High Specific Capacity Nanomaterials as Lithium ion battery anodes

Hsing-Yu Tuan（段興宇）

Professor, Department of Chemical Engineering, National Tsing Hua University, Taiwan, R.O.C.

Nanomaterials: size, shape, composition, phase control property investigation, large-scale synthesis

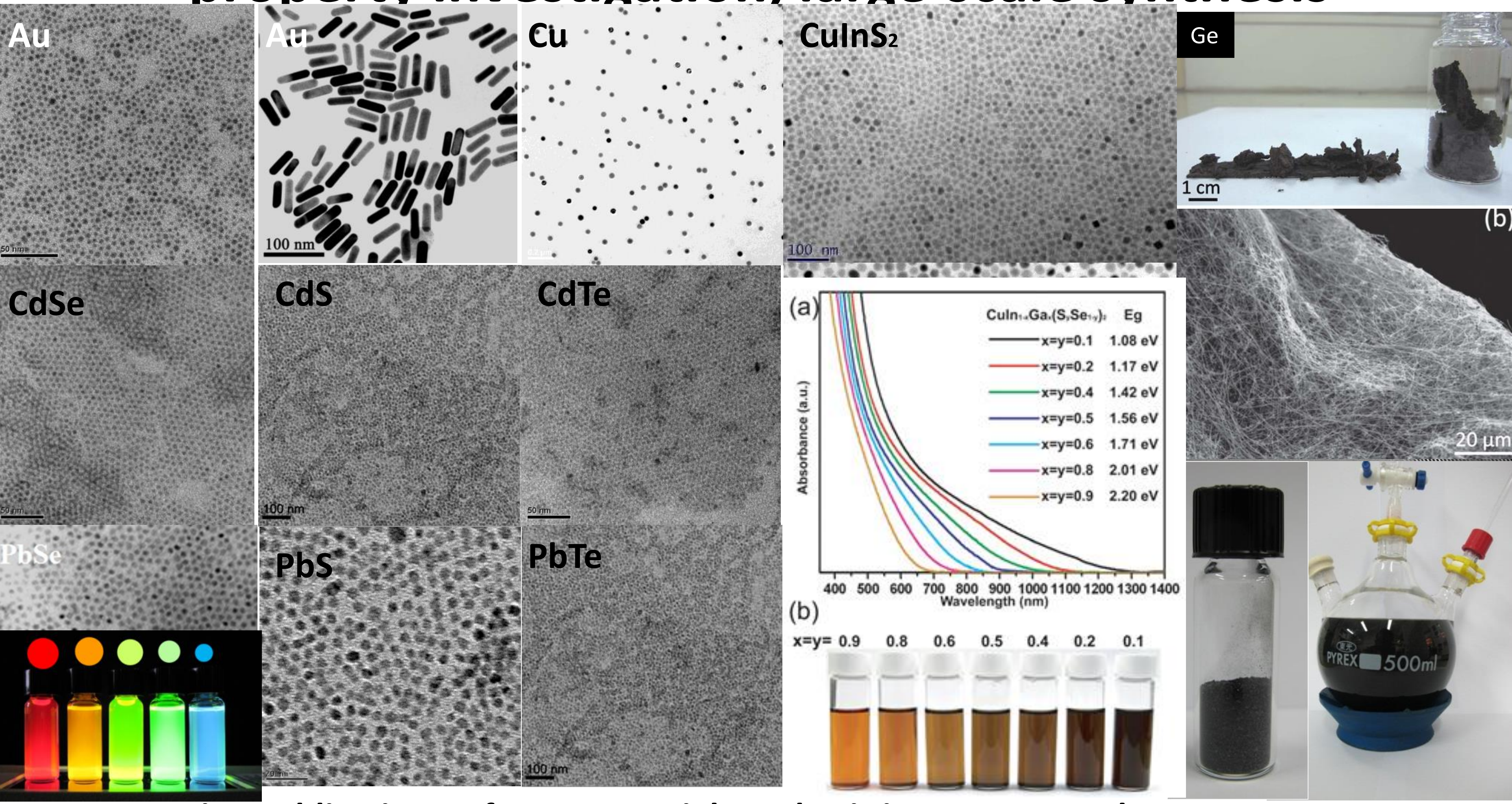

Representative Publications of Nanomaterial Synthesis in Tuan research group

Angew Chem.Int.2006, 45, 5184
J. Am. Chem. Soc, 2008, 130, 8900
J. Am. Chem. Soc, 2008, 130, 5436
J. Am. Chem. Soc, 2007, 129, 1733
Nano Letters., 2005,5,681

Chem. Mater., 2008, 20, 2306
Chem. Mater., 2008, 20, 1239
Chem. Com., 2010, 46, 6105
J. Phys. Chem. C, 2011, 115, 1592
Cry. Growth. Des., 2010, 10, 4741

J. Phys. Chem. C, 2013, 117, 21955
Nanoscale, 2013, 5, 9875
Nanoscale, 2012, 4, 4562
J. Mater. Chem., 2011, 21, 13793

Nanomaterials-based applications

High-capacity anode materials for lithium and sodium ion batteries

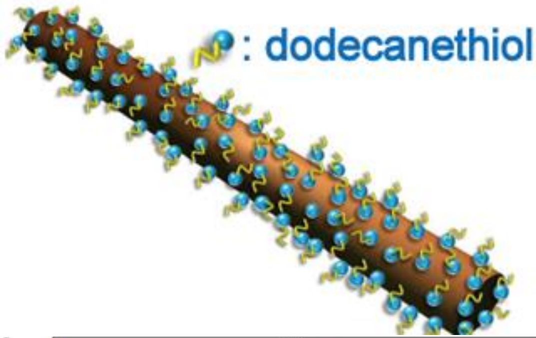

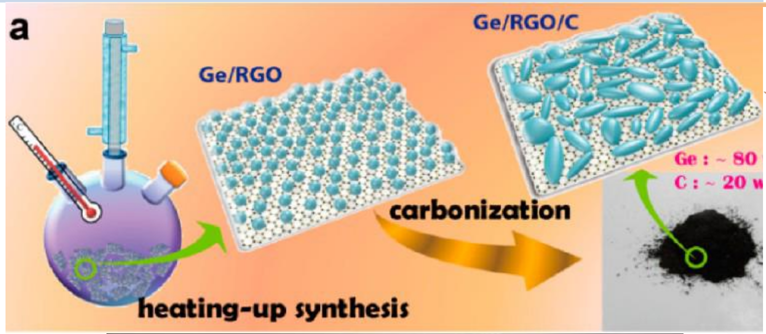

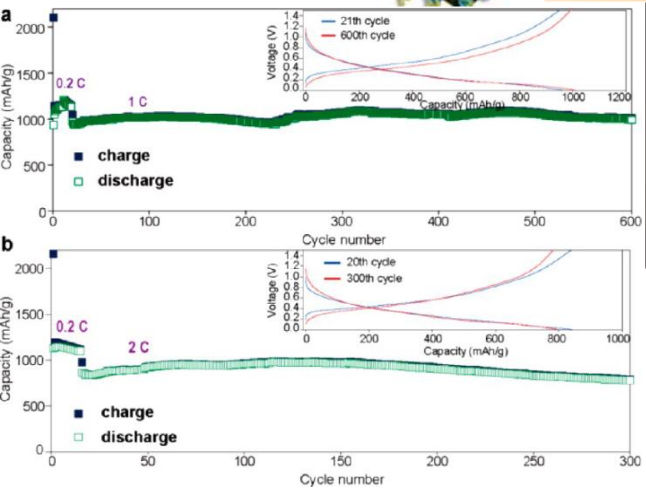

Rapid hydrogen production

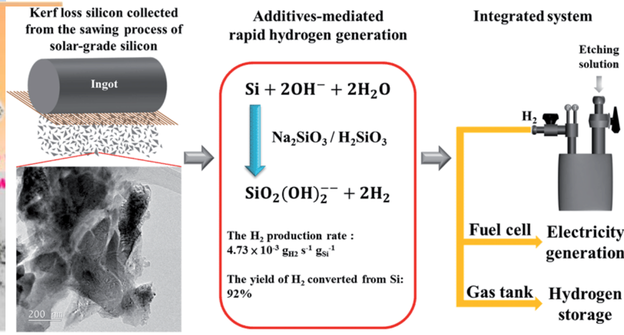

Nanocrystal-based photovoltaic electrodes

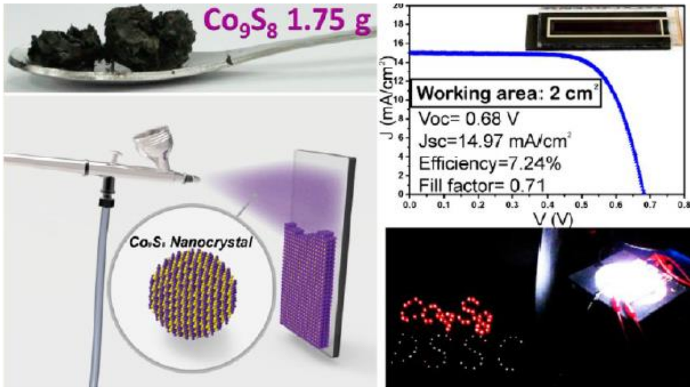

Representative Publications of Nanomaterial Applications in Tuan research group

Nano Letters, 2013, 13, 4036
Nano Letters, 2012, 12 6372
Nano Letters, 2017, 17, 1240-1247
Energy&Environ. Science, 2011, 4, 4929
ACS Nano, 2016, accepted
ACS Nano, 2013, 7, 9443

ACS Nano, 2012, 6, 9932
ACS Nano, 2010, 4, 6278
ACS Nano, 2012, 6, 5710
Biomaterials, 2012, 33, 6559
Biomaterials, 2012, 33, 4108
Chem. Mater., 2015, 12, 4

Chem. Mater., 2014, 26, 2172
Chem. Mater., 2014, 26, 1785
J. Materi. Chem. A, 2017 in press
J. Mater. Chem. A, 2016, 4, 12921
J. Mater. Chem., (cover story) 2012, 22, 2215
ACS AMI, 2016, 5, 5
ACS AMI, 2016, 12, 2

Development of the lithium ion battery

Macbook Air 2008

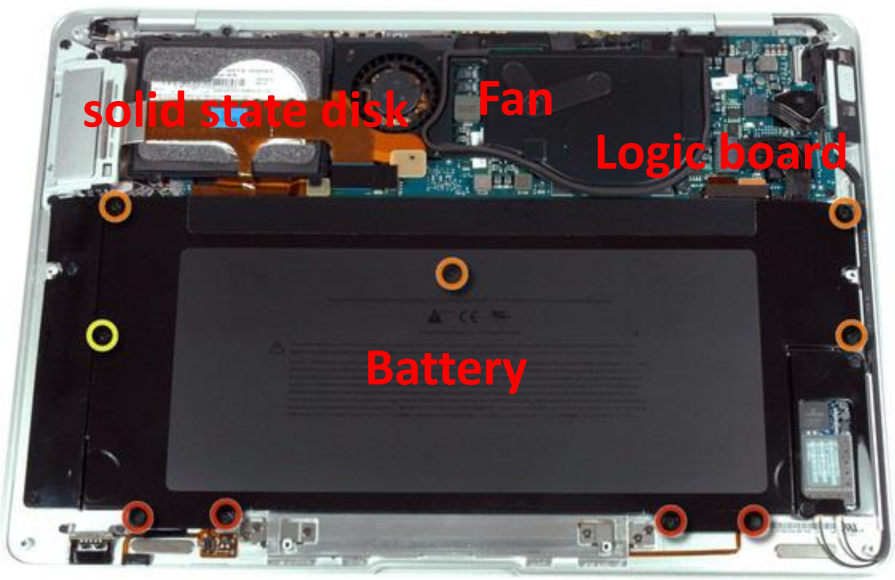

37 Wh lithium ion battery

New macbook 2015

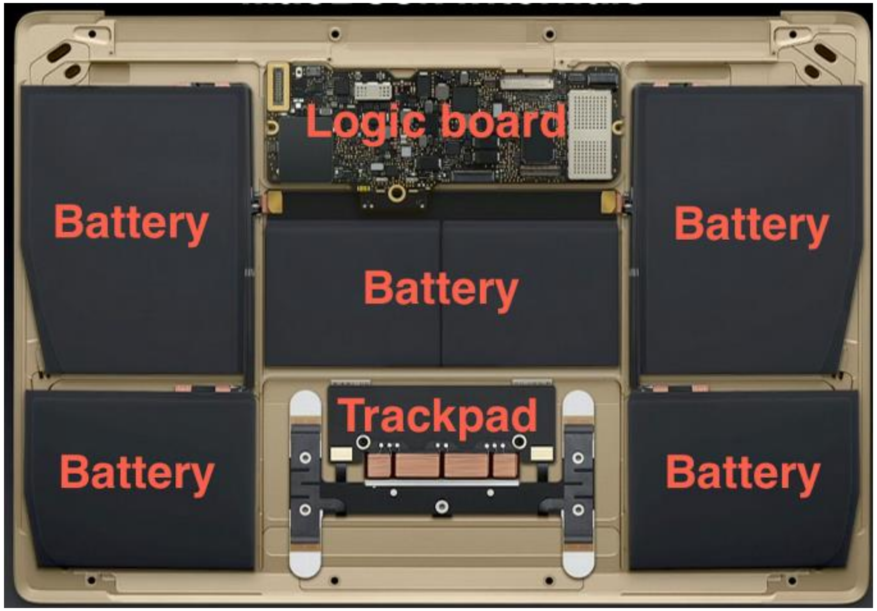

39.7 Wh lithium ion battery

Nanomaterials: size, shape, composition, phase control property investigation, large-scale synthesis

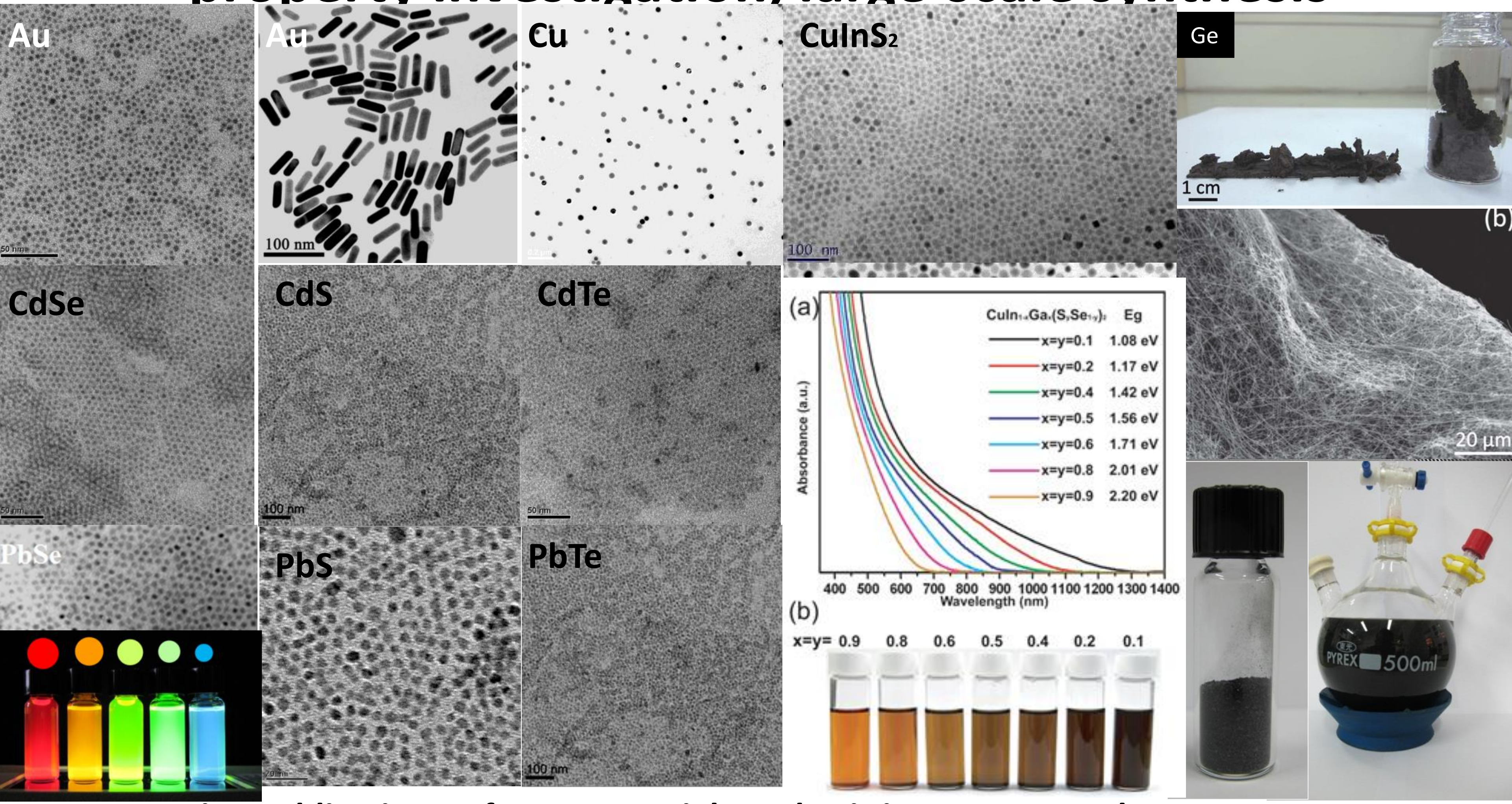

Representative Publications of Nanomaterial Synthesis in Tuan research group

Angew Chem.Int.2006, 45, 5184
J. Am. Chem. Soc, 2008, 130, 8900
J. Am. Chem. Soc, 2008, 130, 5436
J. Am. Chem. Soc, 2007, 129, 1733
Nano Letters., 2005,5,681
Chem. Mater., 2008, 20, 2306
Chem. Mater., 2008, 20, 1239
Chem. Com., 2010, 46, 6105
J. Phys. Chem. C, 2011, 115, 1592
Cry. Growth. Des., 2010, 10, 4741
J. Phys. Chem. C, 2013, 117, 21955
Nanoscale, 2013, 5, 9875
Nanoscale, 2012, 4, 4562
J. Mater. Chem., 2011, 21, 13793

Nanomaterials-based applications

High-capacity anode materials for lithium and sodium ion batteries

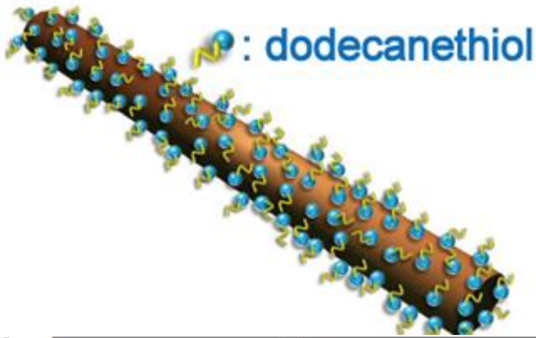

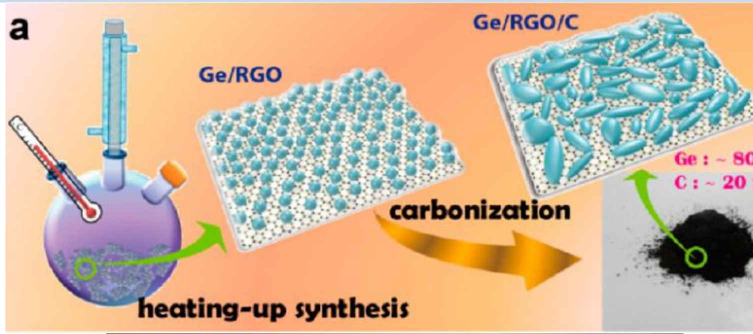

Rapid hydrogen production

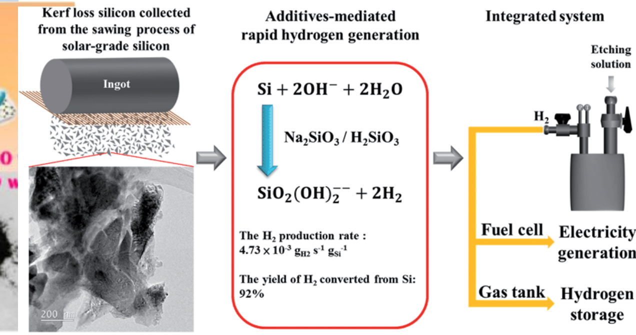

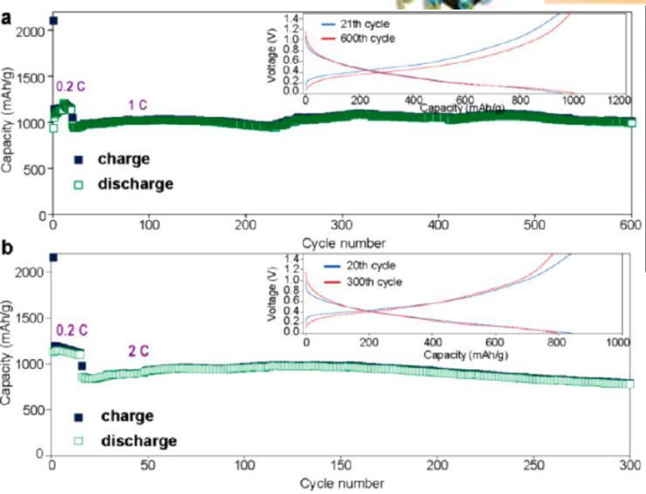

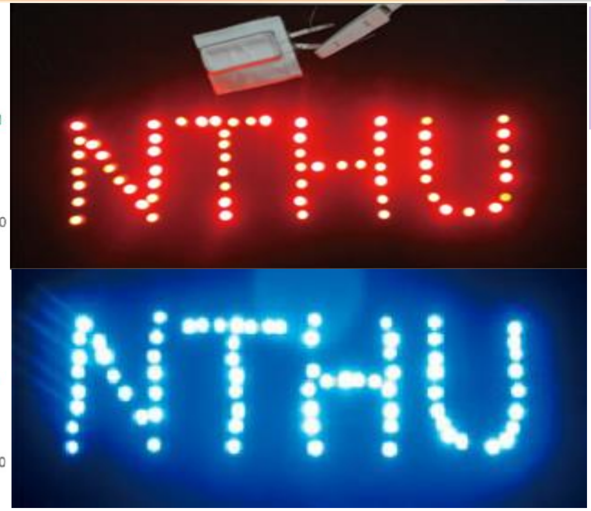

Nanocrystal-based photovoltaic electrodes

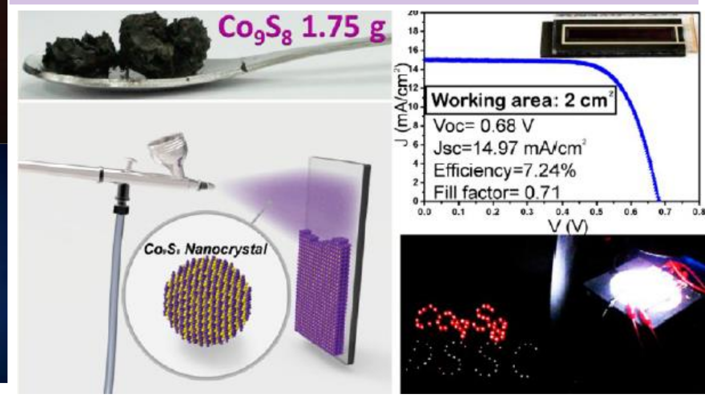

Representative Publications of Nanomaterial Applications in Tuan research group

Nano Letters, 2013, 13, 4036
Nano Letters, 2012, 12 6372
Energy&Environ. Science, 2011, 4, 4929
ACS Nano, 2016, accepted
ACS Nano, 2013, 7, 9443

ACS Nano, 2012, 6, 9932
ACS Nano, 2010, 4, 6278
ACS Nano, 2012, 6, 5710
Biomaterials, 2012, 33, 6559
Biomaterials, 2012, 33, 4108
Chem. Mater., 2015, 12, 4

Chem. Mater., 2014, 26, 2172
Chem. Mater., 2014, 26, 1785
J. Mater. Chem. A, 2016, 4, 12921
J. Mater. Chem., (cover story) 2012, 22, 2215
ACS AMI, 2016, 5, 5
ACS AMI, 2016, 12, 2

Development trend of energy density of lithium ion batteries

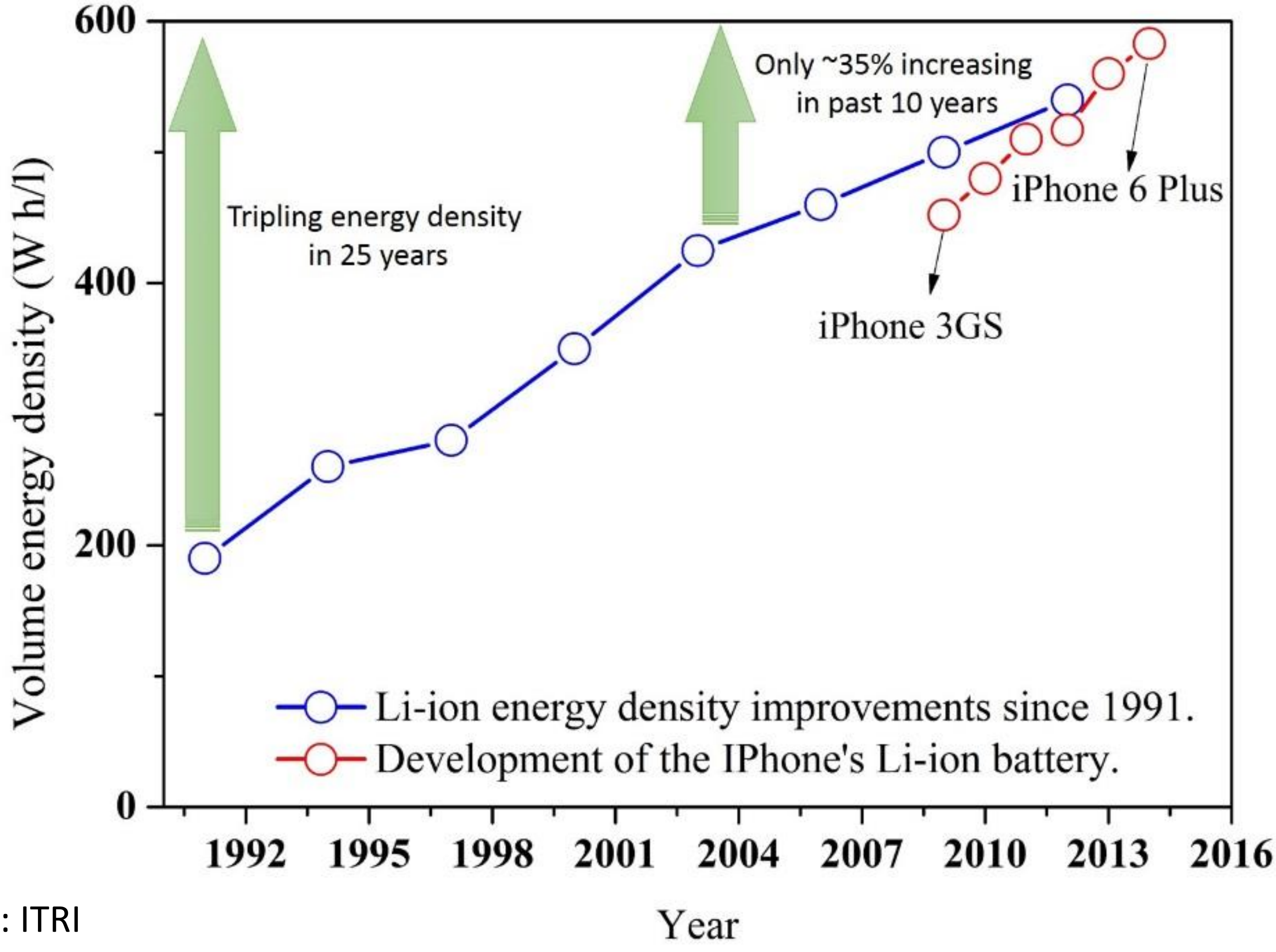

Source: ITRI

LIB: Mechanism and Anode Capacity

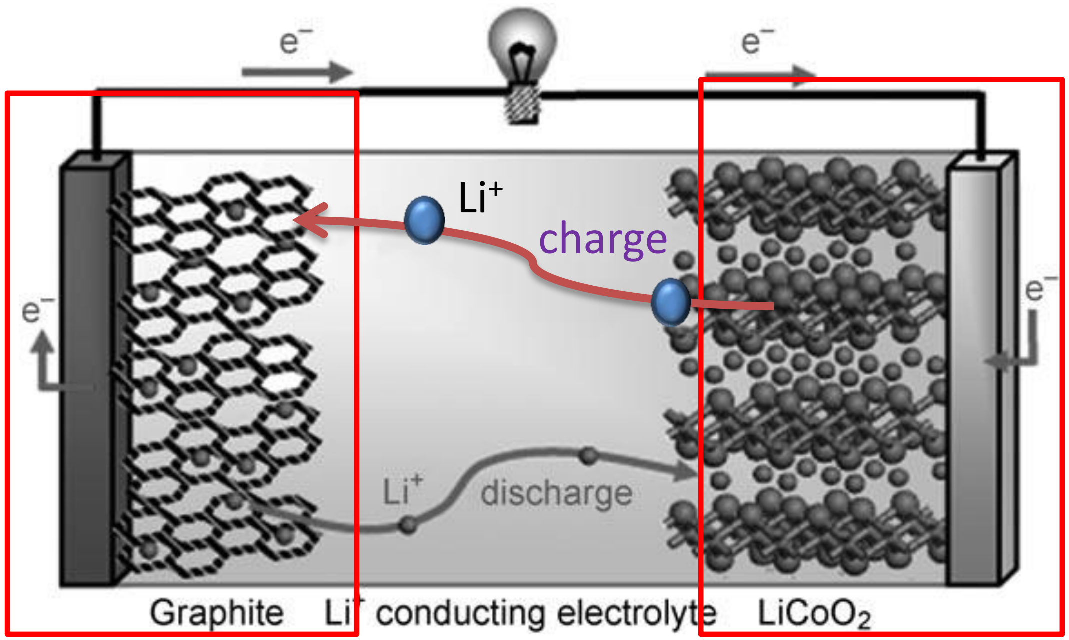

charge reaction :

Cathode : $\mathbf{LiCoO_2 \rightarrow Li_{1-x}CoO_2 + \mathit{x}Li+ + \mathit{x}e^-}$

Anode : $\mathbf{6C + \mathit{x}Li+ + \mathit{x}e^- \rightarrow Li_xC_6}$

Graphite capacity: only 372 mAh/g

ACS App. Mater. Inter., 2012, 4, 4658

Angew. Chem. Int. Ed. 2008, 47, 2930

Graphite alternative :lithium-alloy type materials

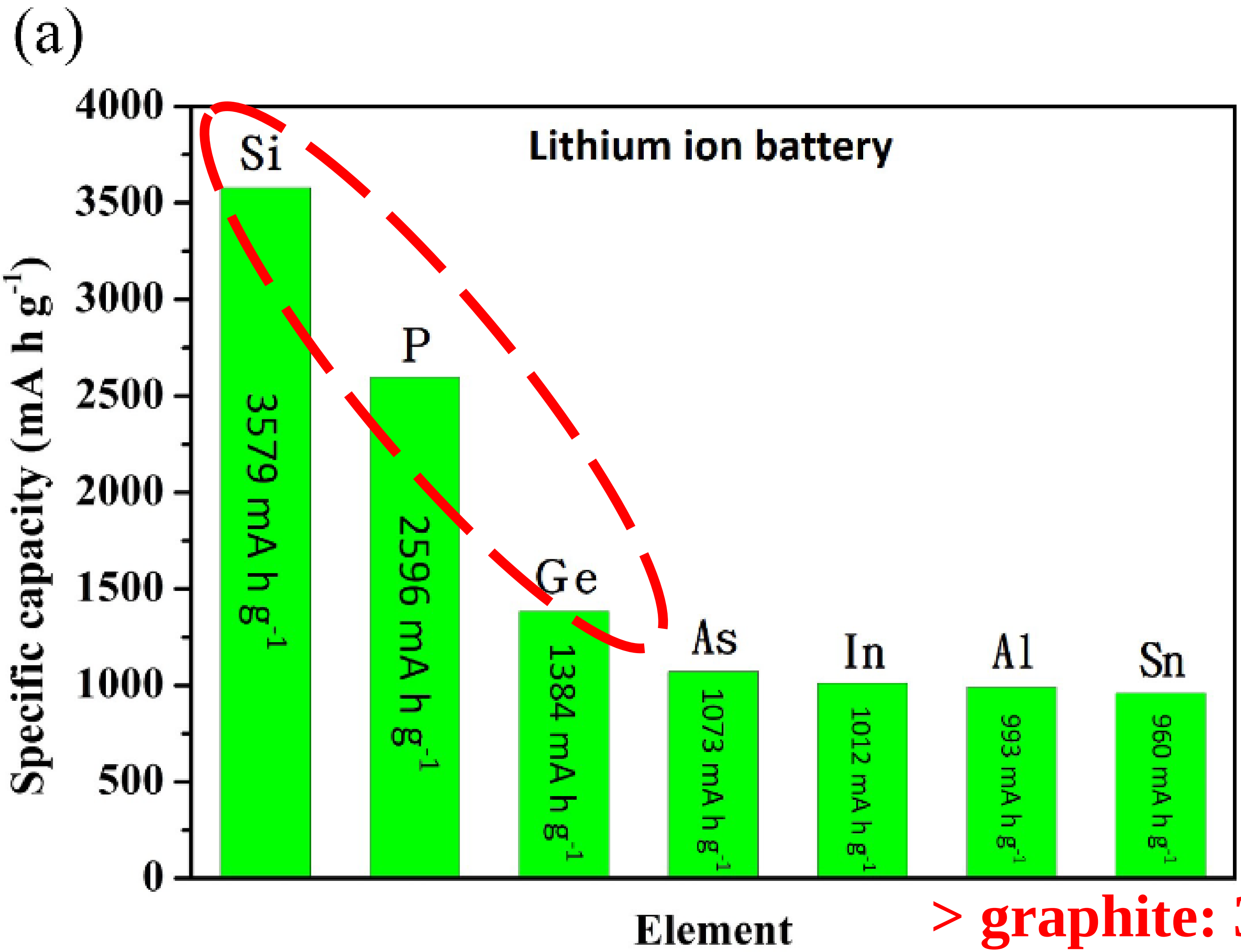

> graphite: 372 mAh/g

Morphological Changes in high-capacity materials During Electrochemical Cycling

micro-size Ge/Si/P particle

~ 300 % volume change

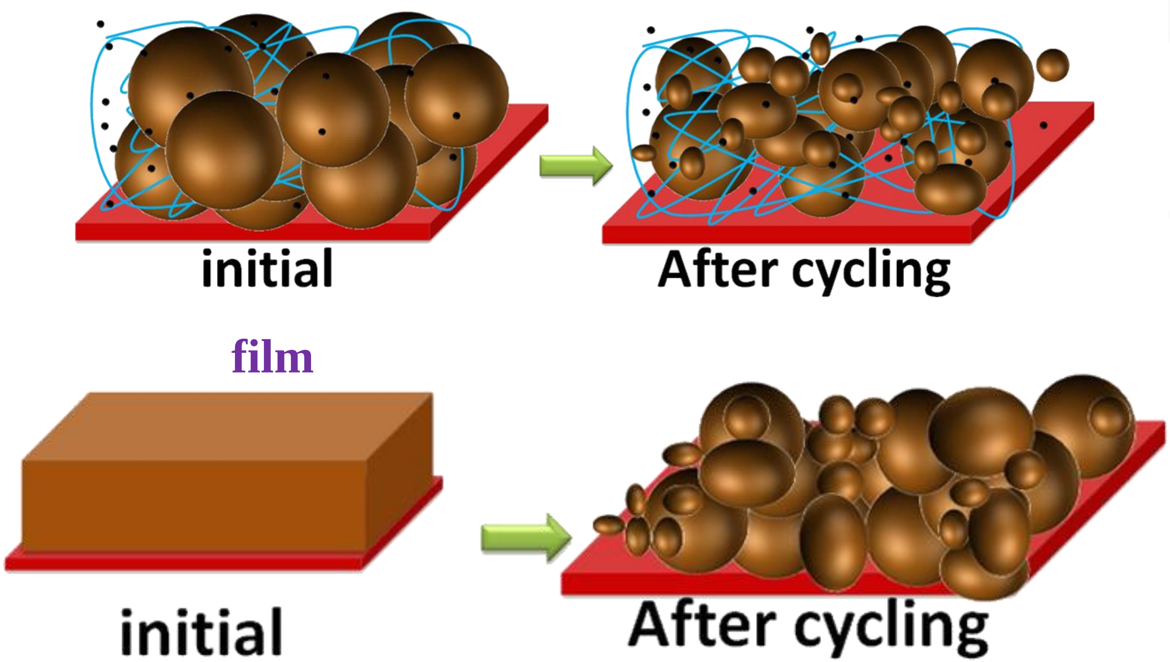

capacity decline rapidly

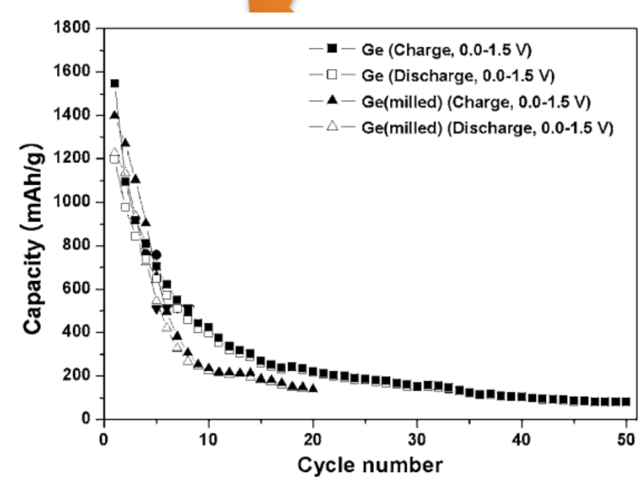

Alloying-based anode materials suffers from pulverization while cycled

J. Electrochem. Soc., 2009, 106, A169

Yoon et al., Electrochem. Solid State Lett., 2008

Nanowires as LIB anodes

- Diameter: 1 to 100 nm
- High surface area
- Unique morphology
- Tunable surface chemistry
- Colloid solution

•Effectivly accommodate the volume changes
•Tolerate reaxed mechanical strain
•Provide channels for
•Efficient electron transport

Raw Ge nanowires for Lithium-Ion Batteries

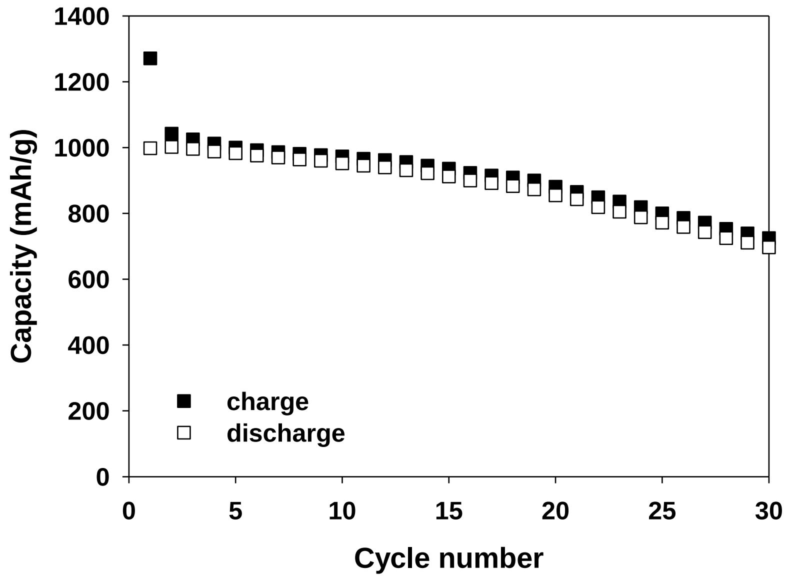

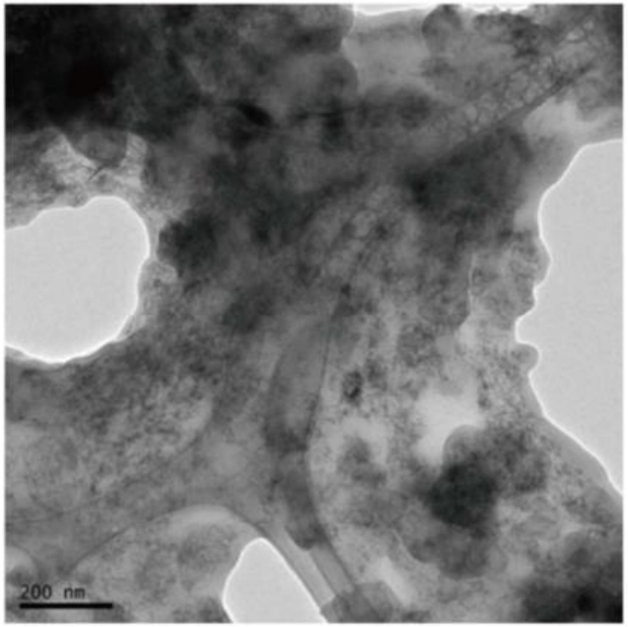

TEM image of Ge nanowires after 30 cycles

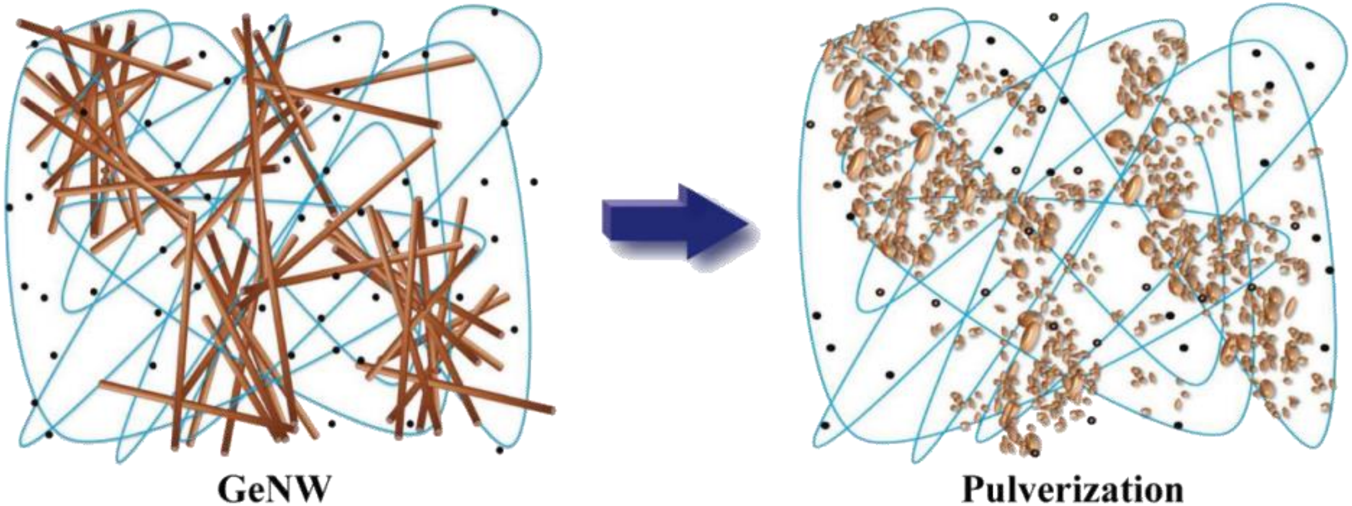

Our approach: alkanethiol-passivated Ge nanowires as LIB anode

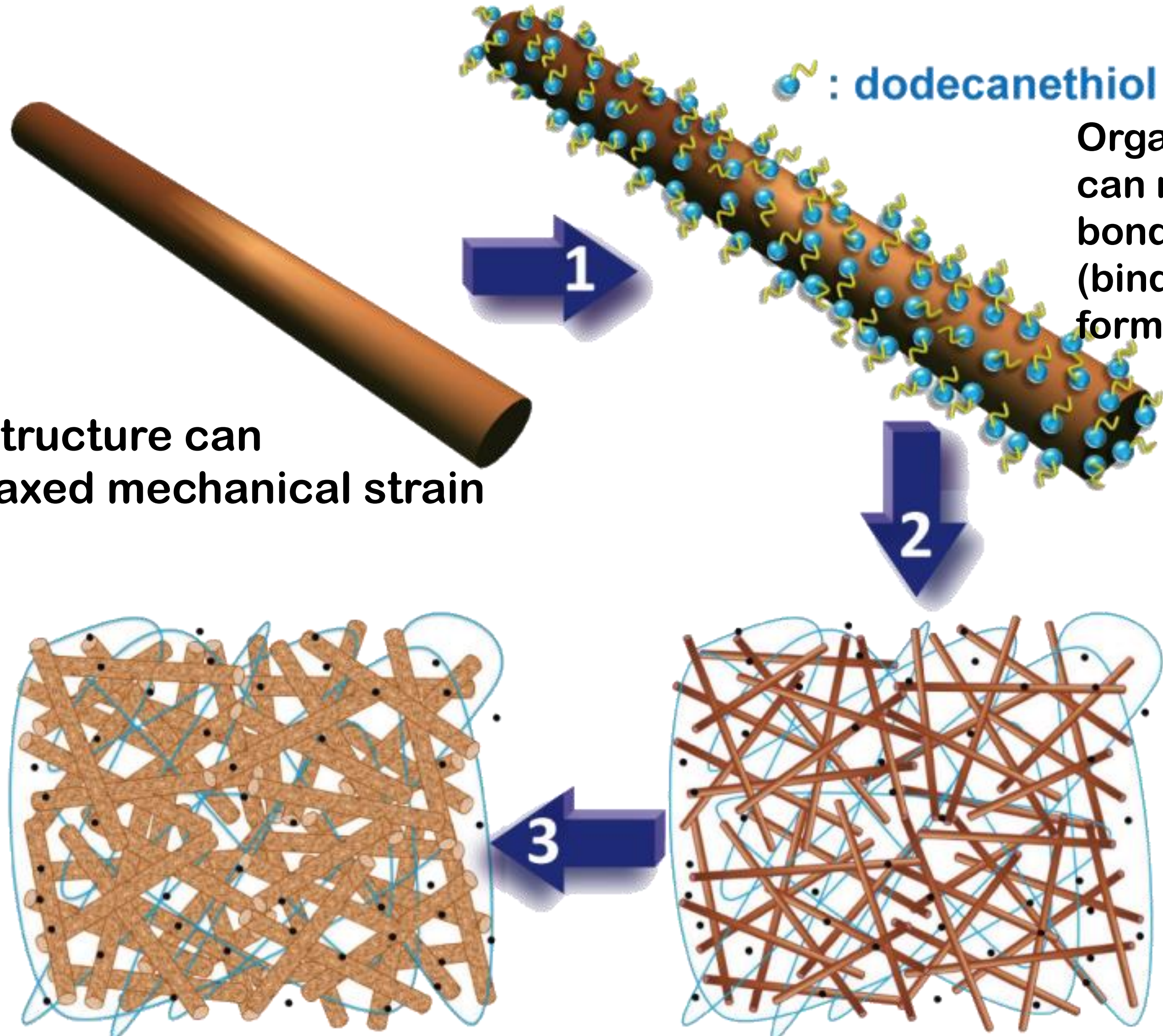

Organic surfactant can make a better bonding with PVdF (binder) to form good composites

Nanowire structure can tolerate relaxed mechanical strain

Germanium nanowires for LIB applications

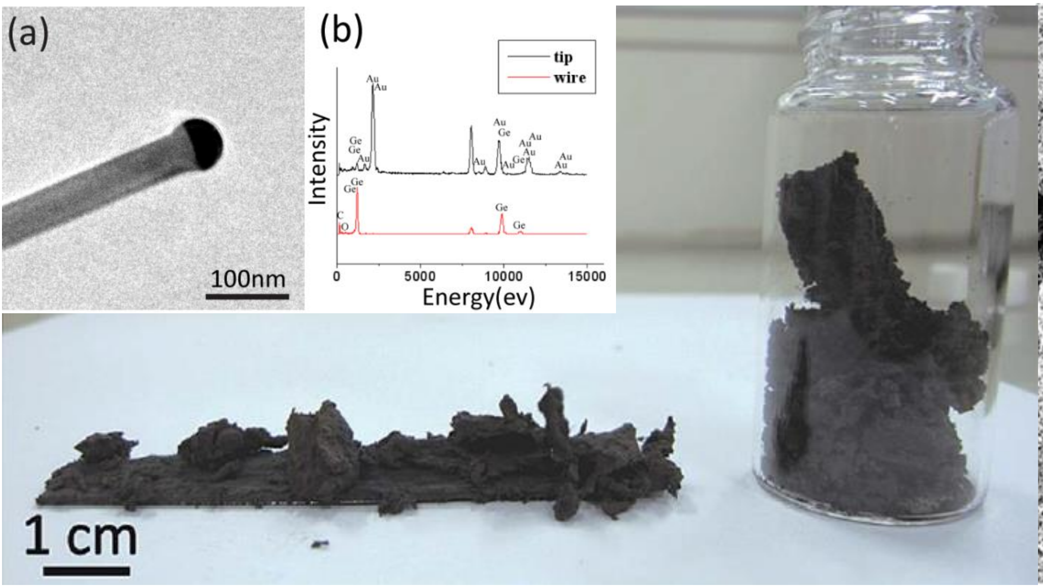

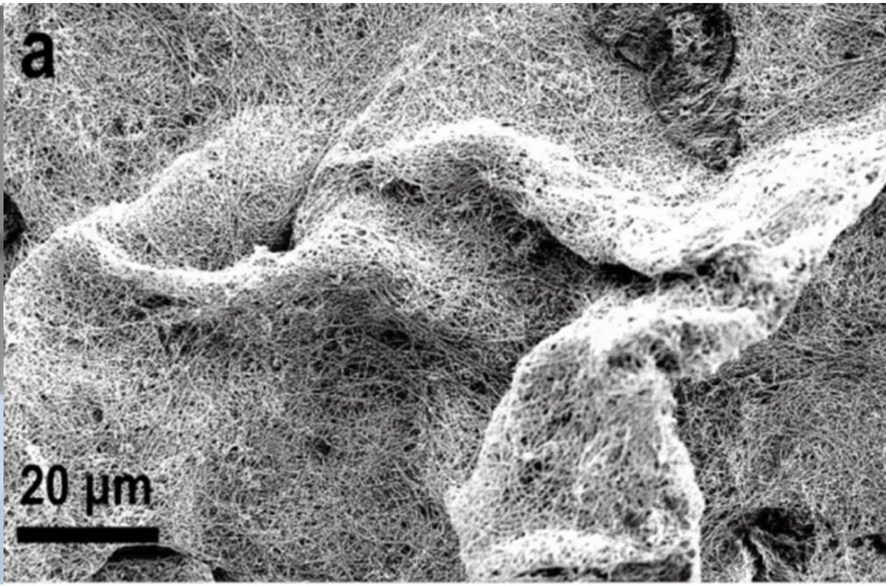

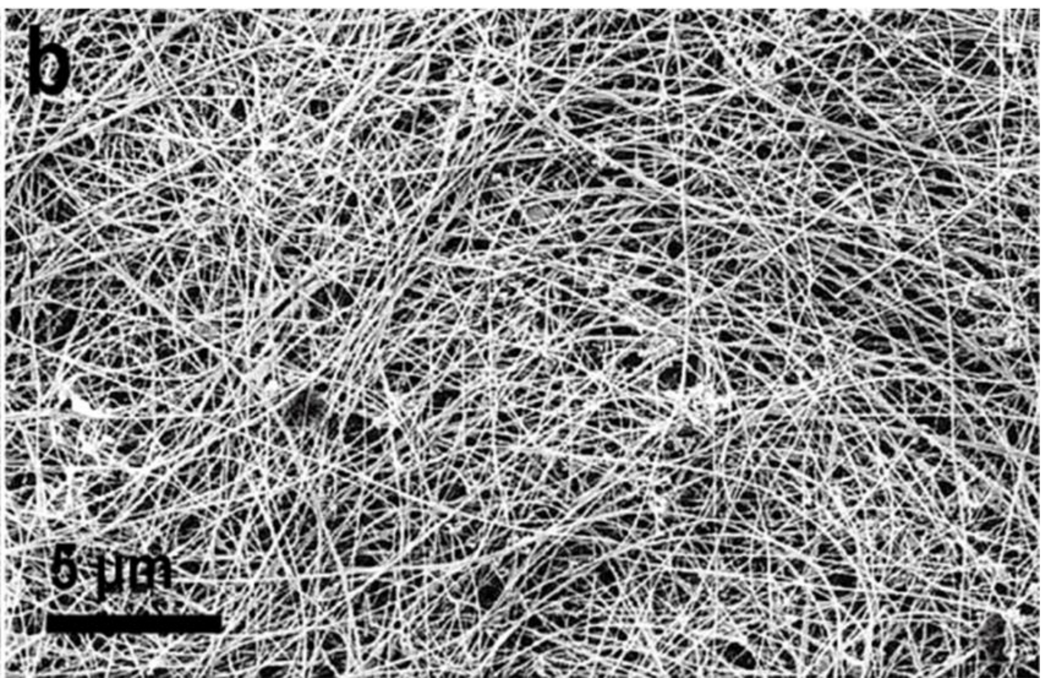

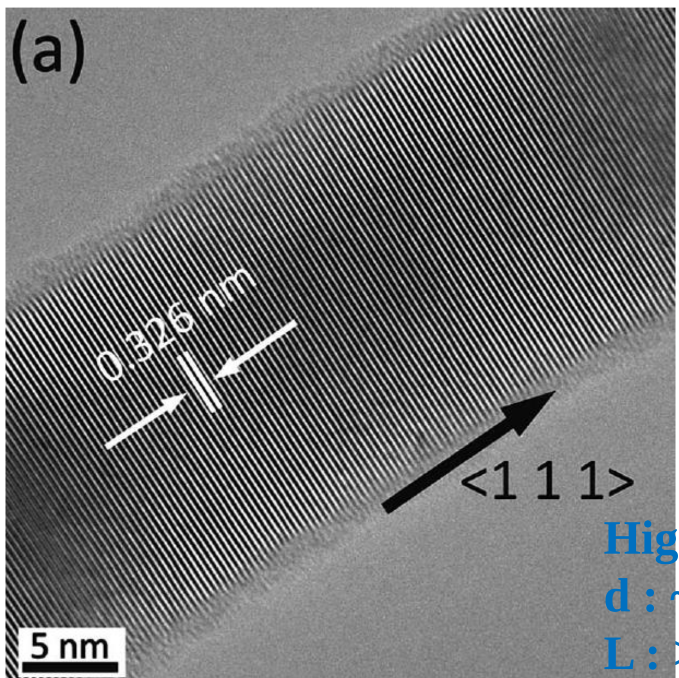

High quality
d : ~ 40 nm
L : >50 µm


METTLER TOLEDO
0.0885 g
→0/T←

Alkanethiol-passivated Ge nanowires

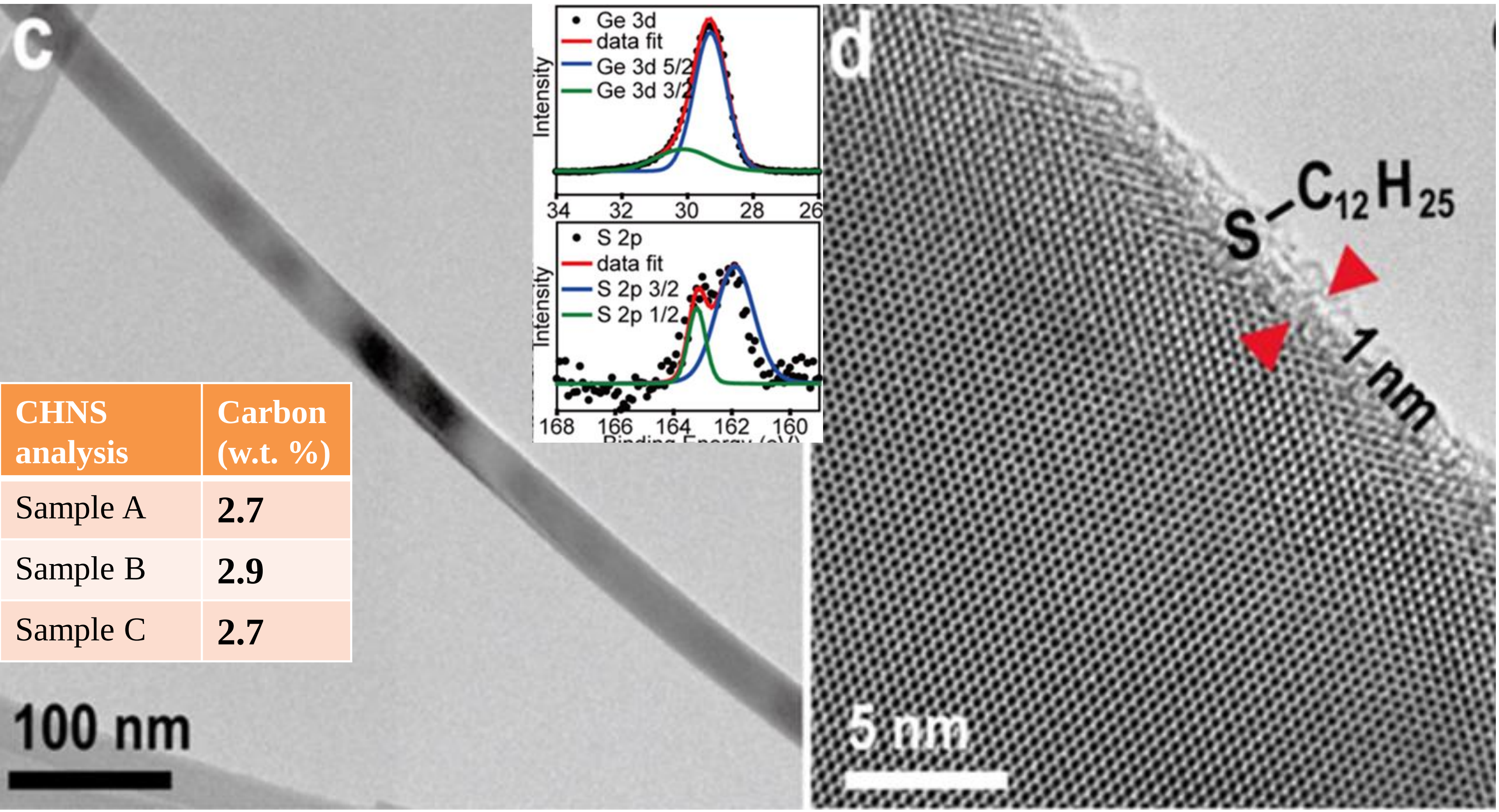

CHNS analysis	Carbon (w.t. %)
Sample A	2.7
Sample B	2.9
Sample C	2.7

Performance of Ge nanowire anode

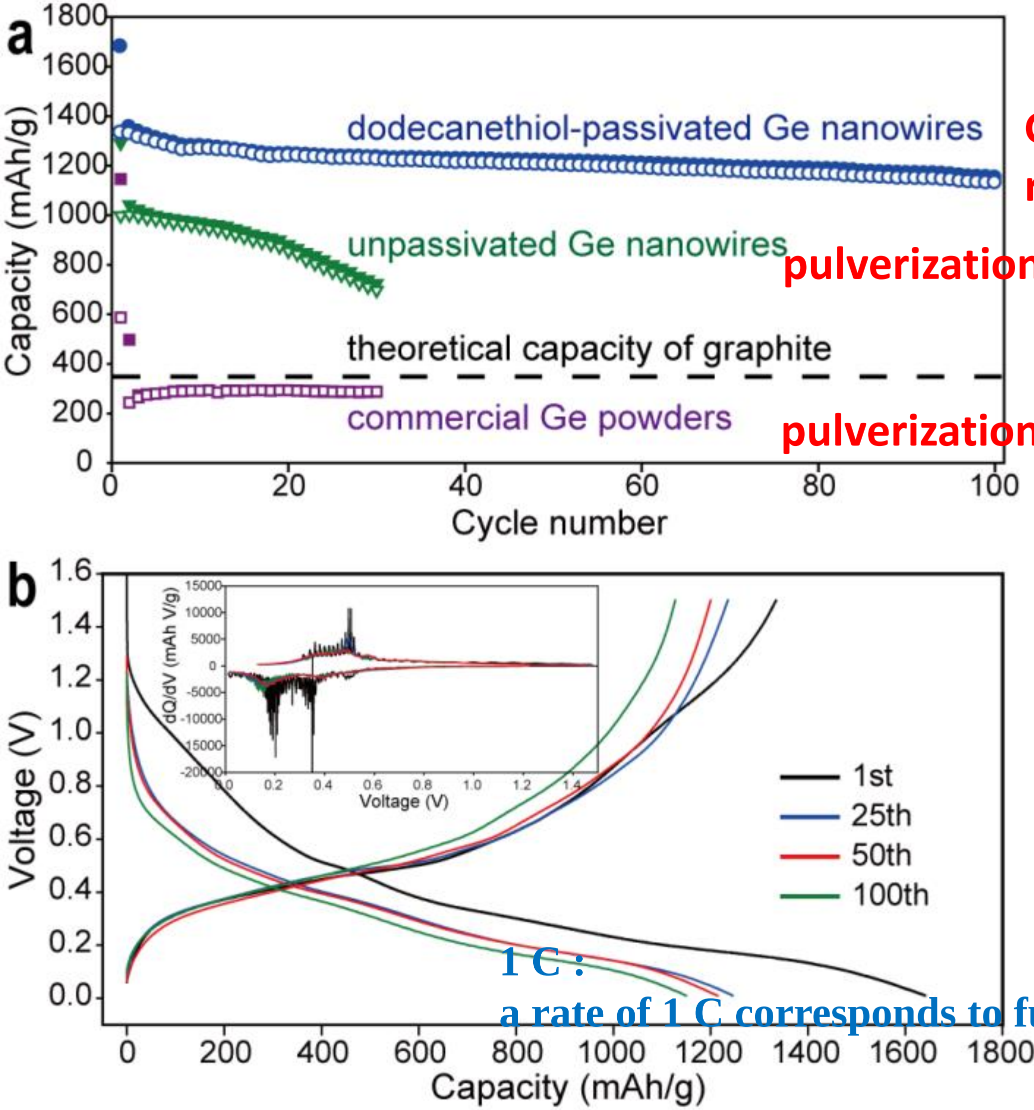

Good capacity retention

pulverization

pulverization

1130 mAh/g (~3 times higher than graphite)

1 C :

a rate of 1 C corresponds to full charge or discharge in 1 hour

High-rate capability of Ge nanowire anode

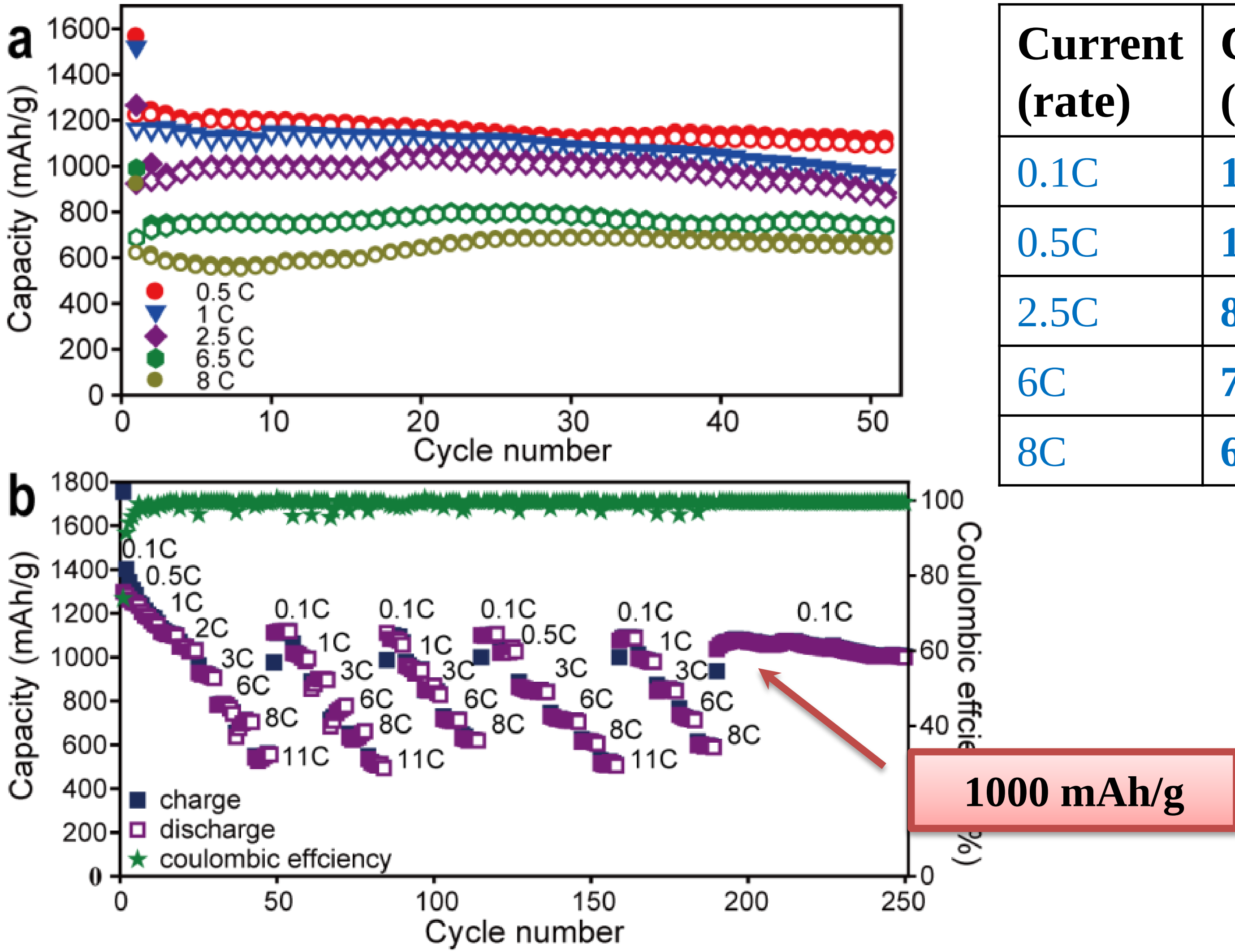

Current (rate)	Capacity (mAh/g)	Cycle number
0.1C	**1130**	100
0.5C	**1090**	50
2.5C	**863**	50
6C	**733**	50
8C	**643**	50

High-temperature performance (55 °C) of Ge nanoiwre anode

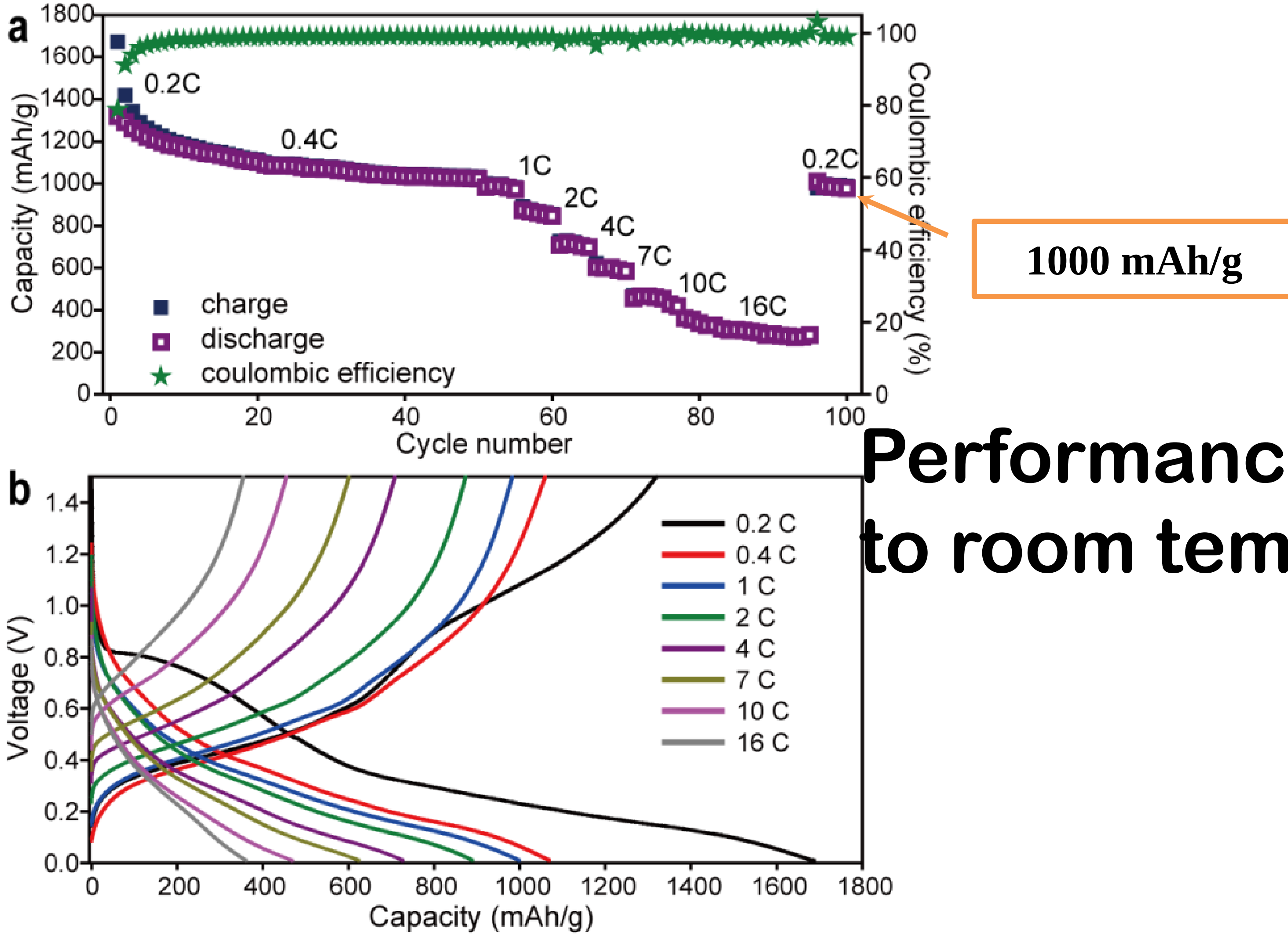

Performance similar to room temperature

Performance of a Full Cell

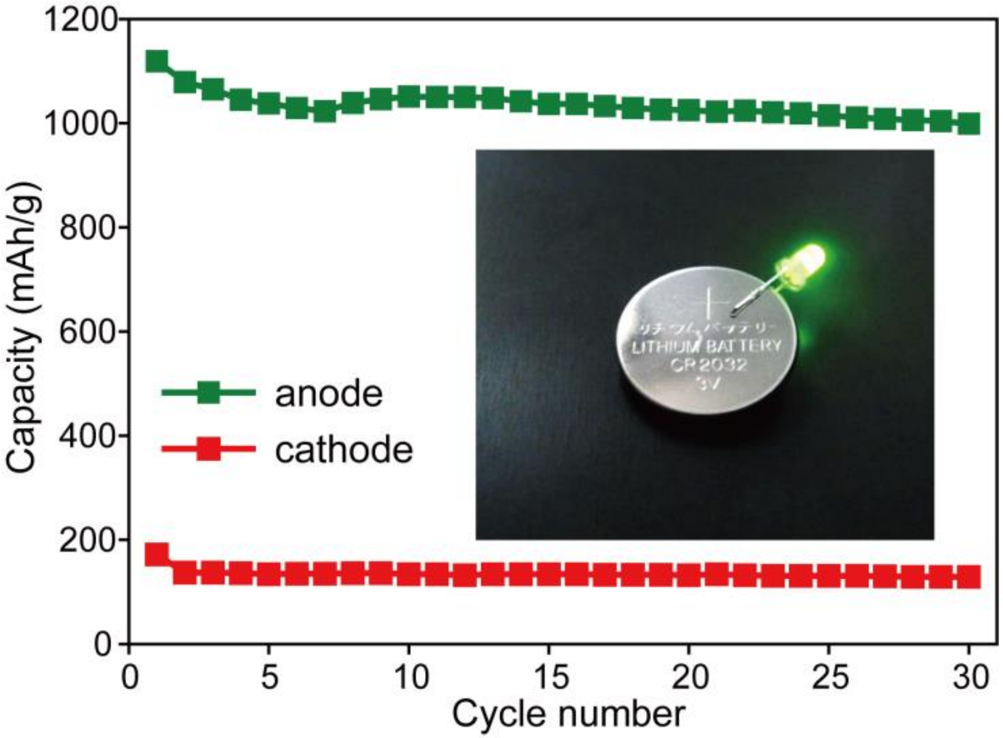

Capacity versus cycle number of a coin full cell between 2.0 and 3.8 V with dodecanethiol-passivated Ge nanowire as the anode and $LiFePO_4$ as the cathode

	anode	cathode
Material	GeNWs	LFP
Loading	~ 1 mg/cm^2	~ 8 mg/cm^2
Capacity	1100 mAh/g	140 mAh/g

Structure evolution of dodecanethiol-passivated Ge nanowires

During lithiation/delithiation process

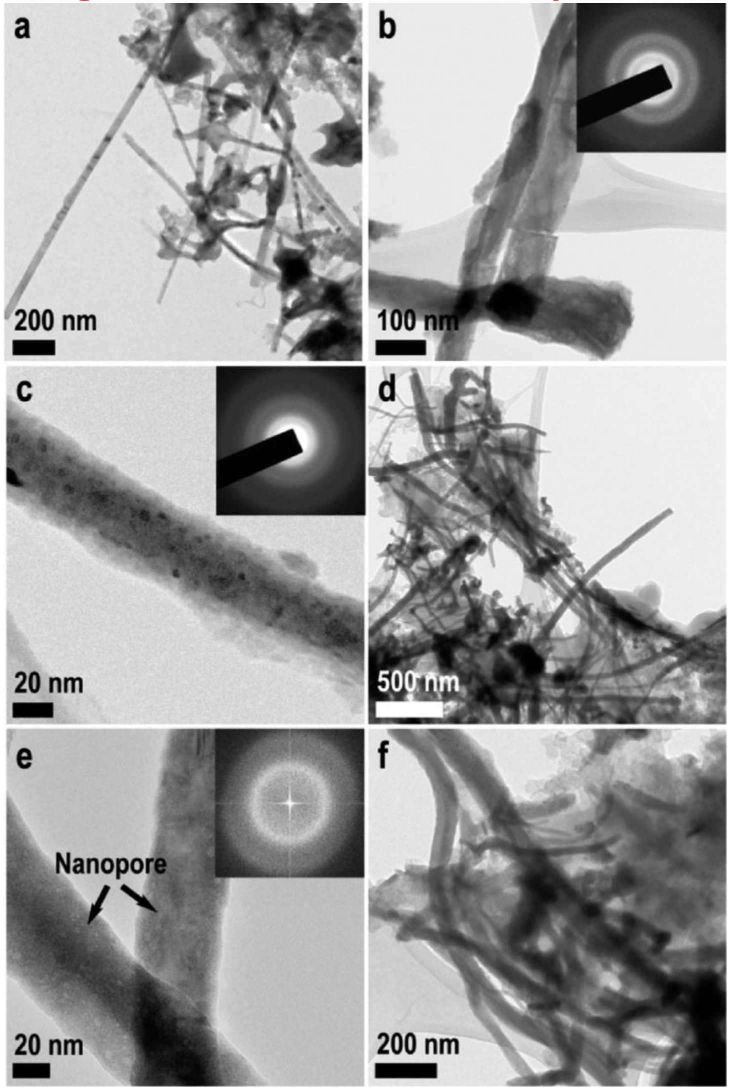

After 100 cycles at 0.1 C

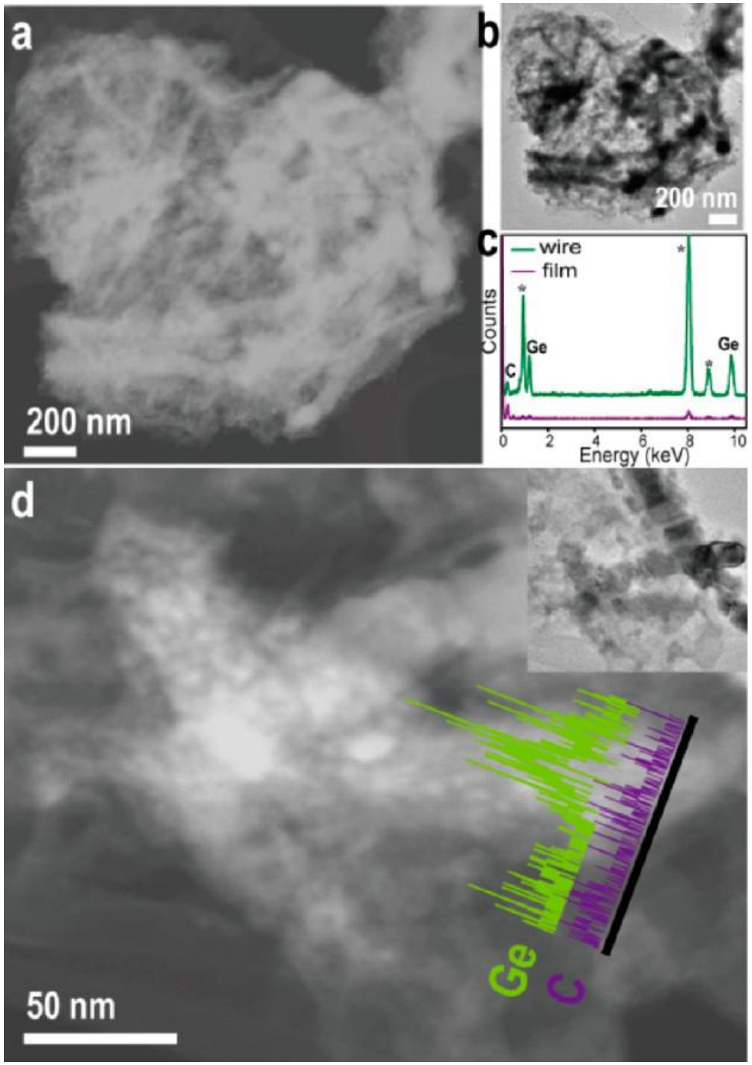

Reduced Graphene Oxide as a supportive materials for performance improvement of high-capacity lithium ion materials

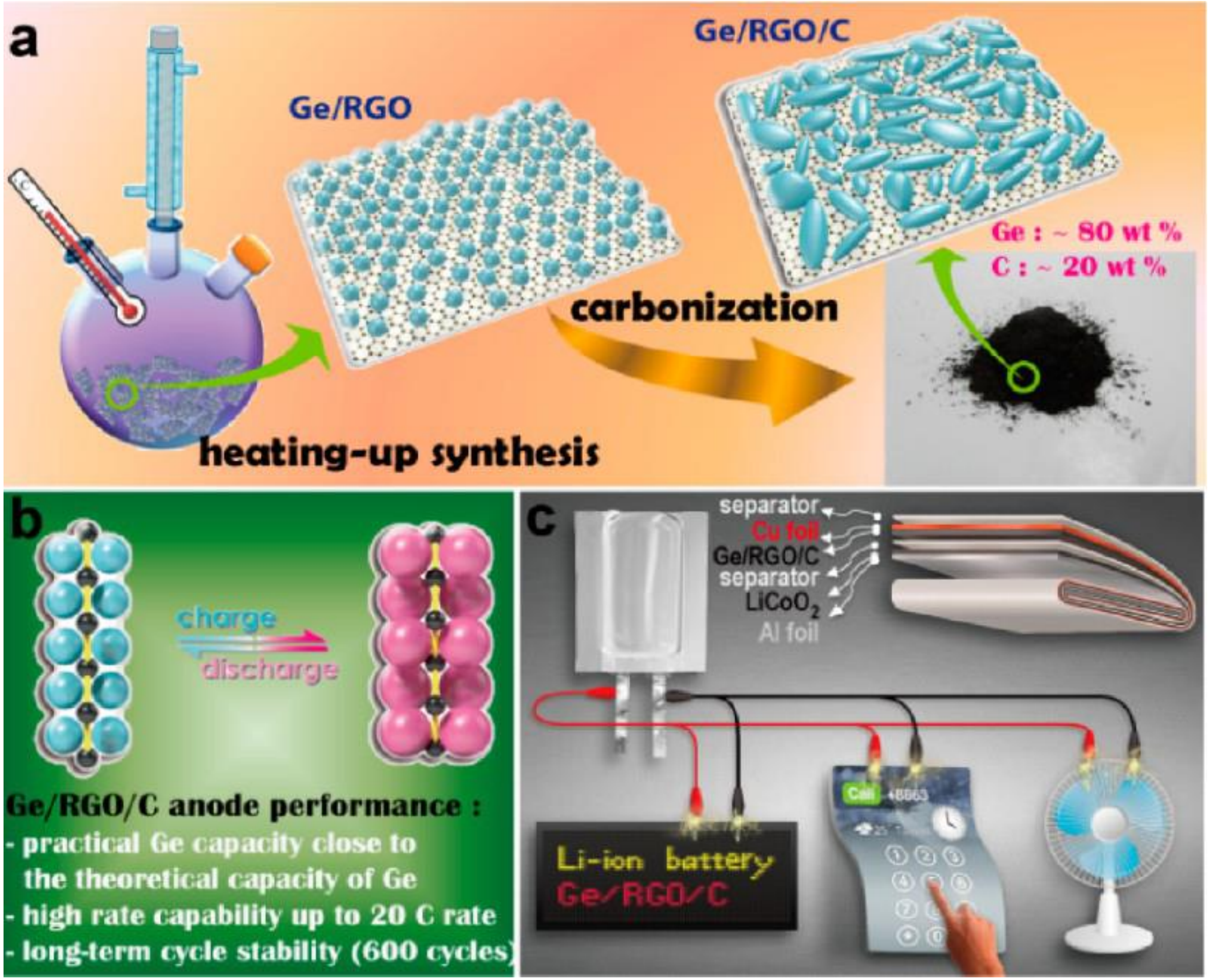

Ge/RGO nanocomposites

Large-scale synthesis **Crystalline&monodisperse**

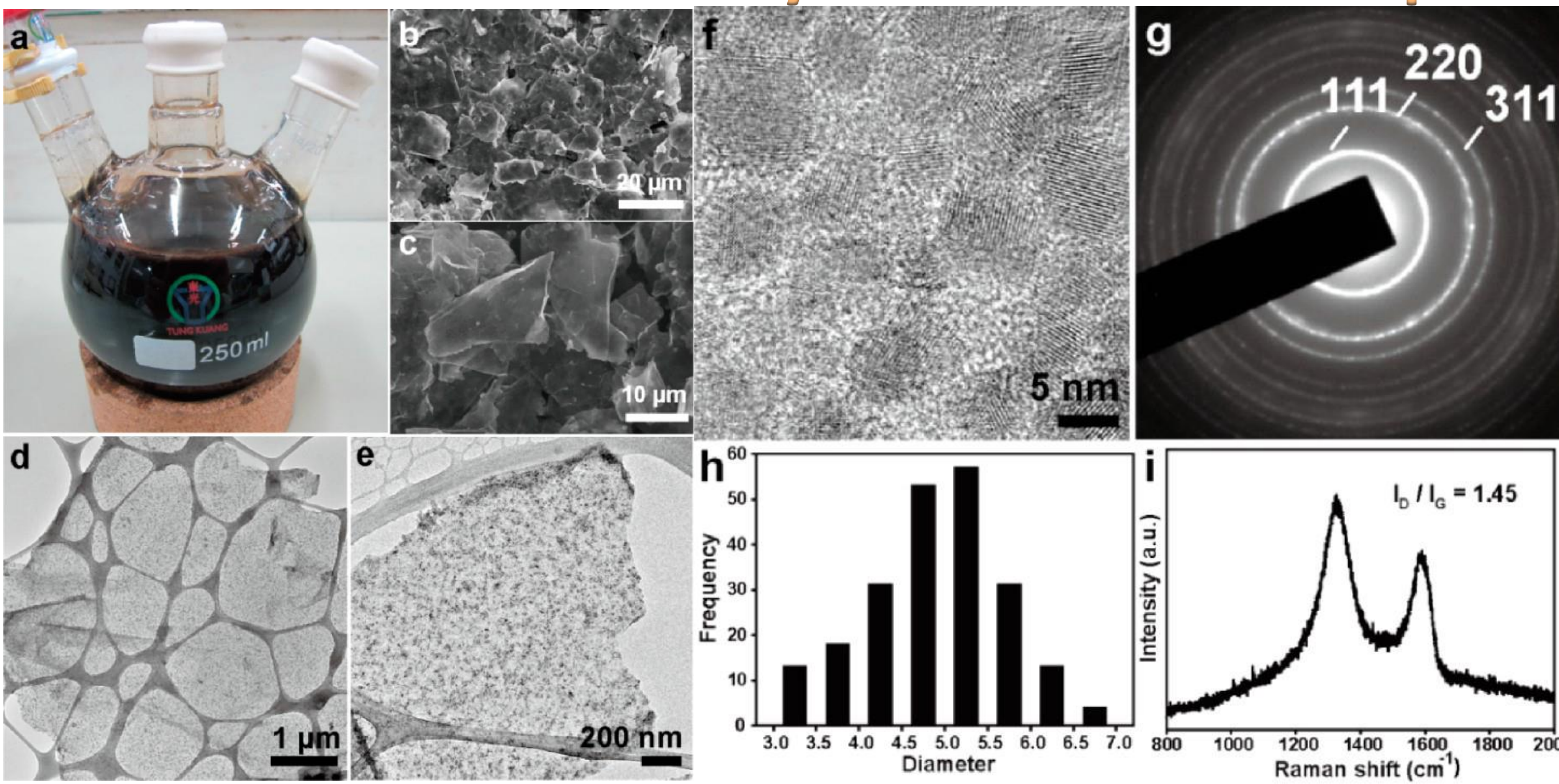

High-density coverage **Small, uniform distribution**

Ge/RGO/C nanocomposites

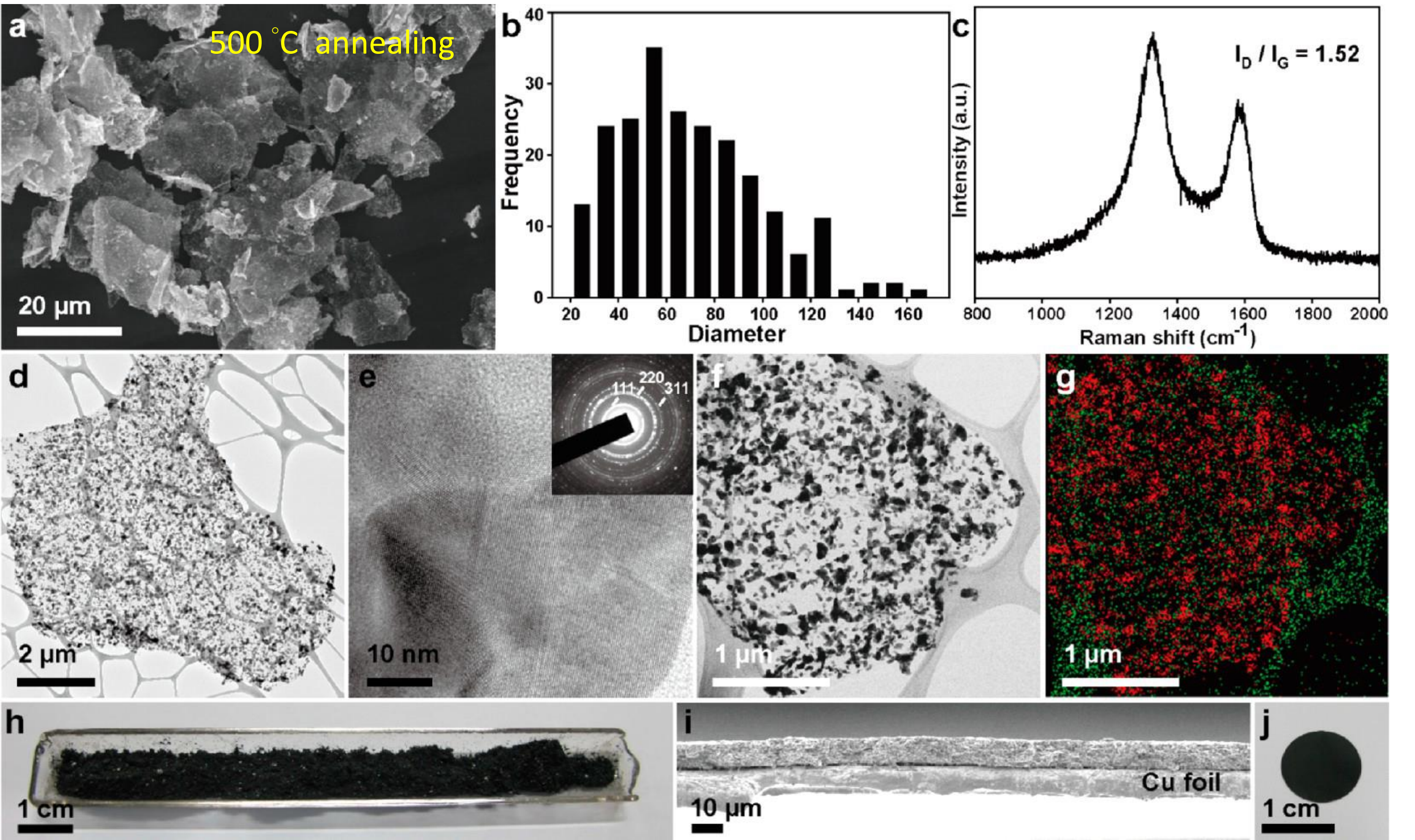

LIB Performance of Ge/RGO/C

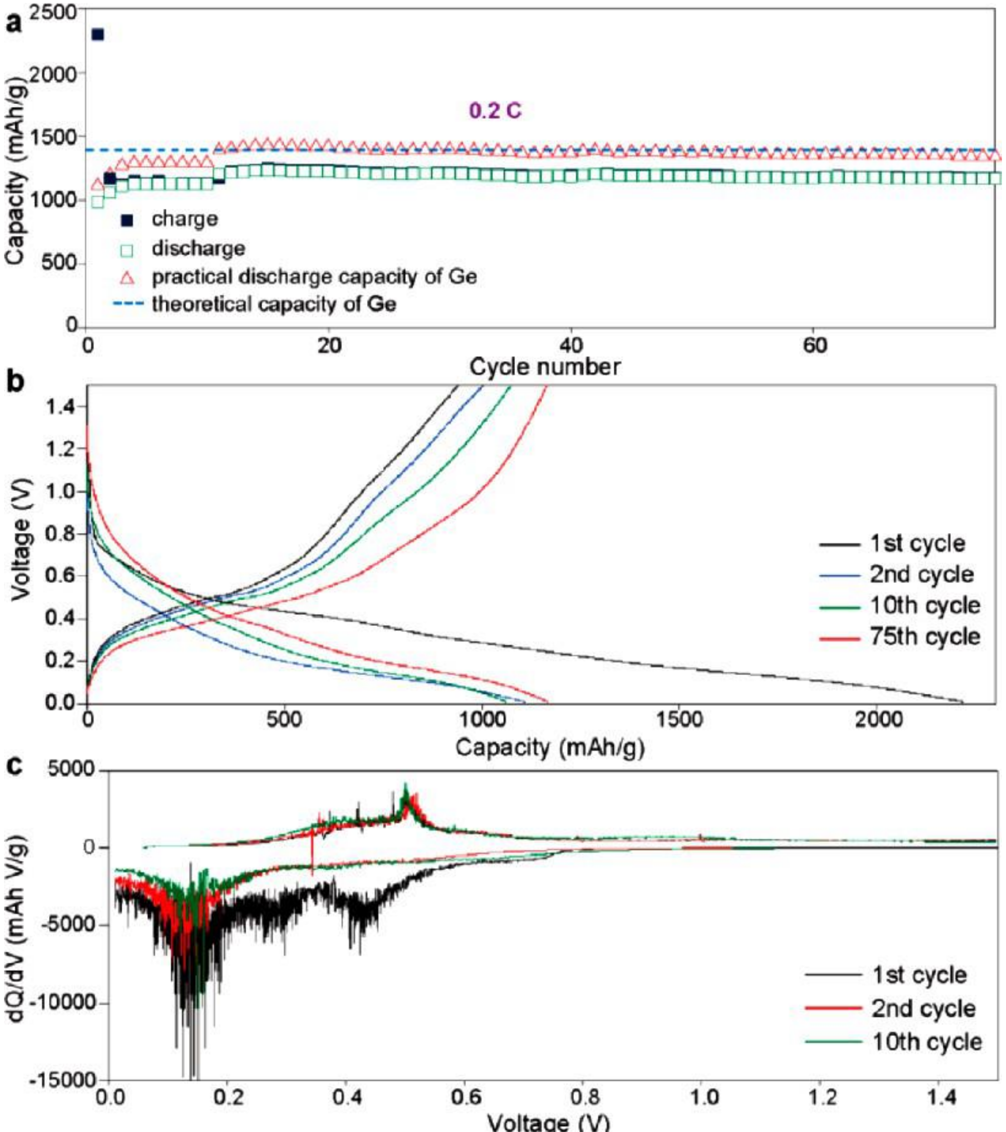

1332 mAh/g over 75 cycles
~96% of theoretical capacity of germanium (1384 mAh/g)

Very consistent electrochemical properties

Cycling performance at 1C

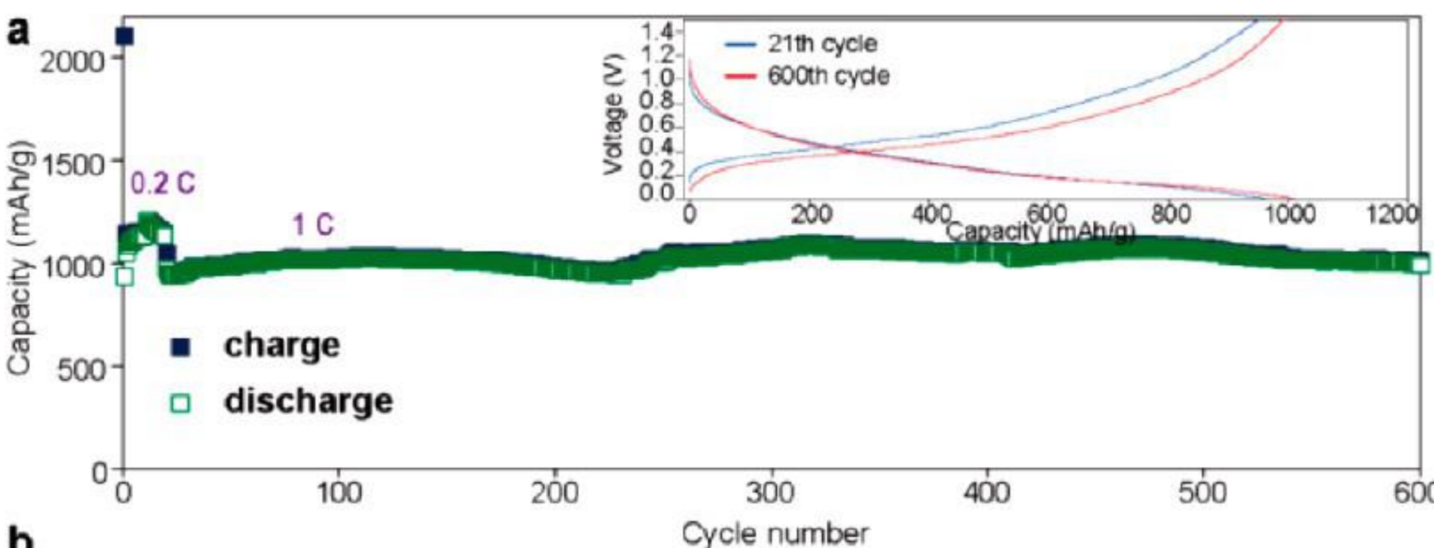

No capacity decade after 600 cycles at 1C

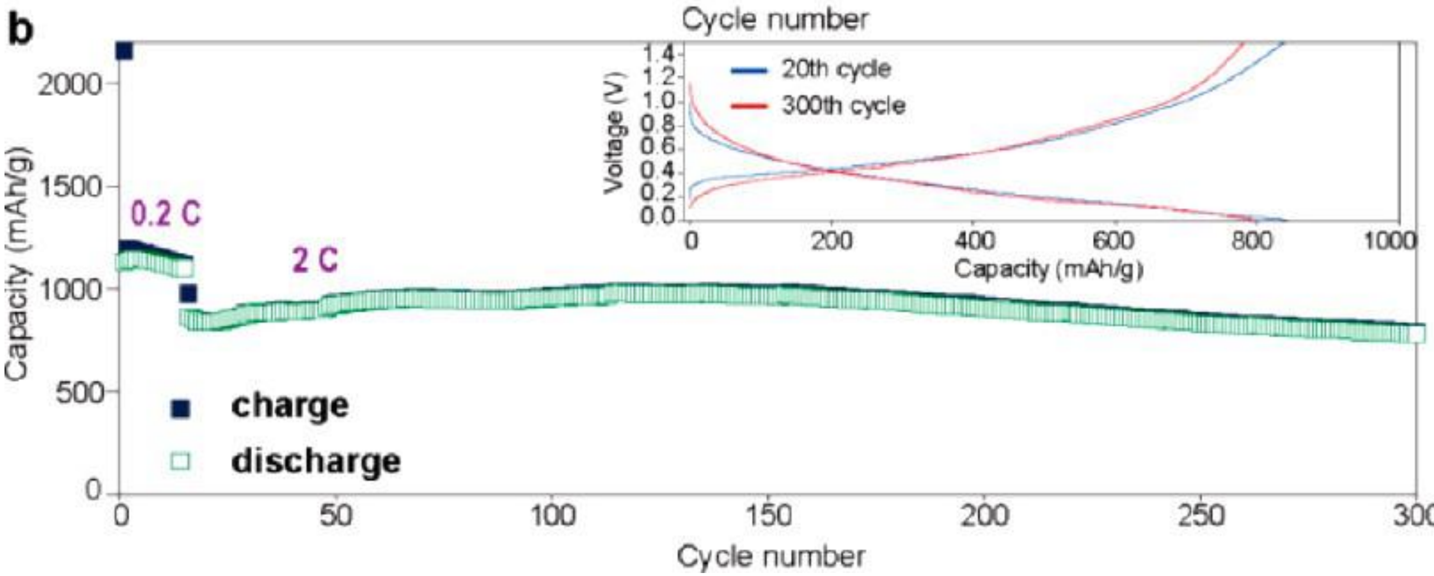

No capacity decade after 300 cycles at 2C

Cycling performance at high rates

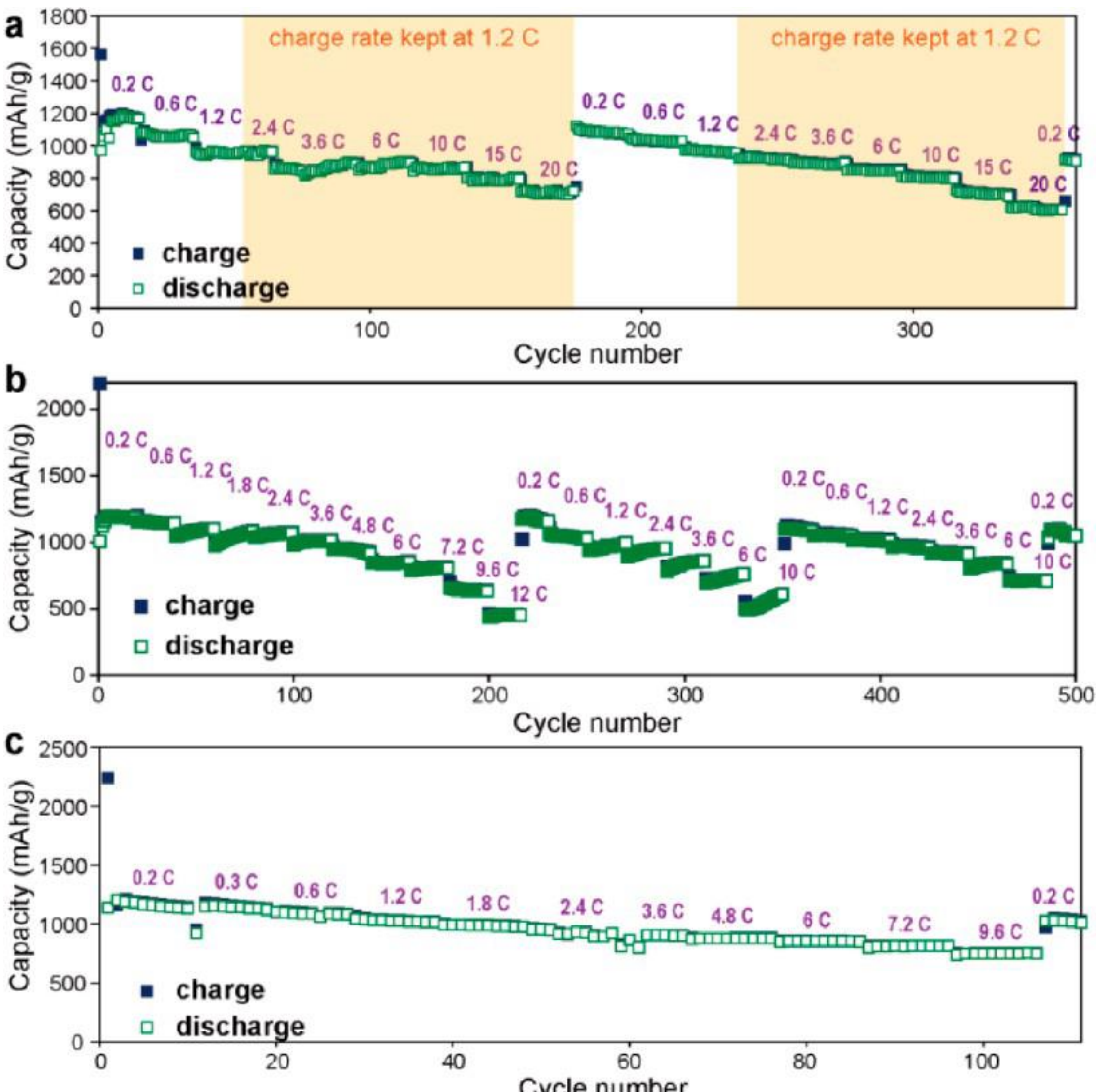

Robust Ge/RGO/C nanocomposites

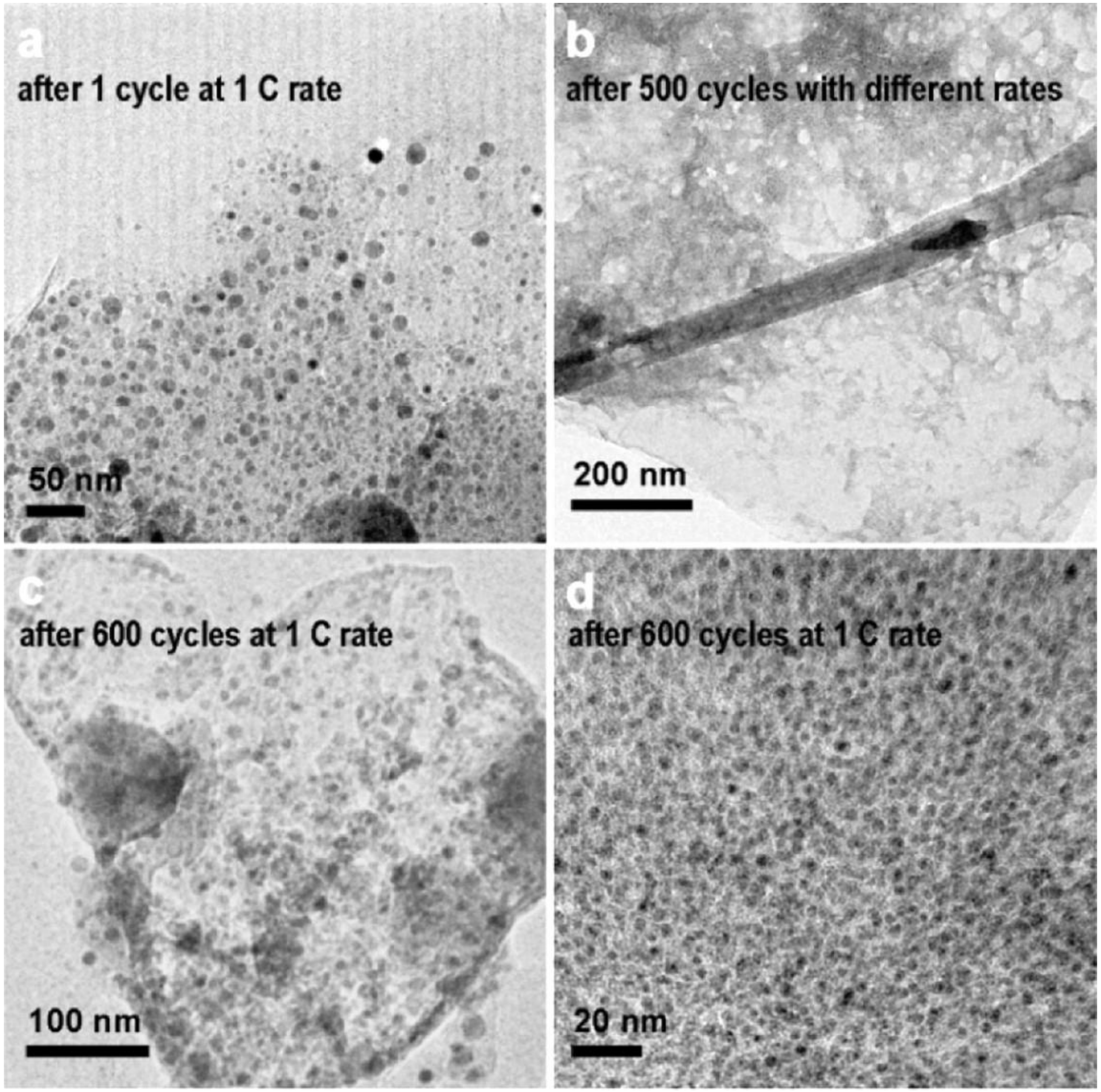

Full cell performance

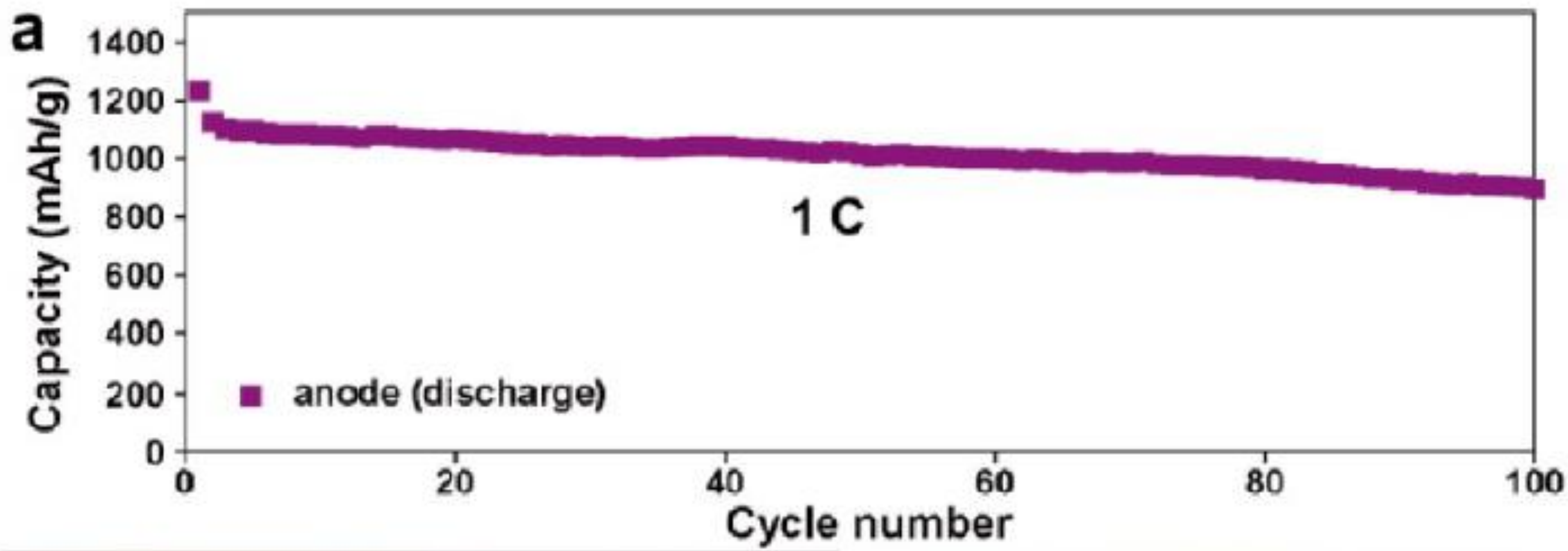

Capacity versus cycle number of a full cell between 2.5 and 4.2 V
Anode: Ge/RGO/C
Cathode: LiCoO2

MoS2 nanoflower sheets as supportive materials for high-capacity anodes

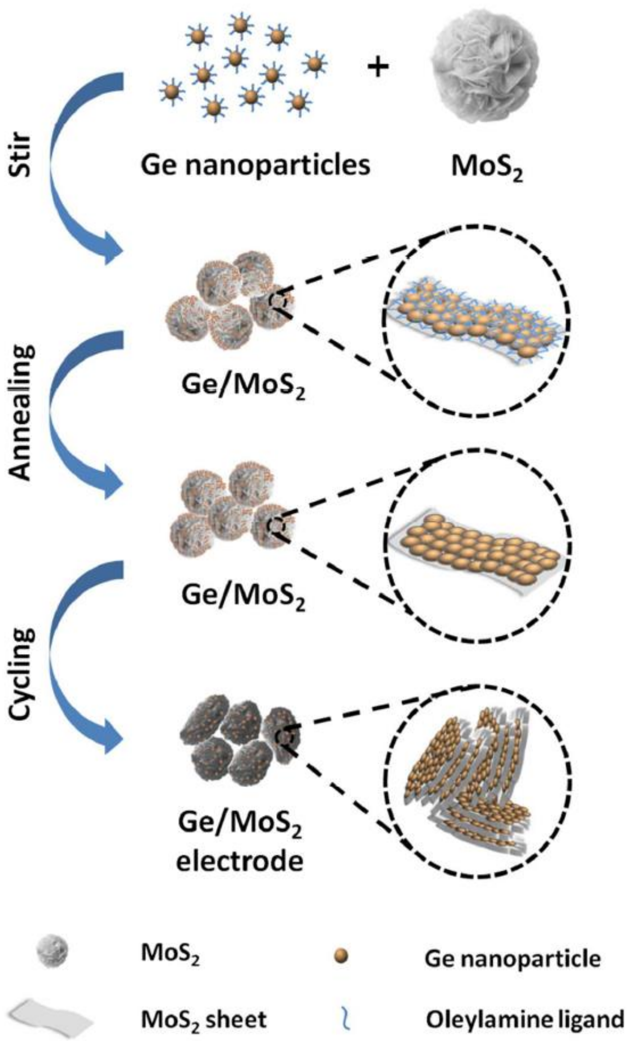

MoS2 nanoflower sheets

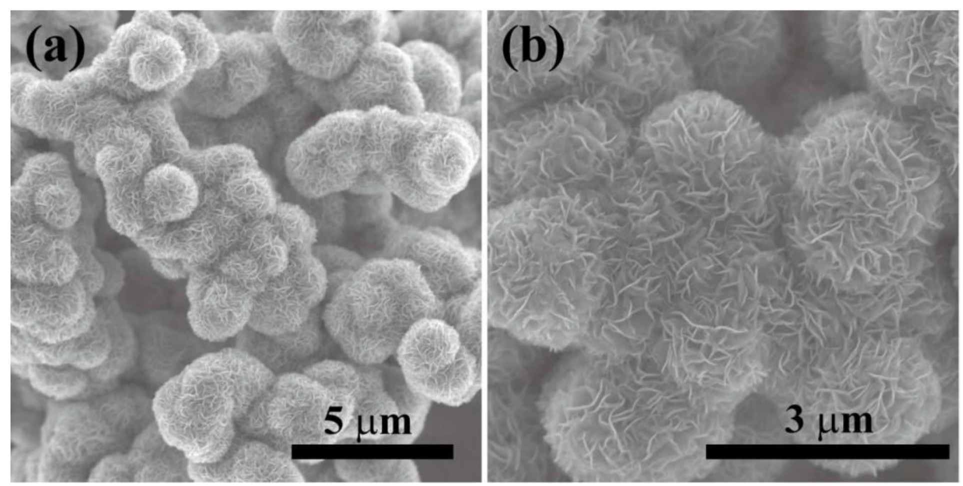

Ge/MoS2 and Ge/MoS2/C nanocomposite

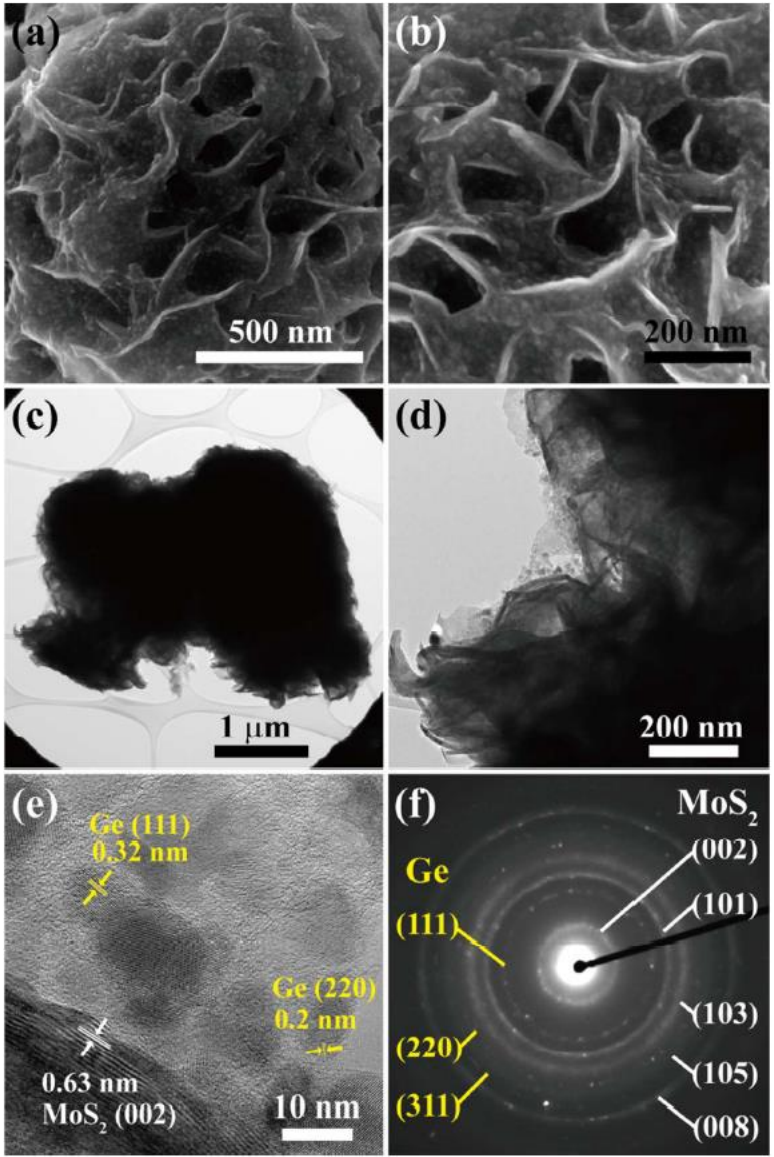

Annealing at 350 °C

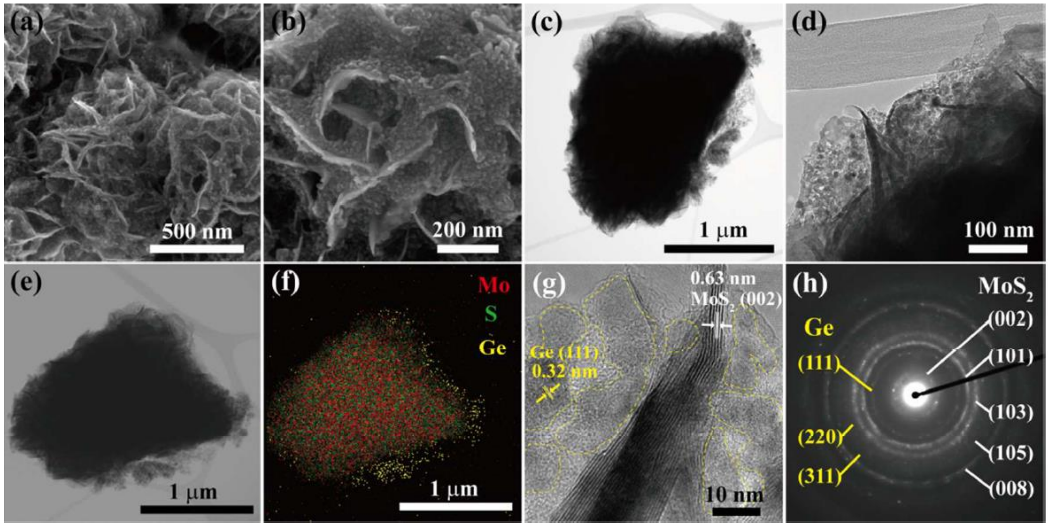

Performance of Ge/MoS2 nanocomposites

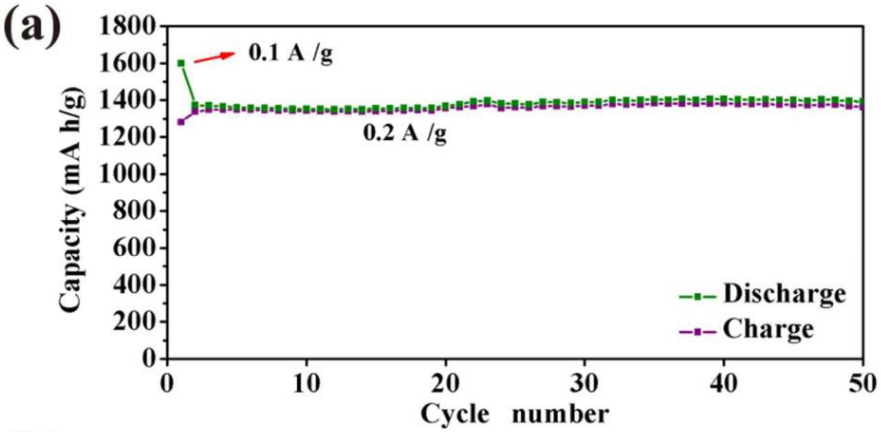

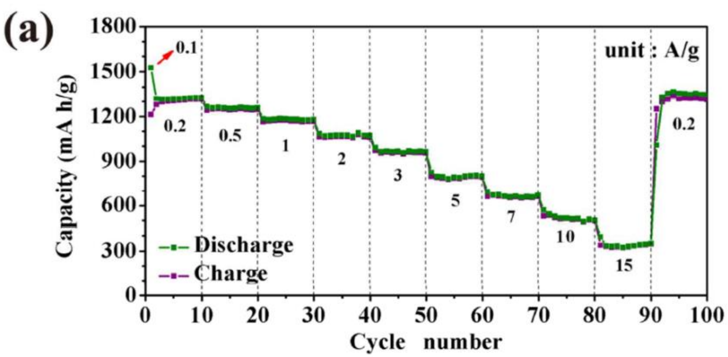

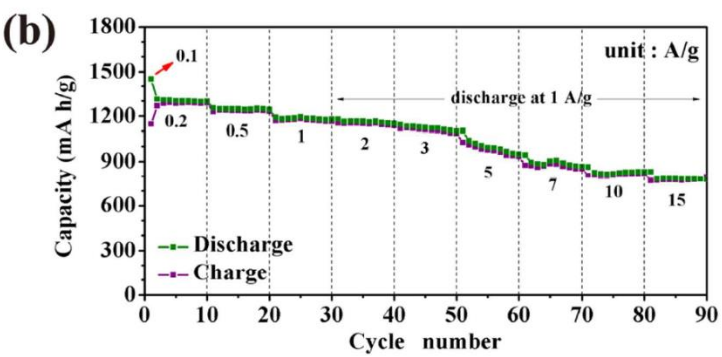

1362 mAh/g: ~98.4% of theoretical capacity of germanium (1384 mAh/g)

Structure evolution of Ge/MoS2 composites after cycling

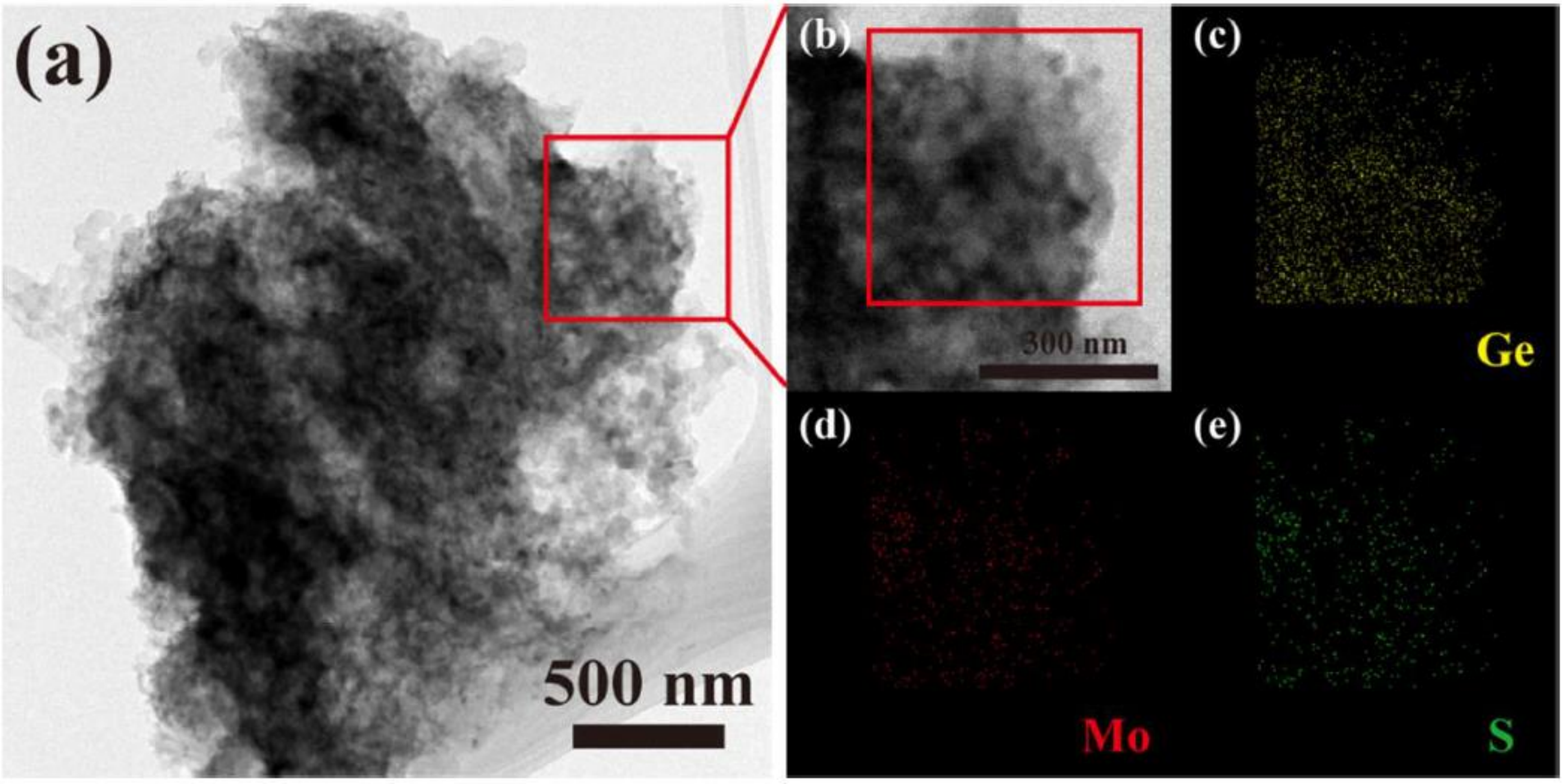

Performance comparison with other work

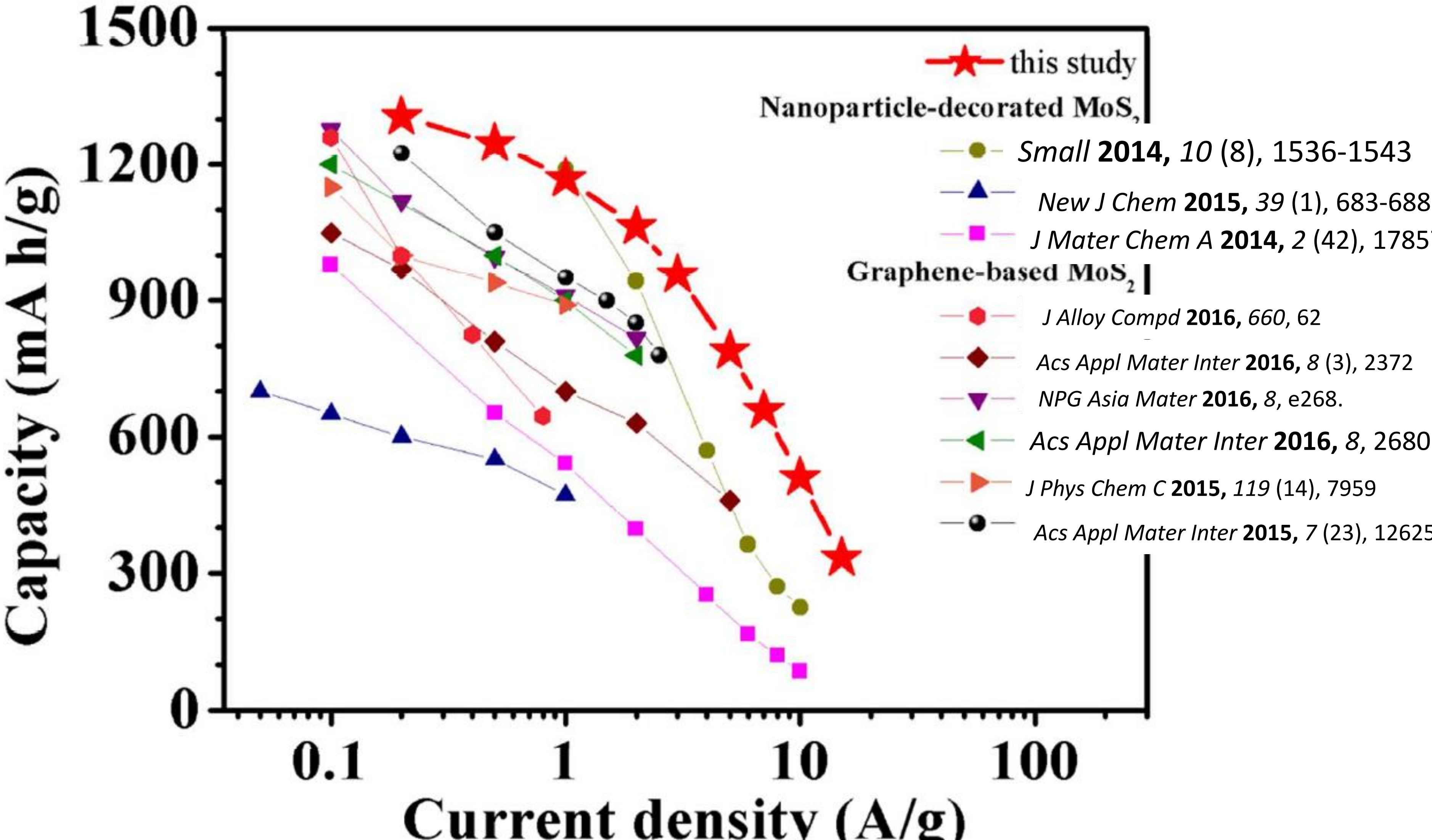

Updated to August, 2016

Full cell with high-areal-volumetric capacity using Ge/MoS2 as anode

3 mA h/Cm2
Areal capacity

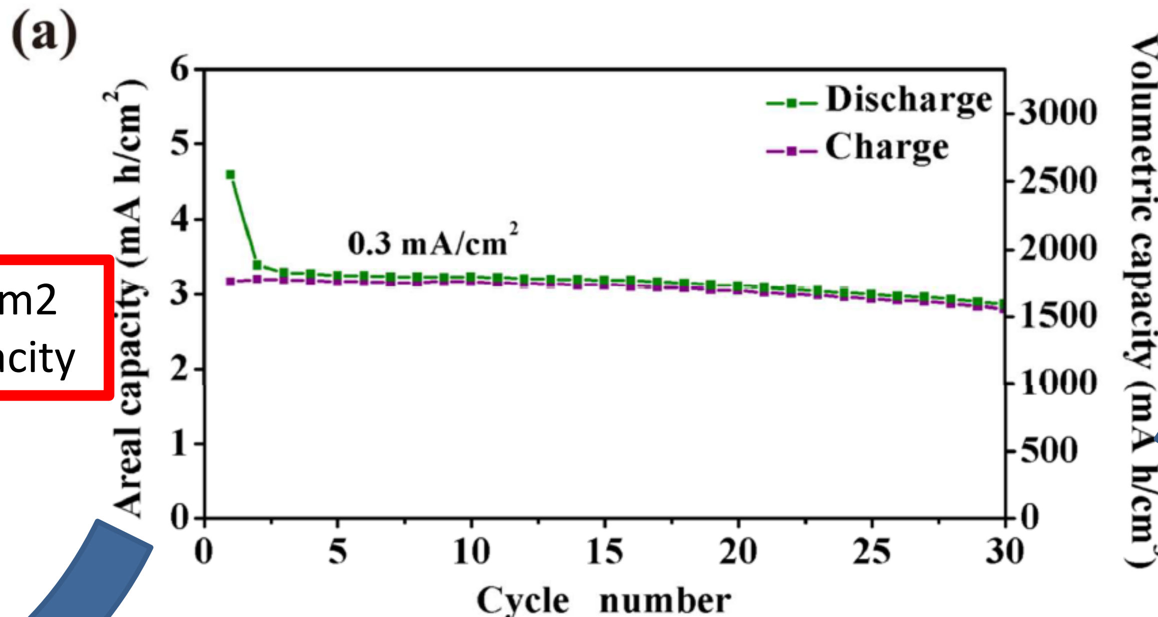

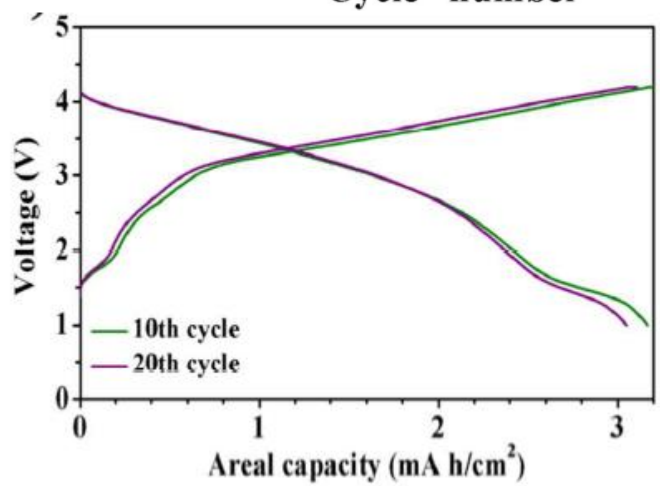

1700 mAh/cm3,
several times higher than the commercial graphite (330-430 mAh/cm3).

GeO2 (Germania) nanoparticles

(a)

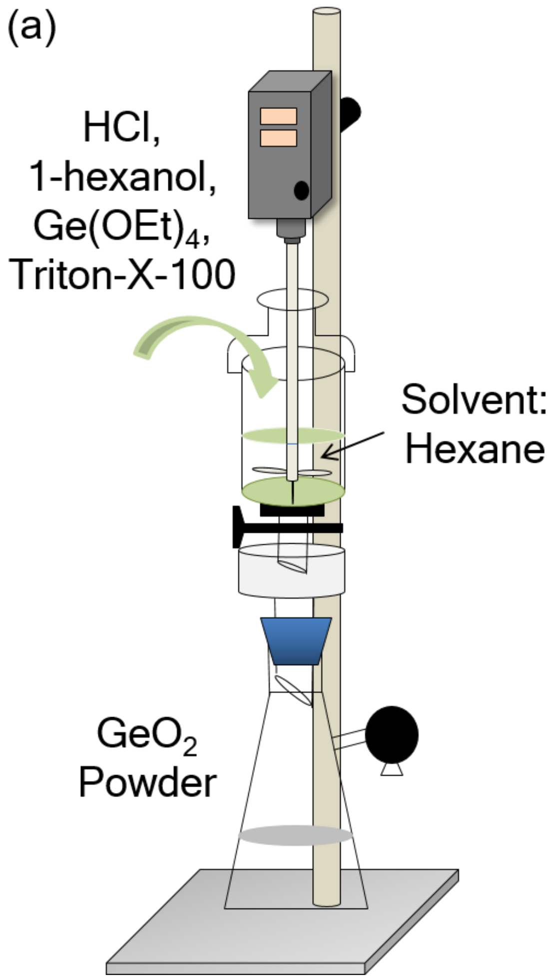

Germania is much less expansive than germanium
Nearly 100 % yield and good crystallinity germanium oxide (GeO_2) nanoparticles
in a reverse micelle system at ambient temperature

Nearly 100% yield, single crystallinity of germania nanoparticles

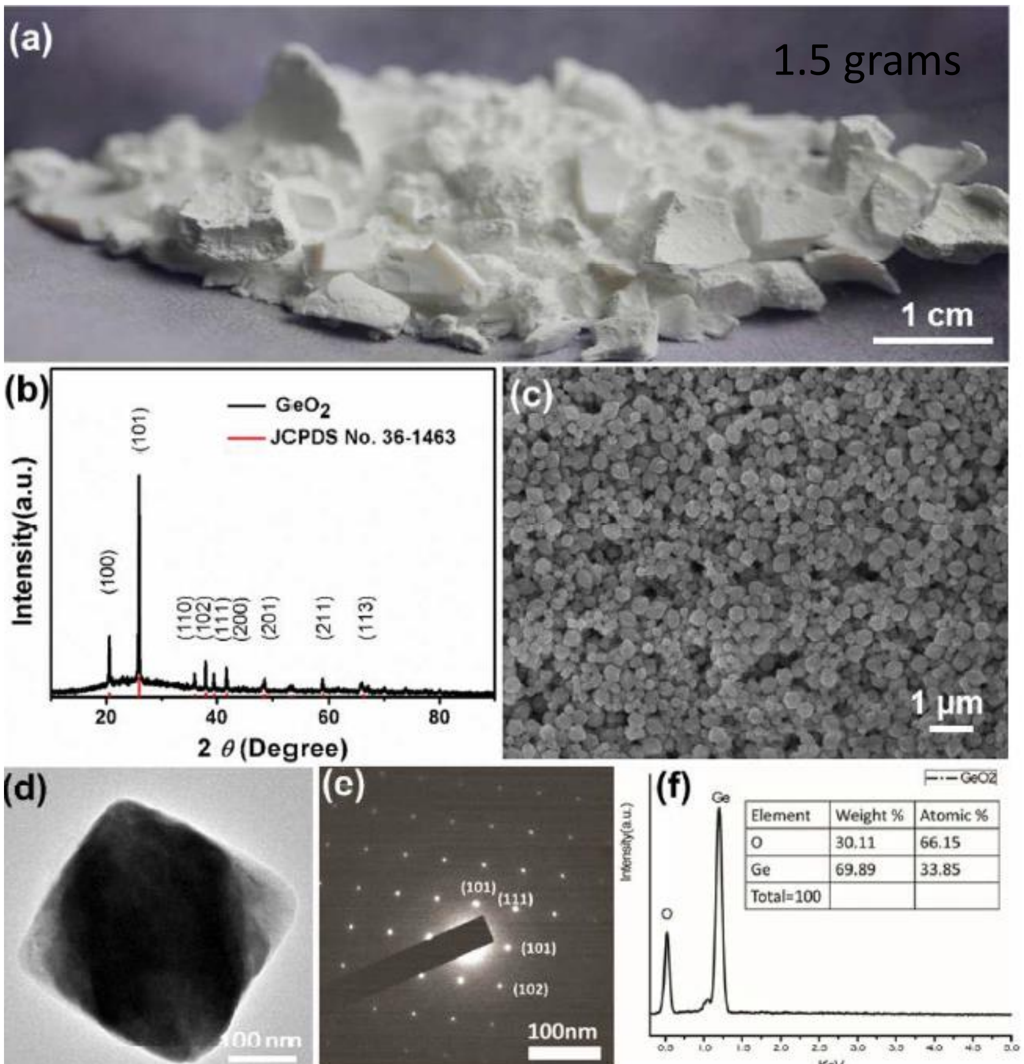

GeO2 anode performance

1100 mAh/g，95.5%
to theoretical capacity
of GeO2 (1100 mAh/g)

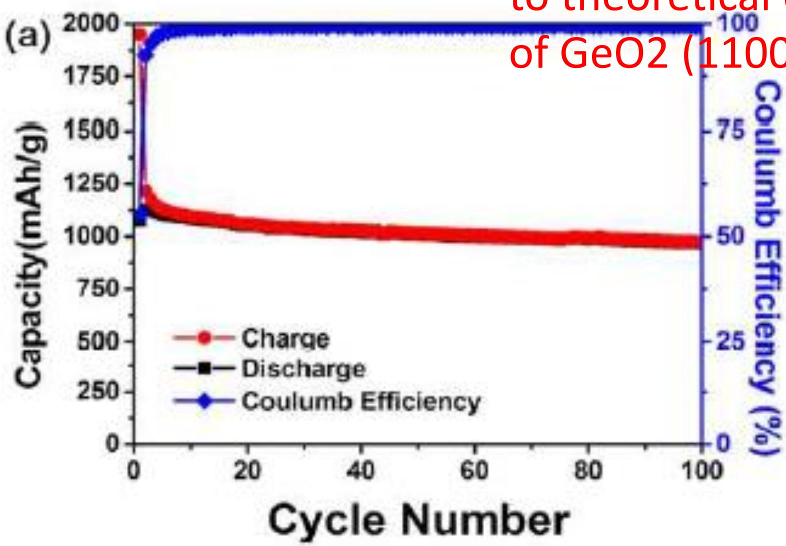

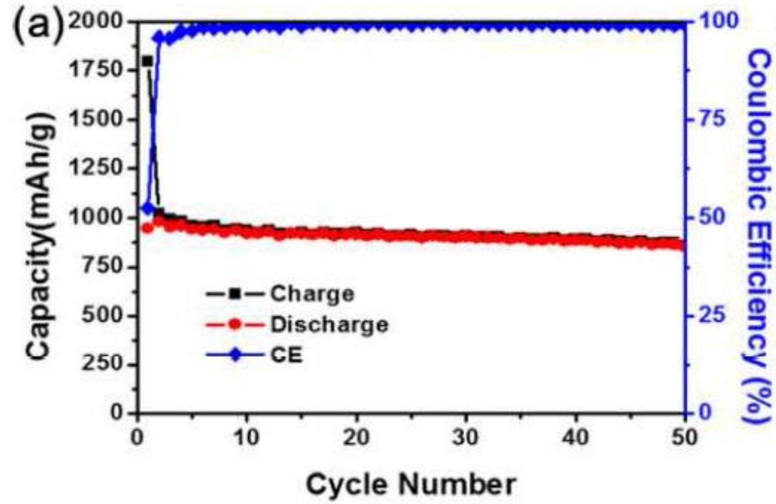

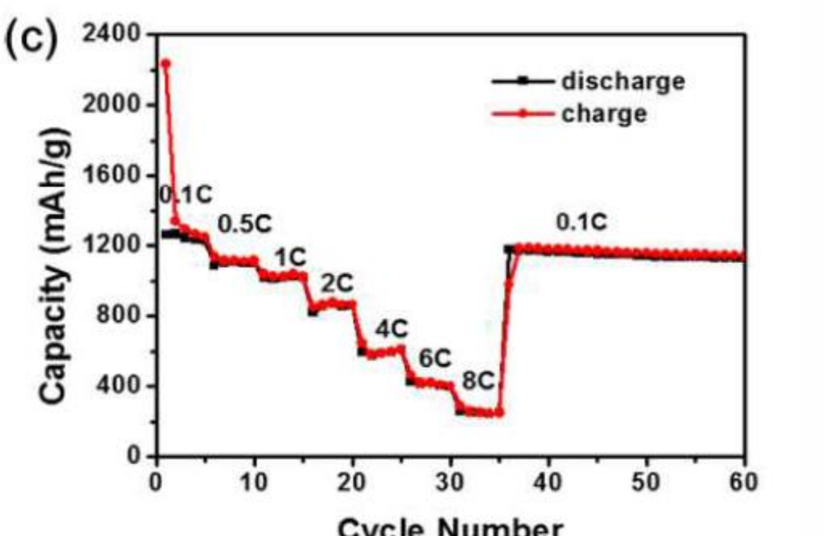

GeO2 → Ge → reversible lithiation process

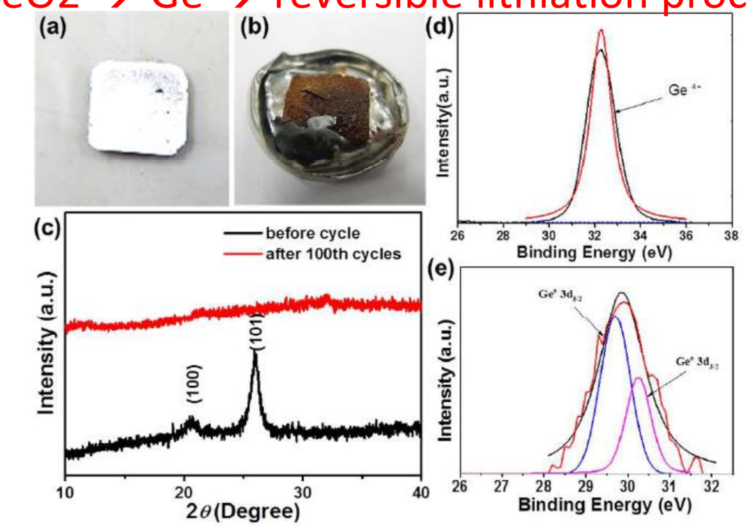

A flexible all inorganic nanowire bilayer mesh as a high-performance lithium-ion battery anode

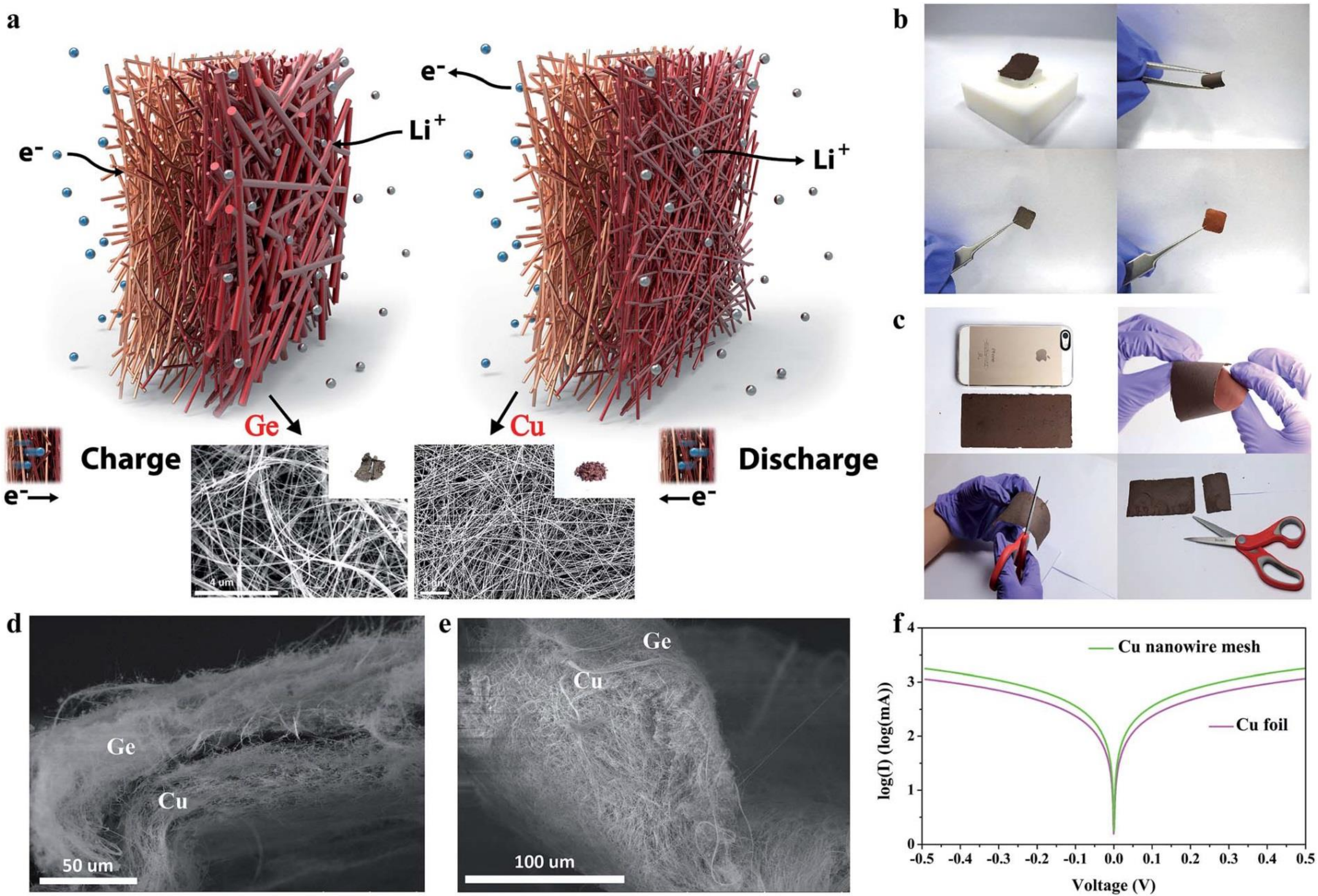

Photographs of the mass of Cu foil and Cu nanowire mesh

a

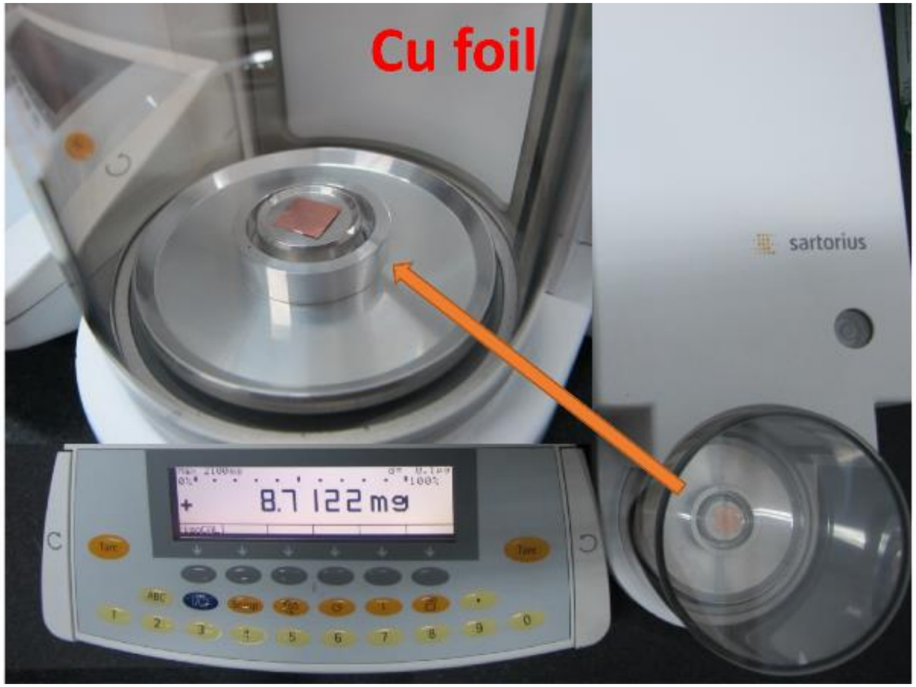

b

Cu nanowire mesh is only 16% of weight compared to Cu foil

Cycling performance of Ge/Cu nanowire fabric

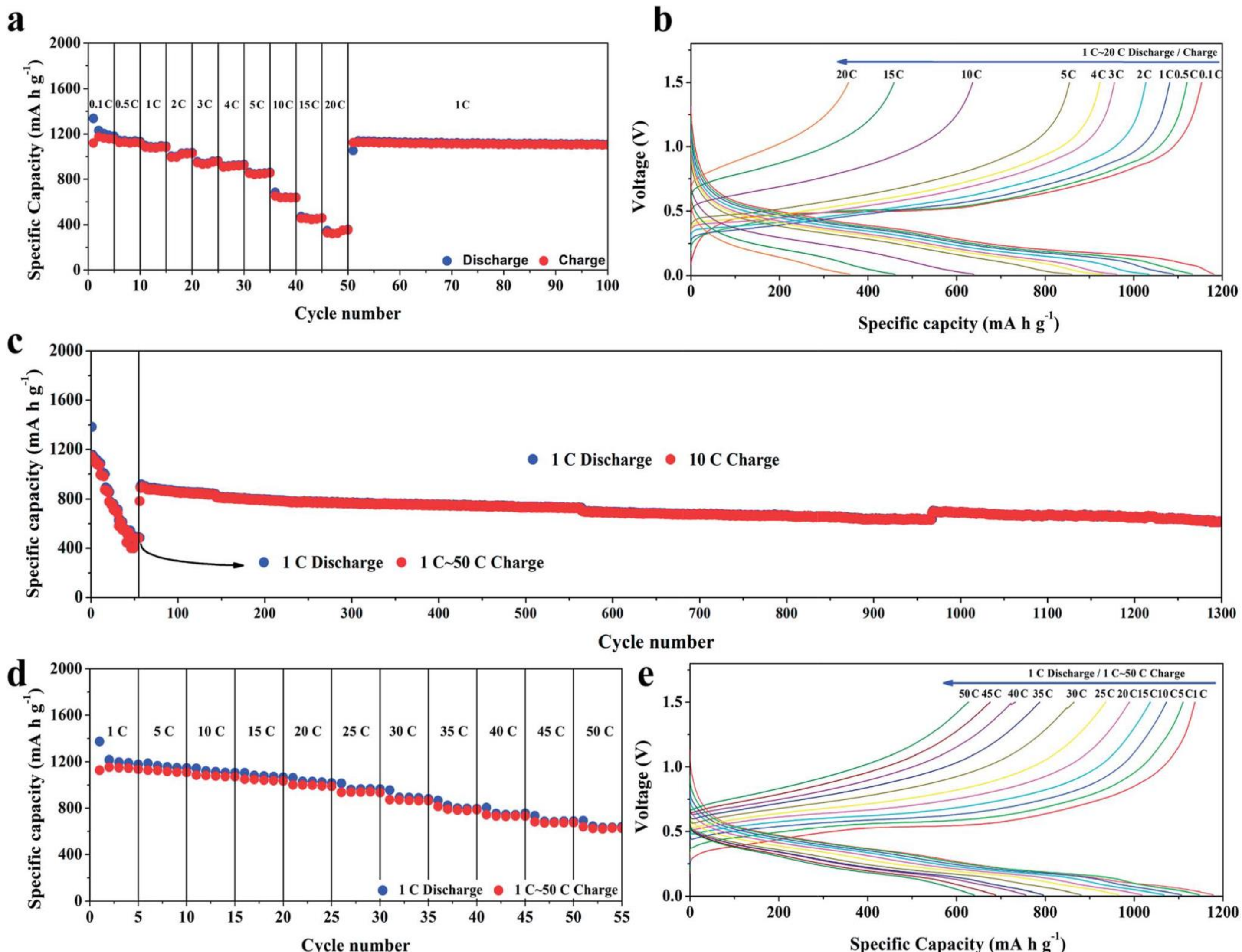

Ge/Cu Nanowire fabric after cycling

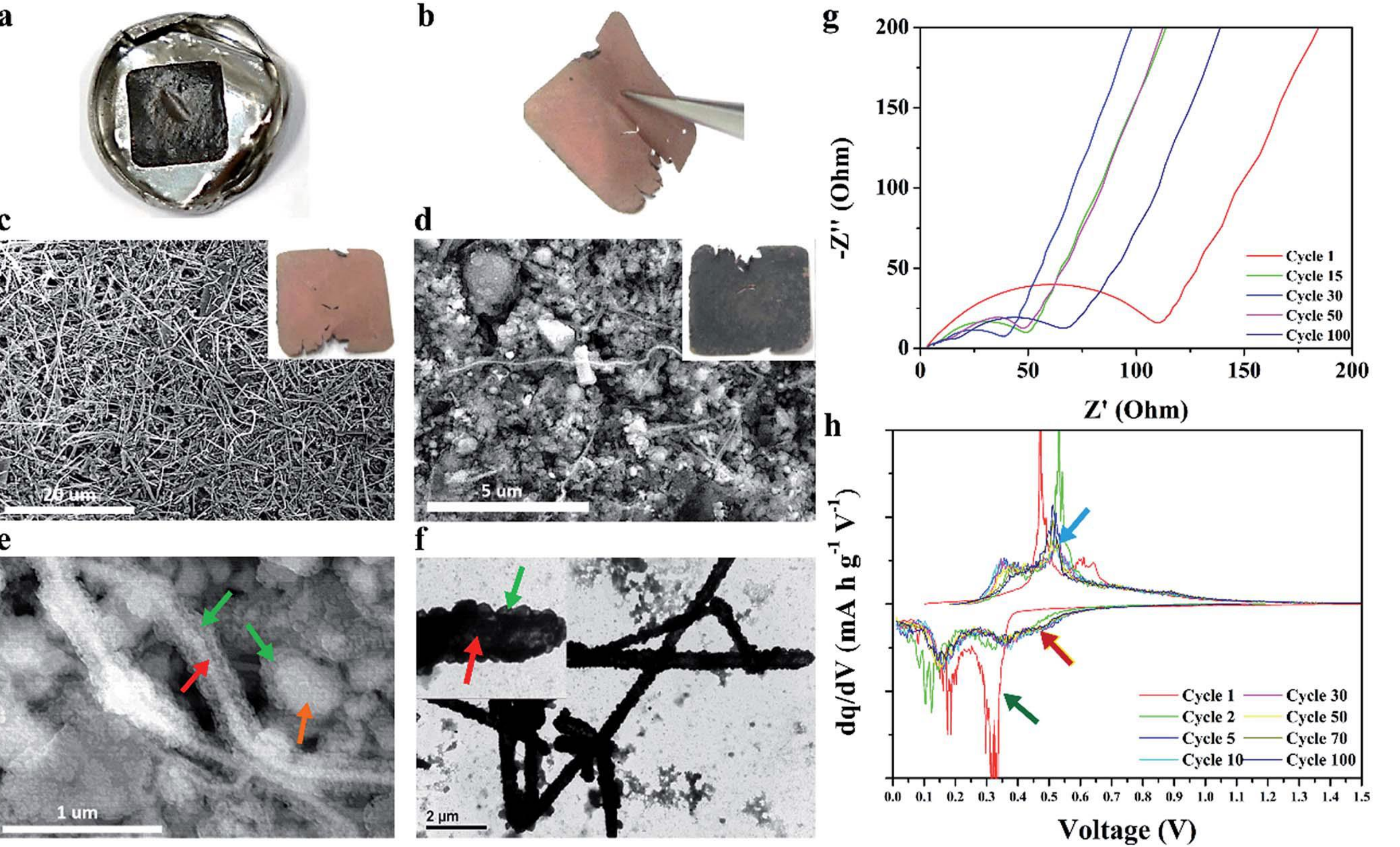

Half-cell test at high loadings of active materials

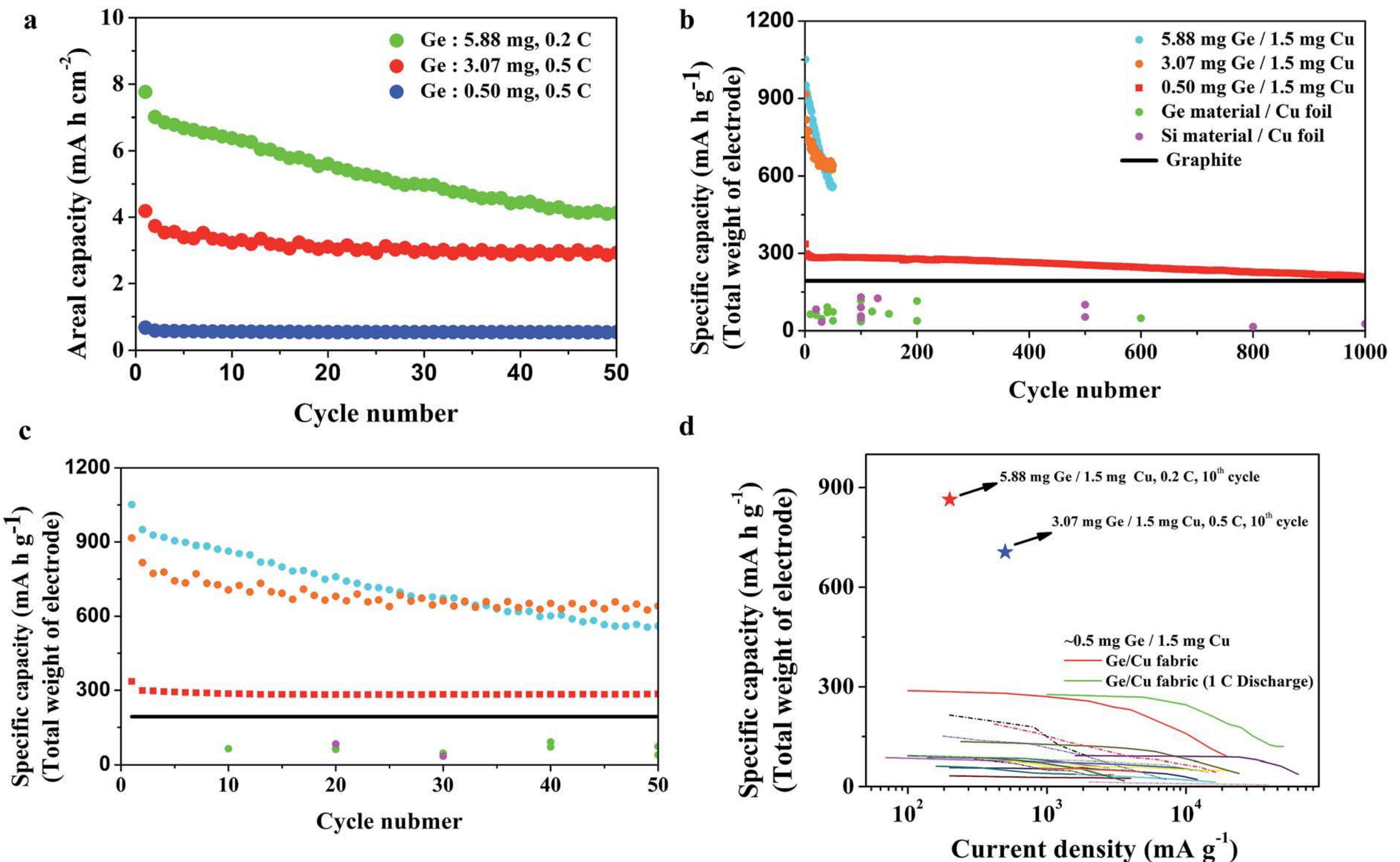

Theoretical Volumetric capacities and full cell demonstration

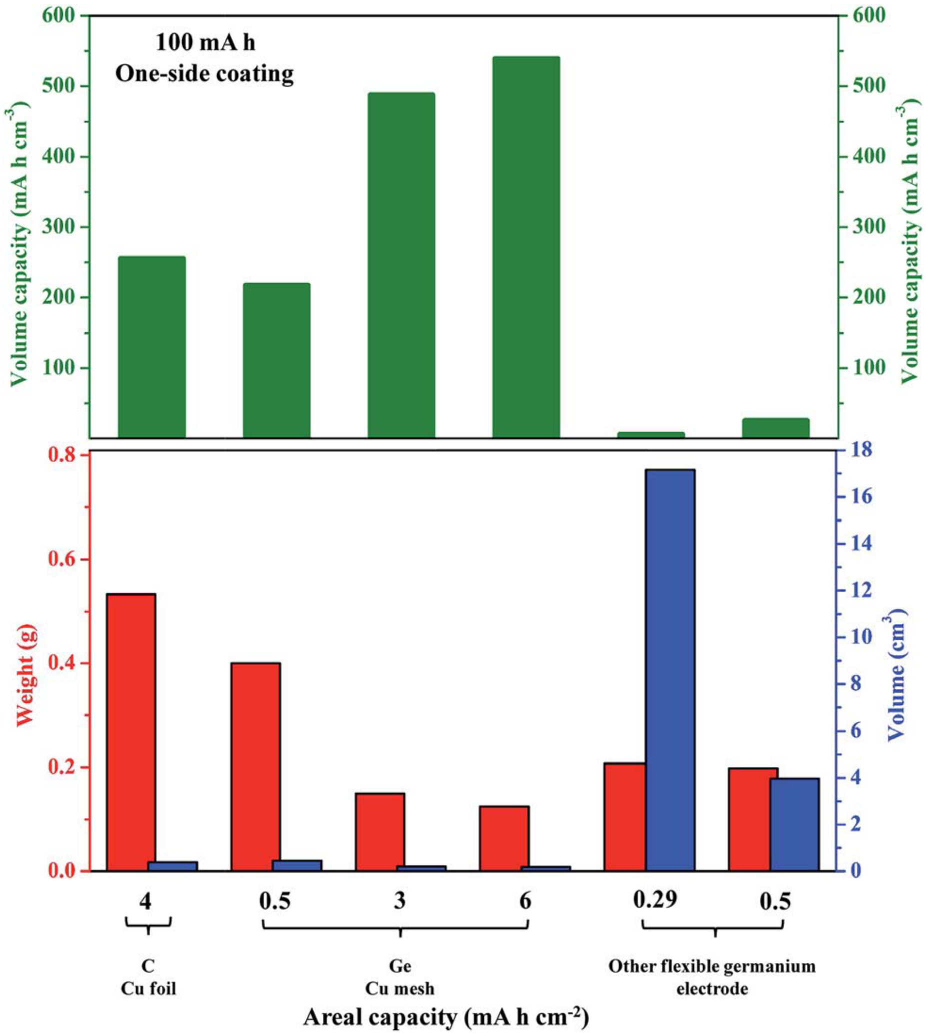

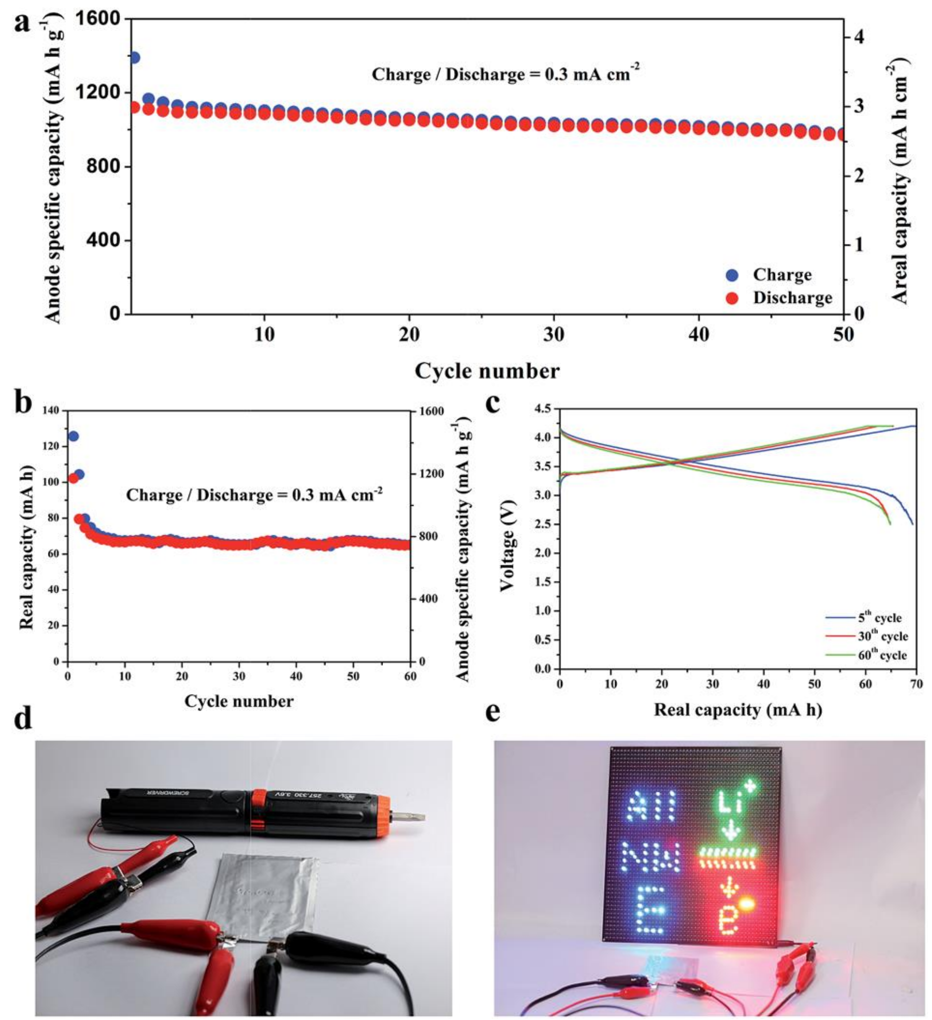

High-performance lithium-ion batteries with 1.5 mm thin copper nanowire foil as a current collector

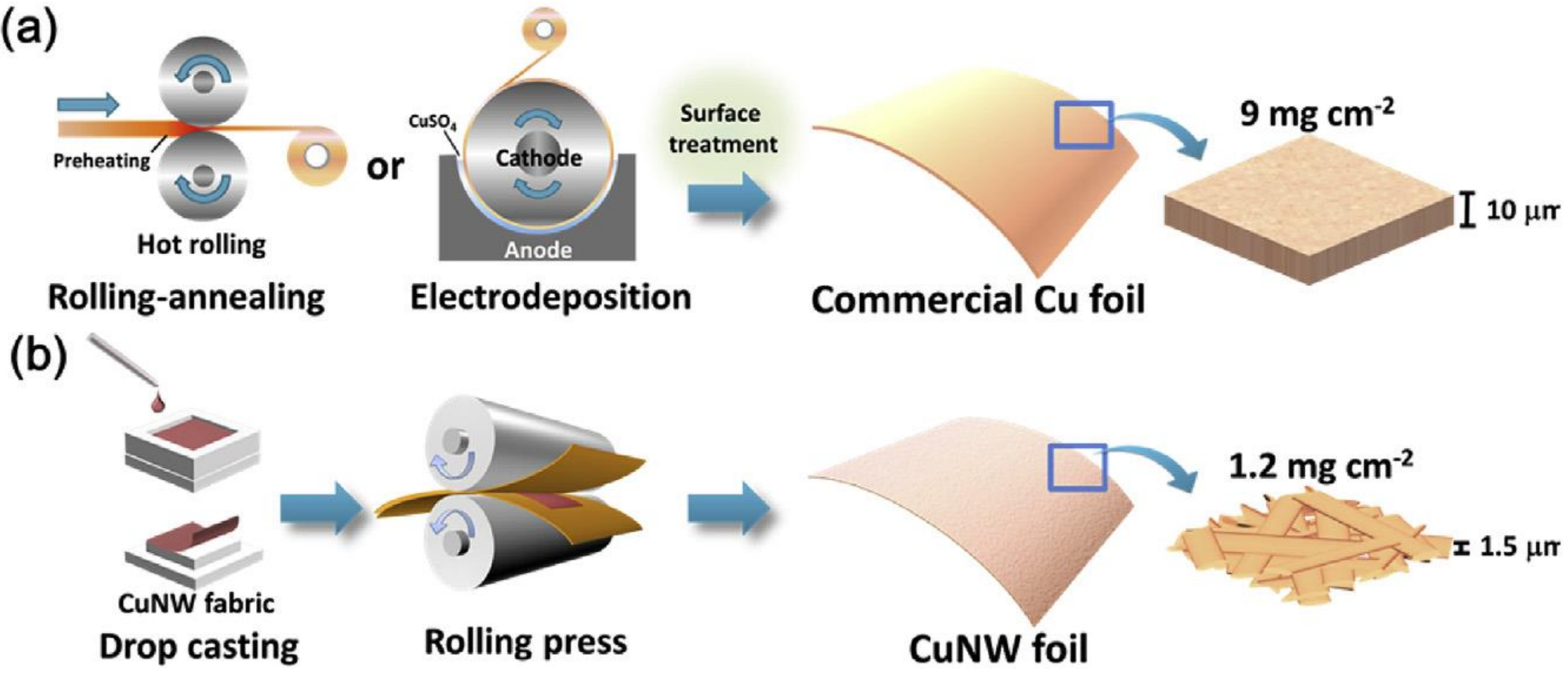

Schematic of the process of (a) conventional Cu foil fabrication process using rolling-annealing or electrodeposition methods and (b) CuNW foil fabrication process using a rolling press method.

Cu NW fabric with tunable thickness

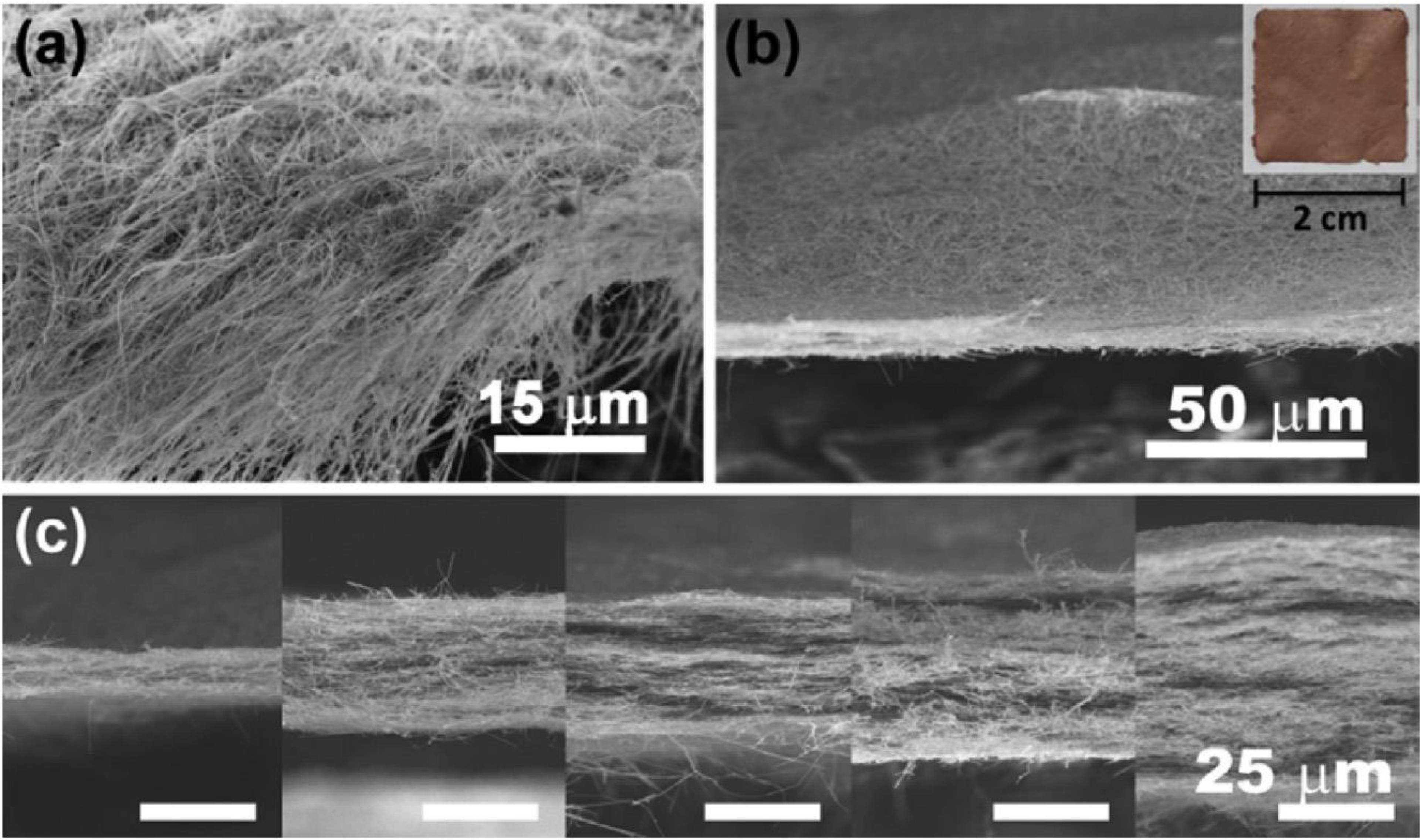

Cu NW foil and their density

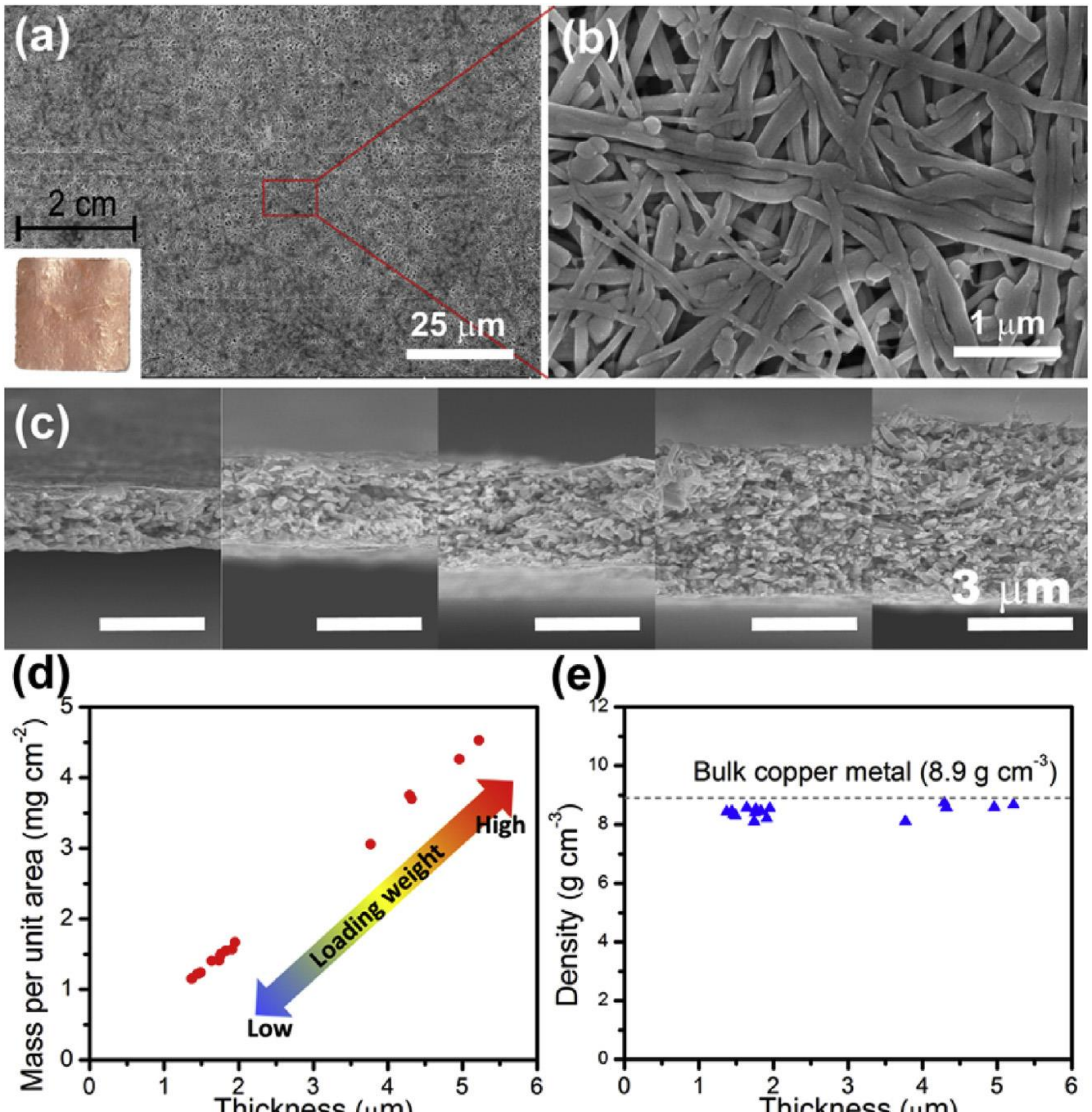

Cu nanowire foil for LIB current collector

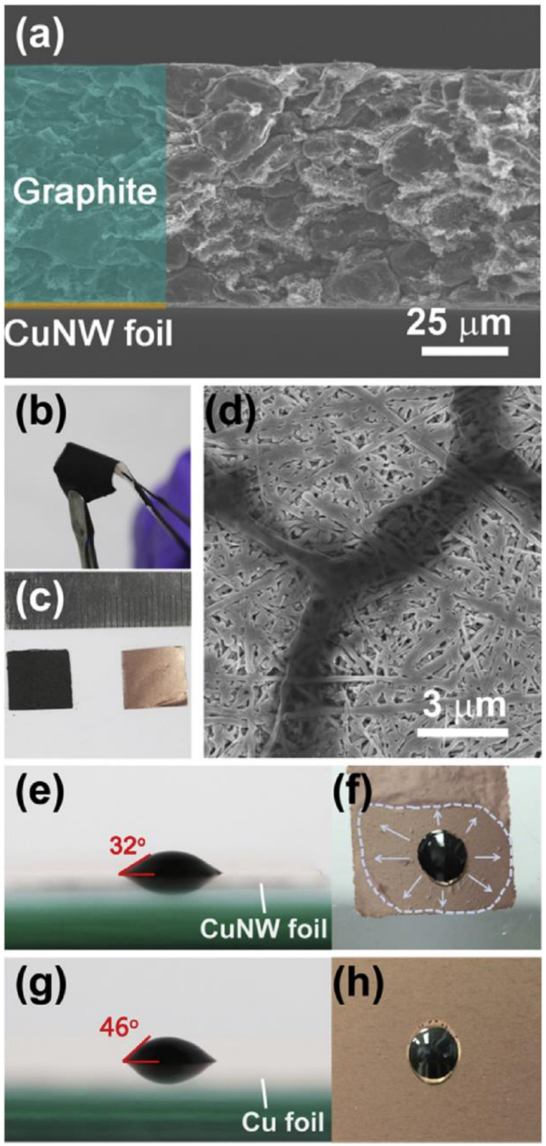

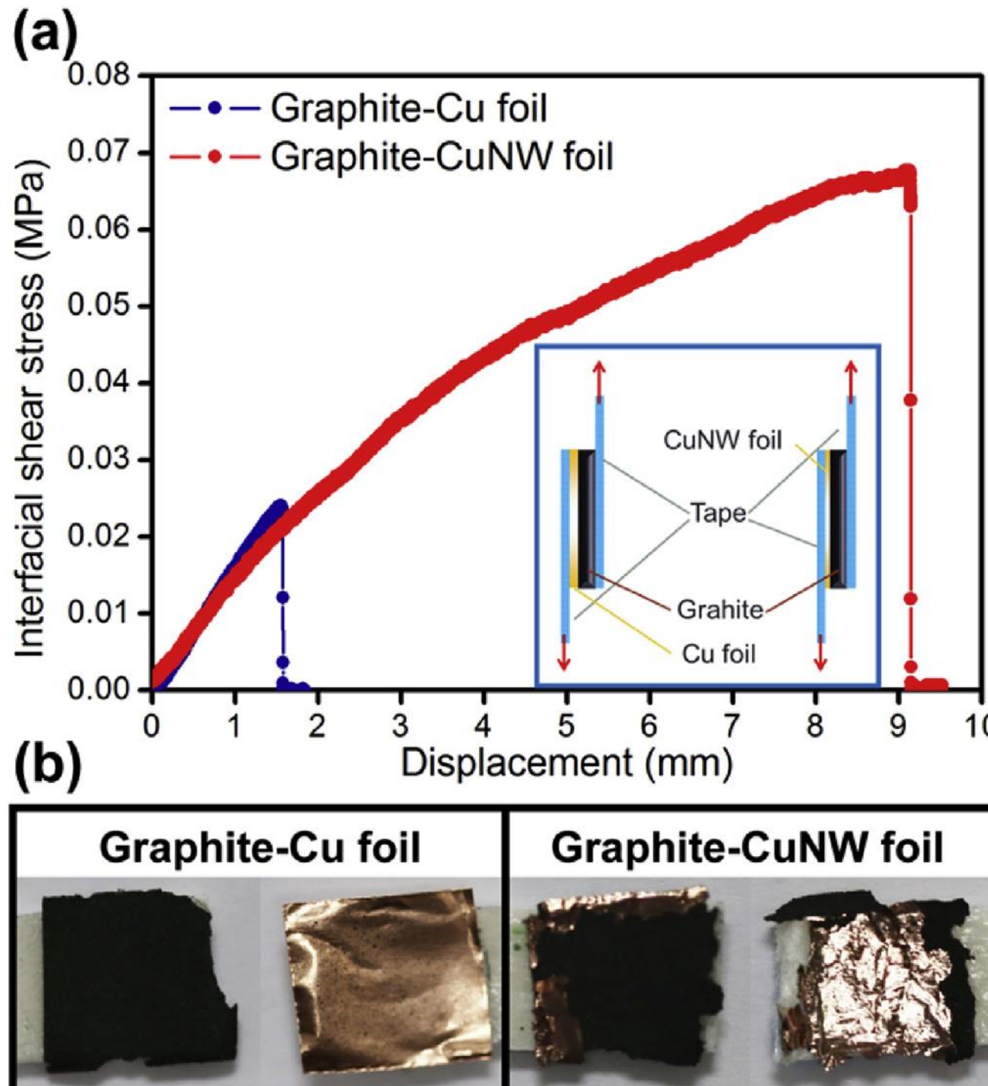

Cycling performance of graphite-CuNW foil

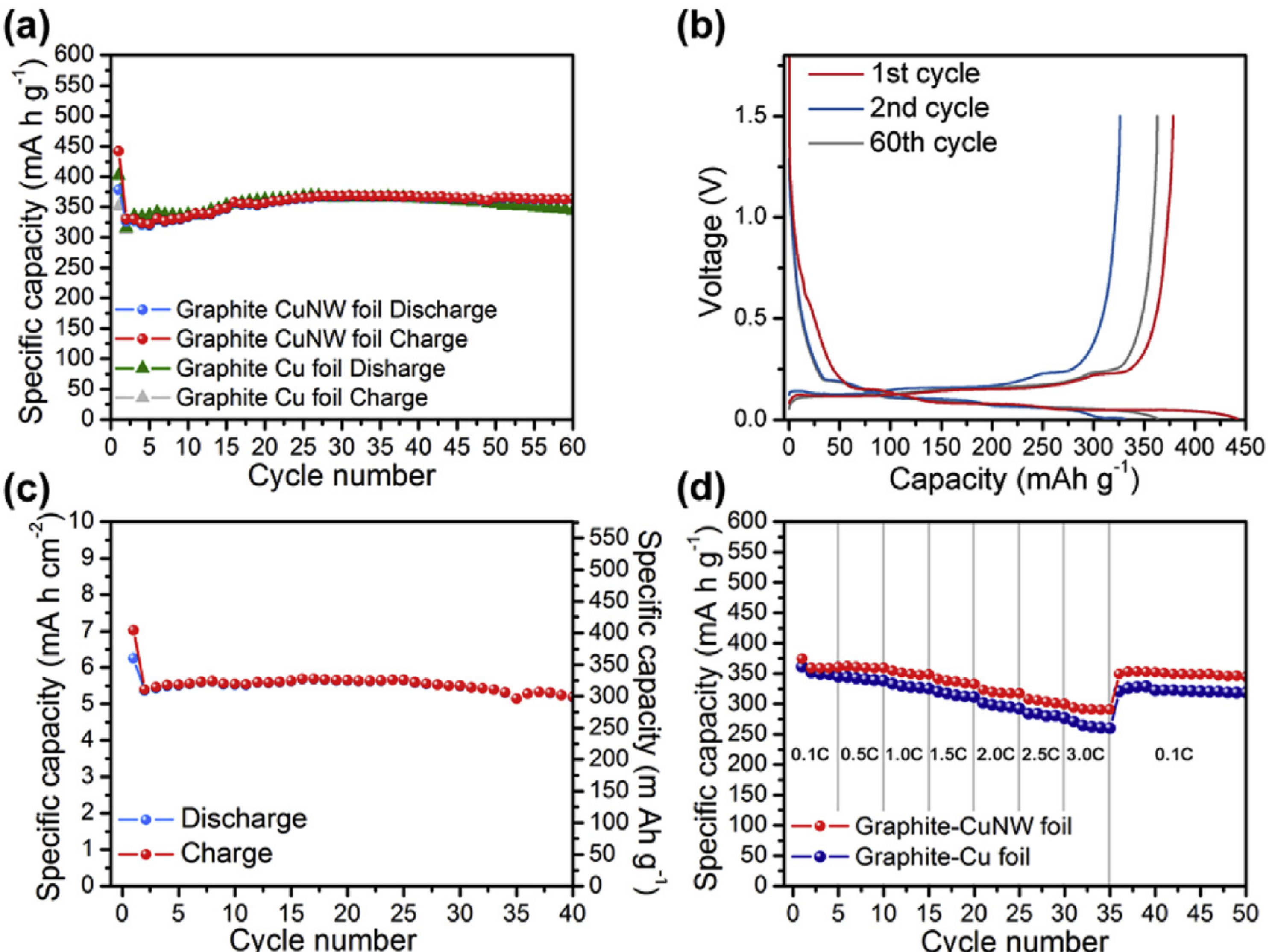

Full cell performance of graphite-CuNW foil

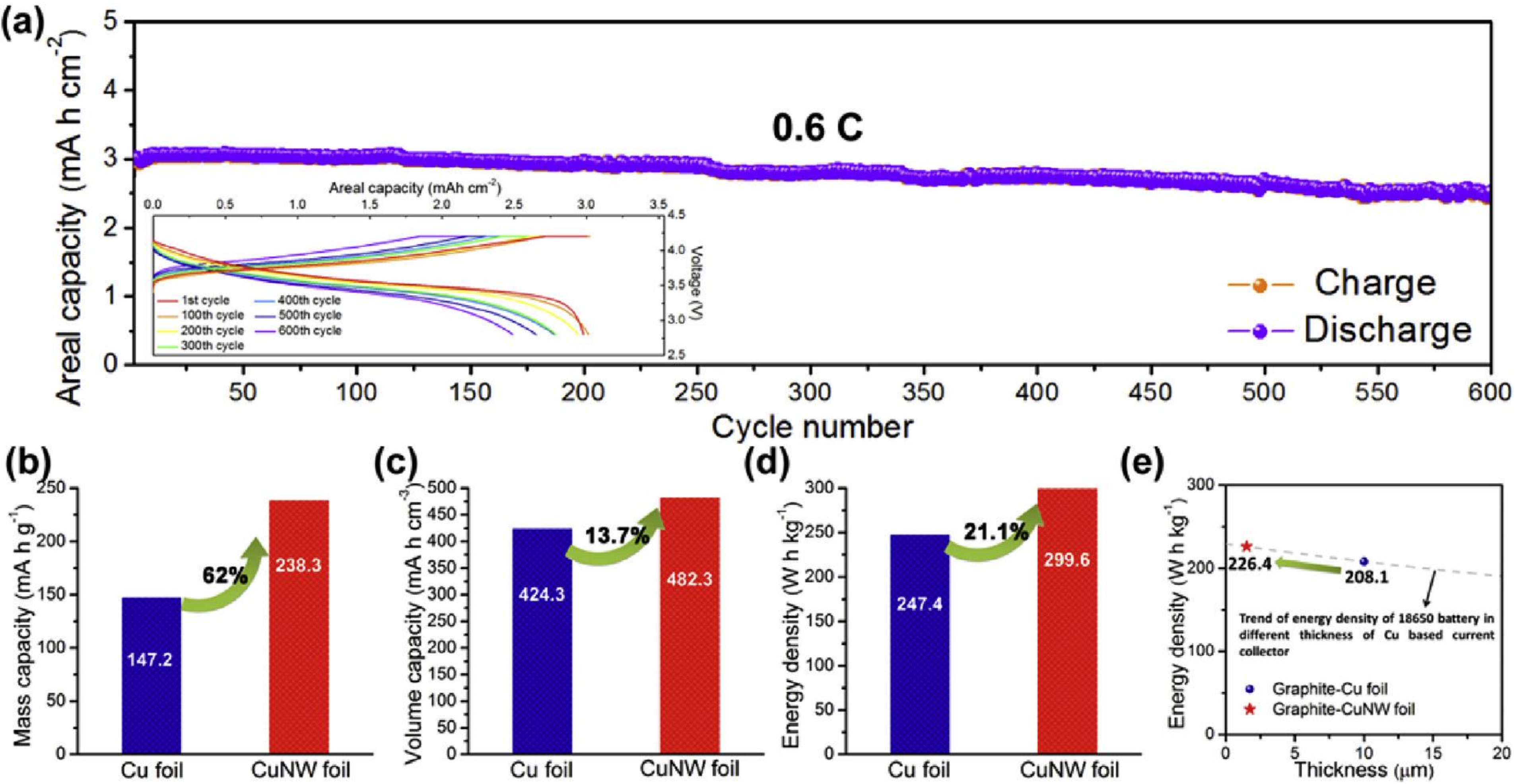

Pouch type full cells using graphite-CuNW foil anodes

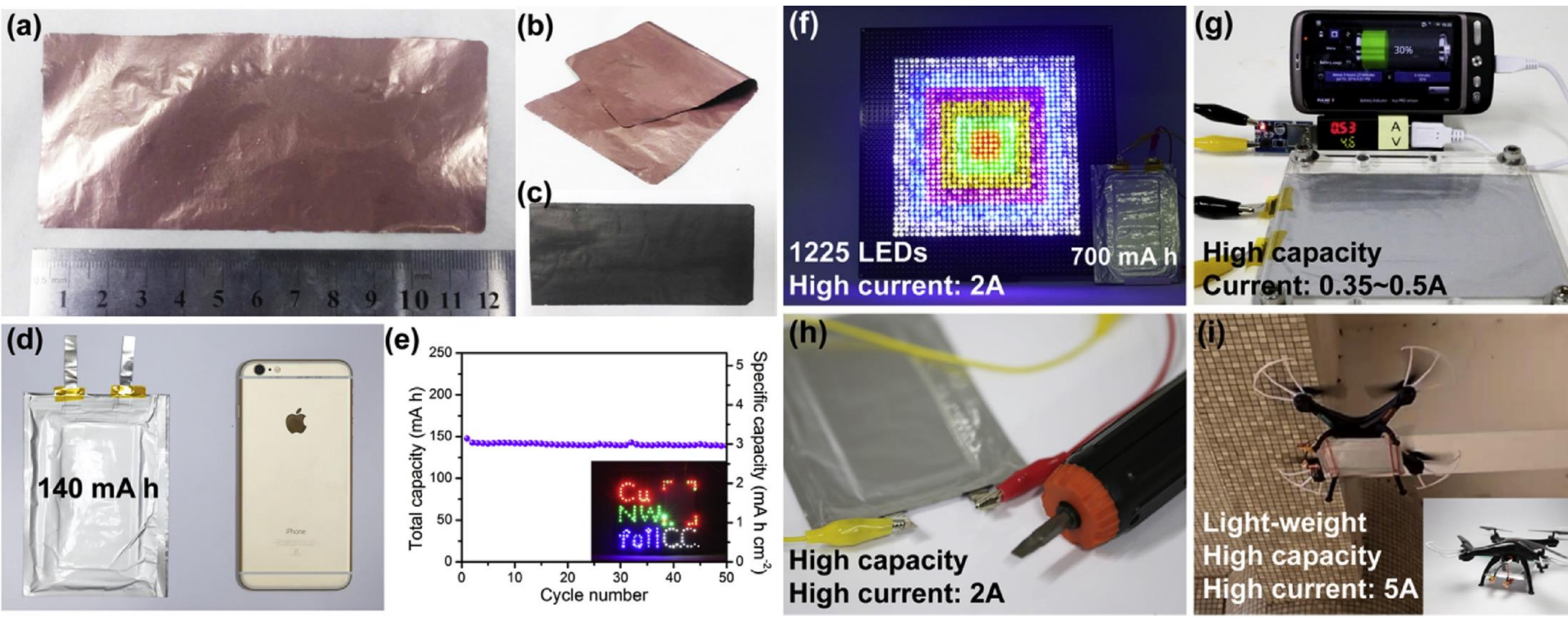

Metal phosphide as anodes for LIB

(a)

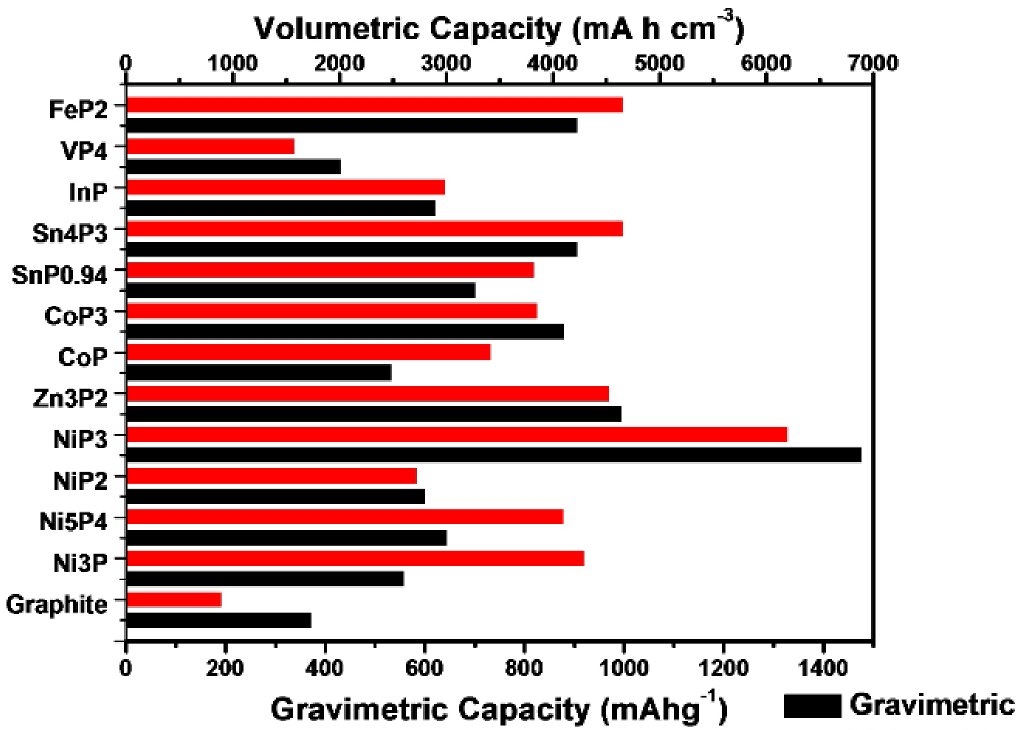

Lithium-ion Battery

Metal phosphide：

- ☐ High gravimetric capacities
- ☐ High volumetric capacities
- ☐ Smaller volume expansion
- ☐ Low polarization
- ☐ Avoid lithium plating during fast charging.

P: 2596 mA h g^{-1}

- Poor conductivity
- large volume expansion

Goal: Synthesis of CuP_2 Nanowires and applied on Lithium ion Batteries

CuP_2 nanowires seeded by Bi nanoparticles

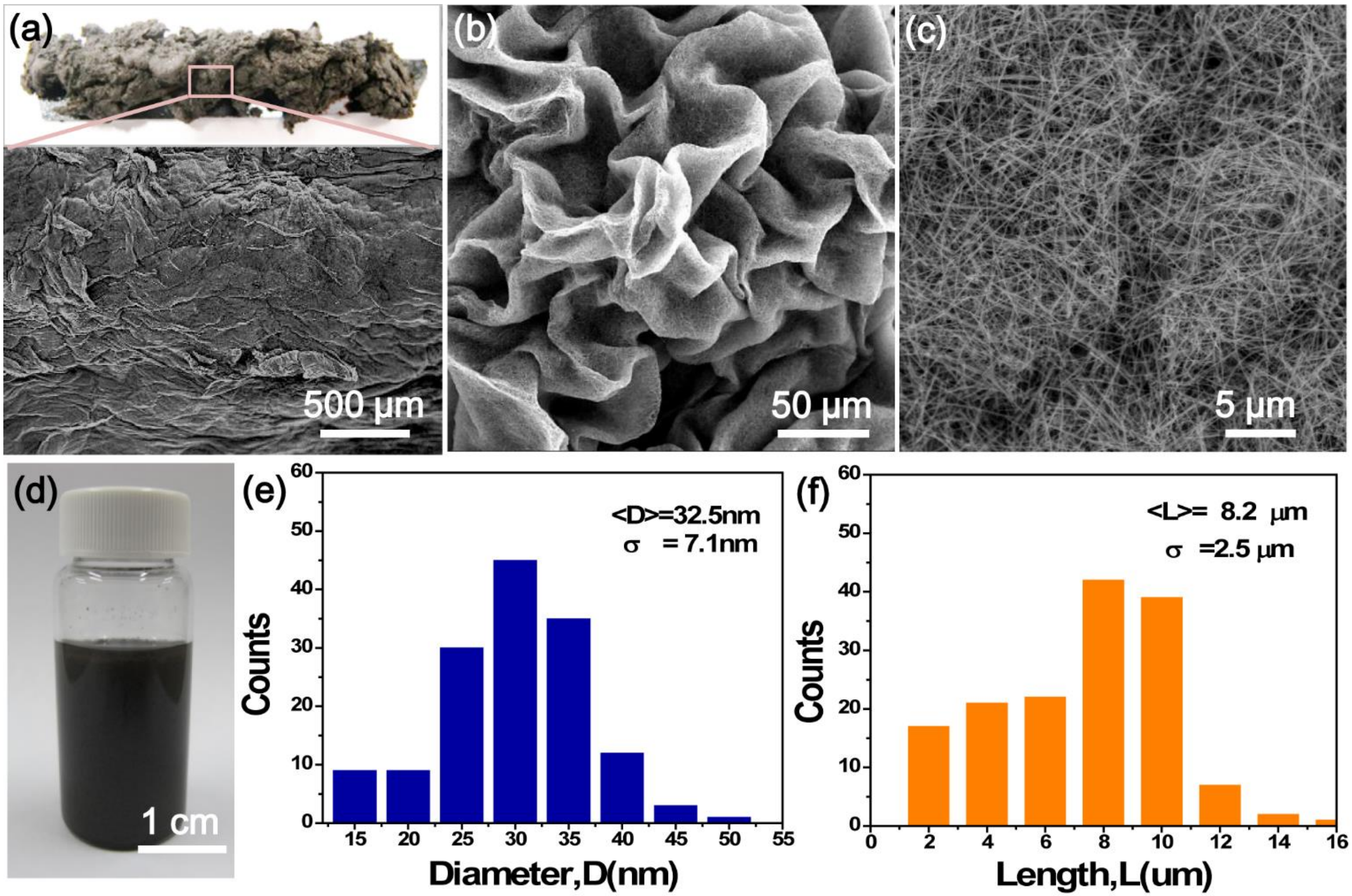

CuP₂ nanowires seeded by Bi nanoparticles

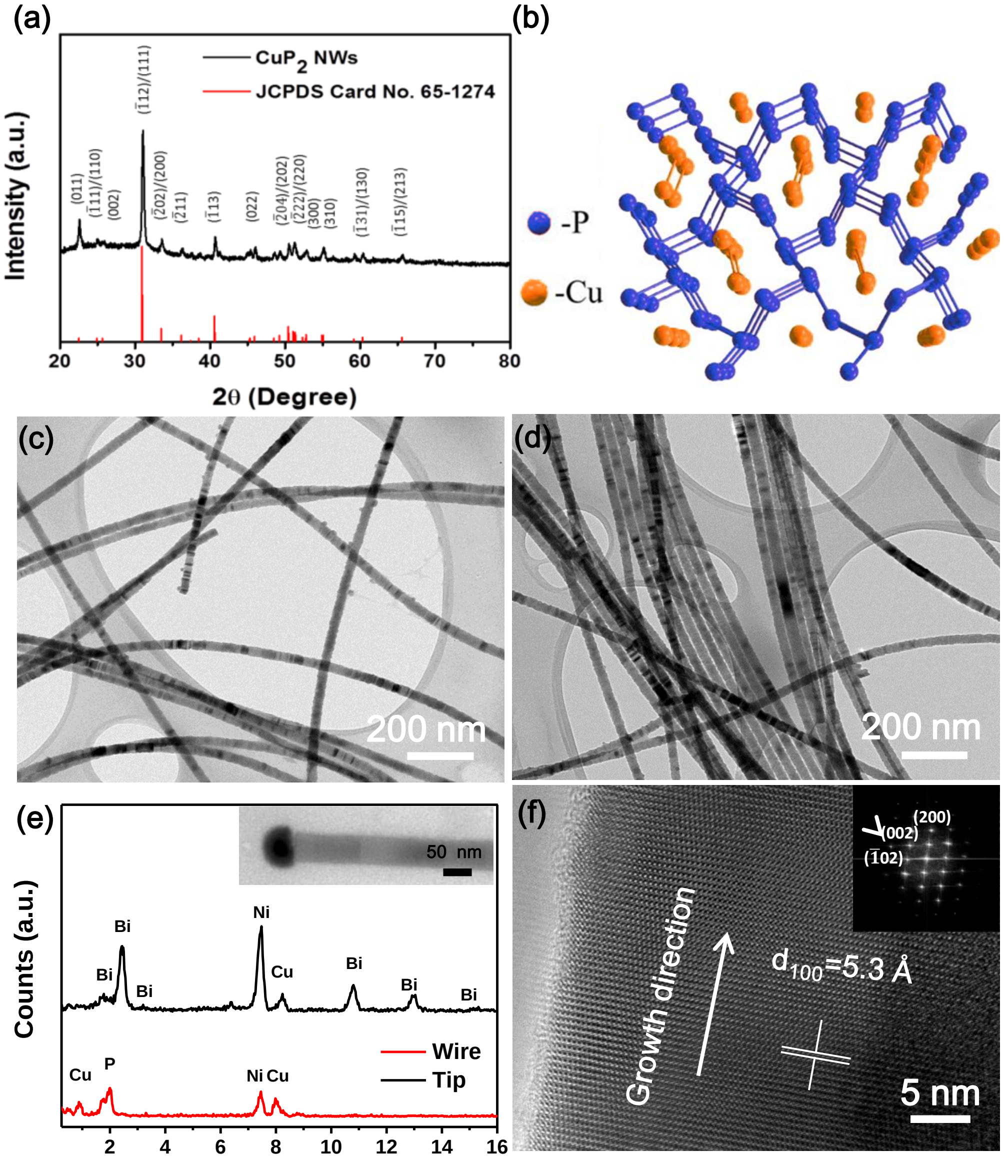

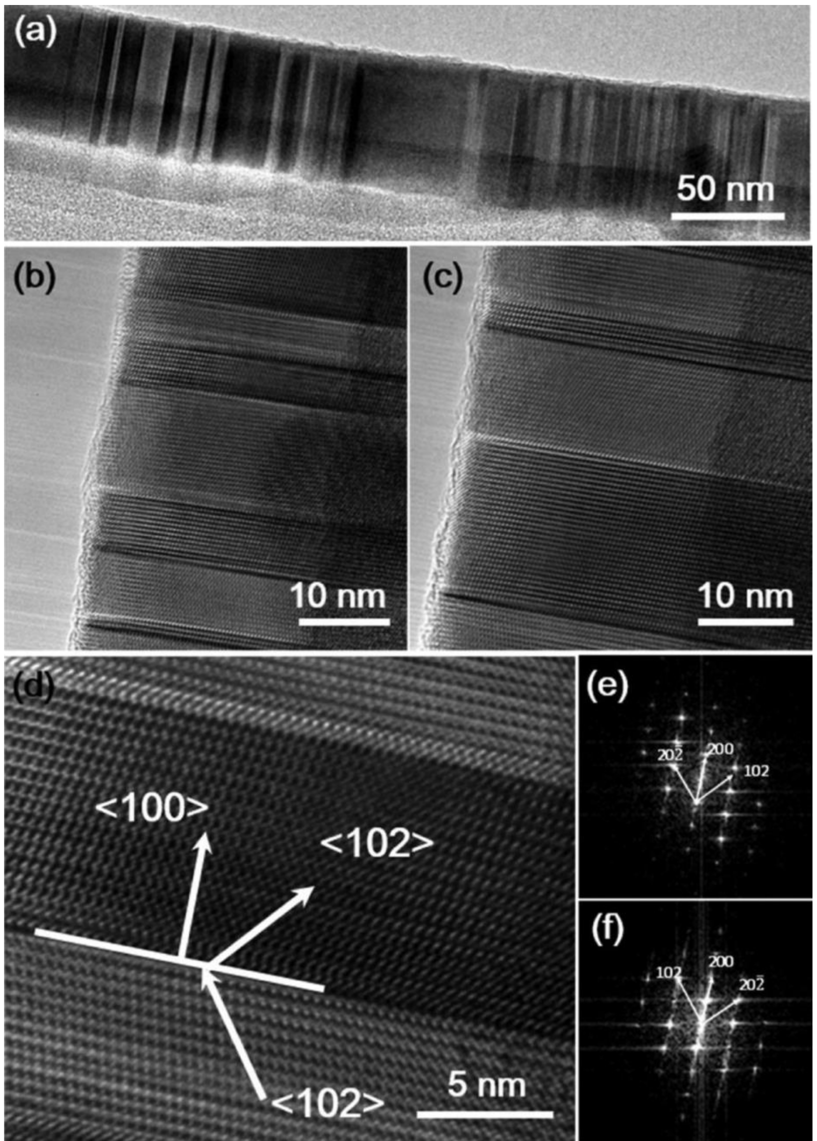

CuP_2 anode performance

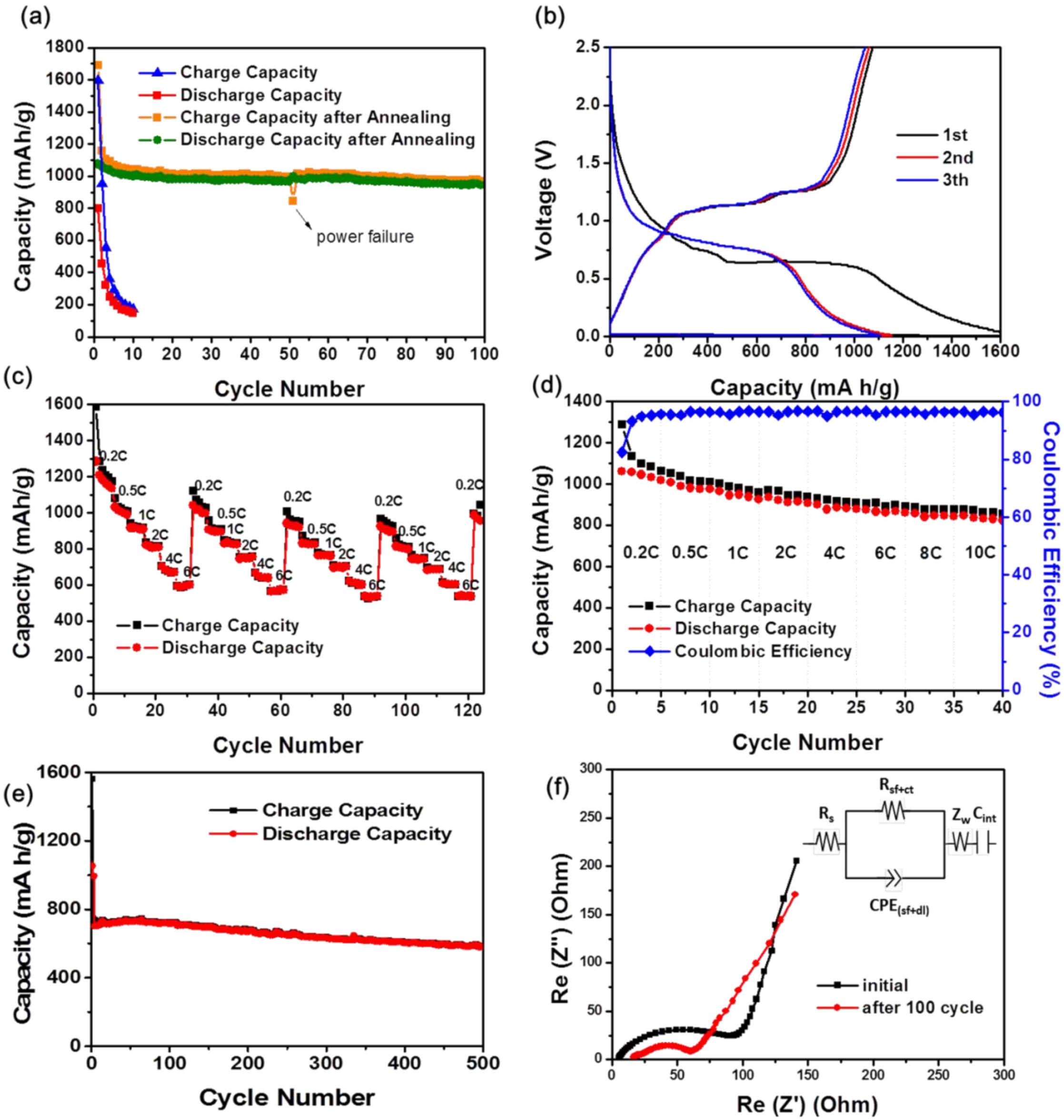

Full cell performance

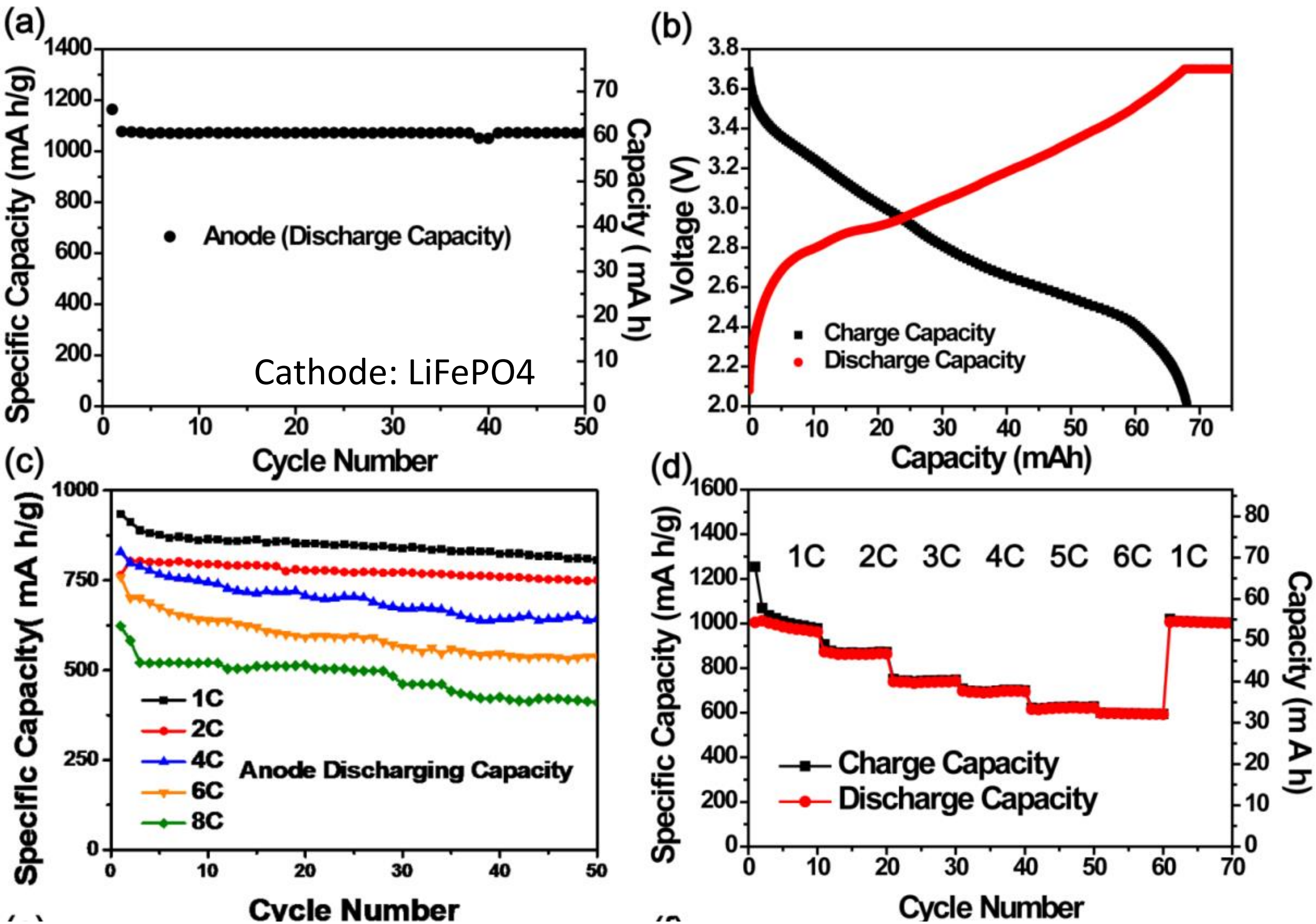

Red phosphorus Nanoparticles (RPNPs)

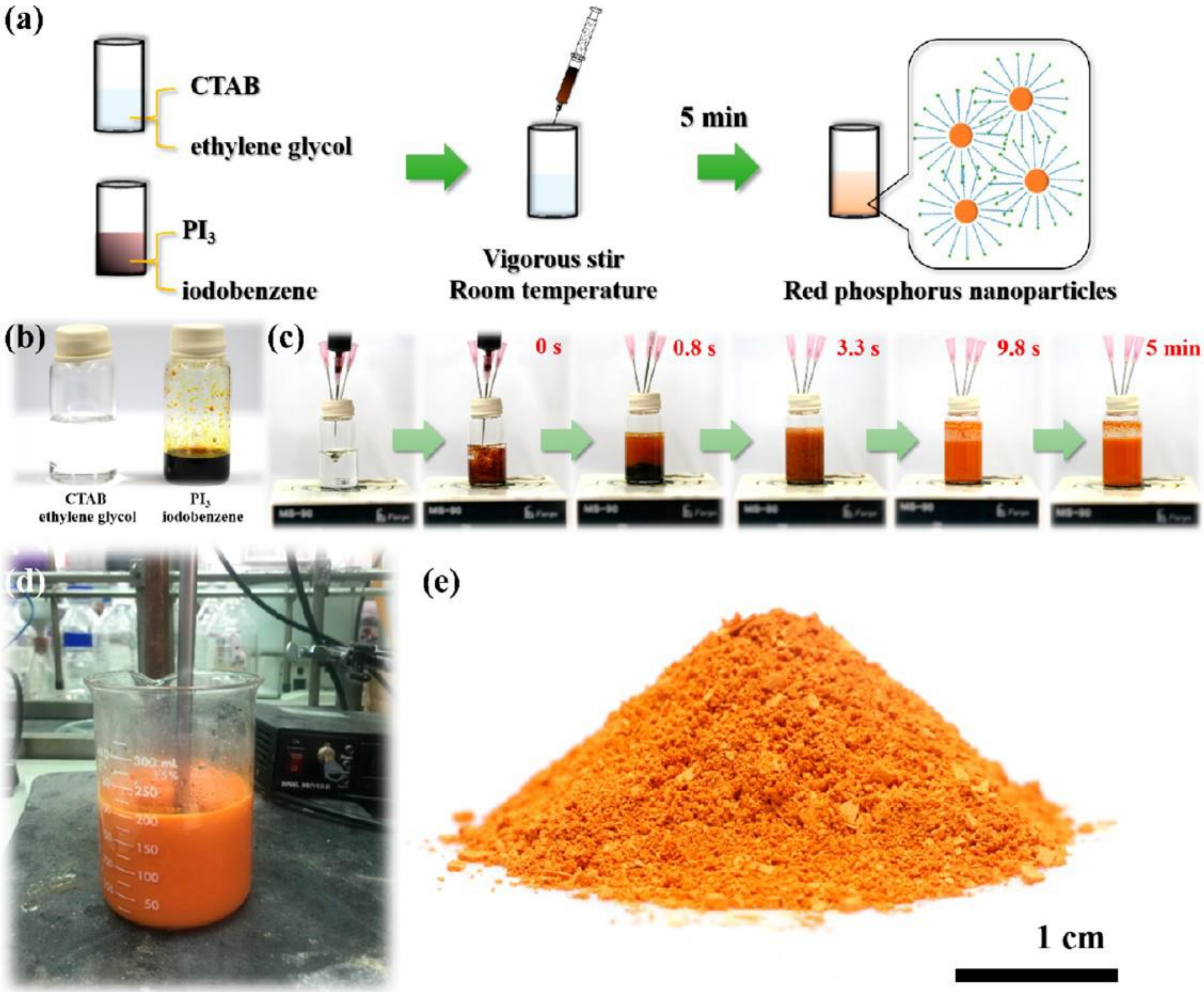

Morphology of RPNPs

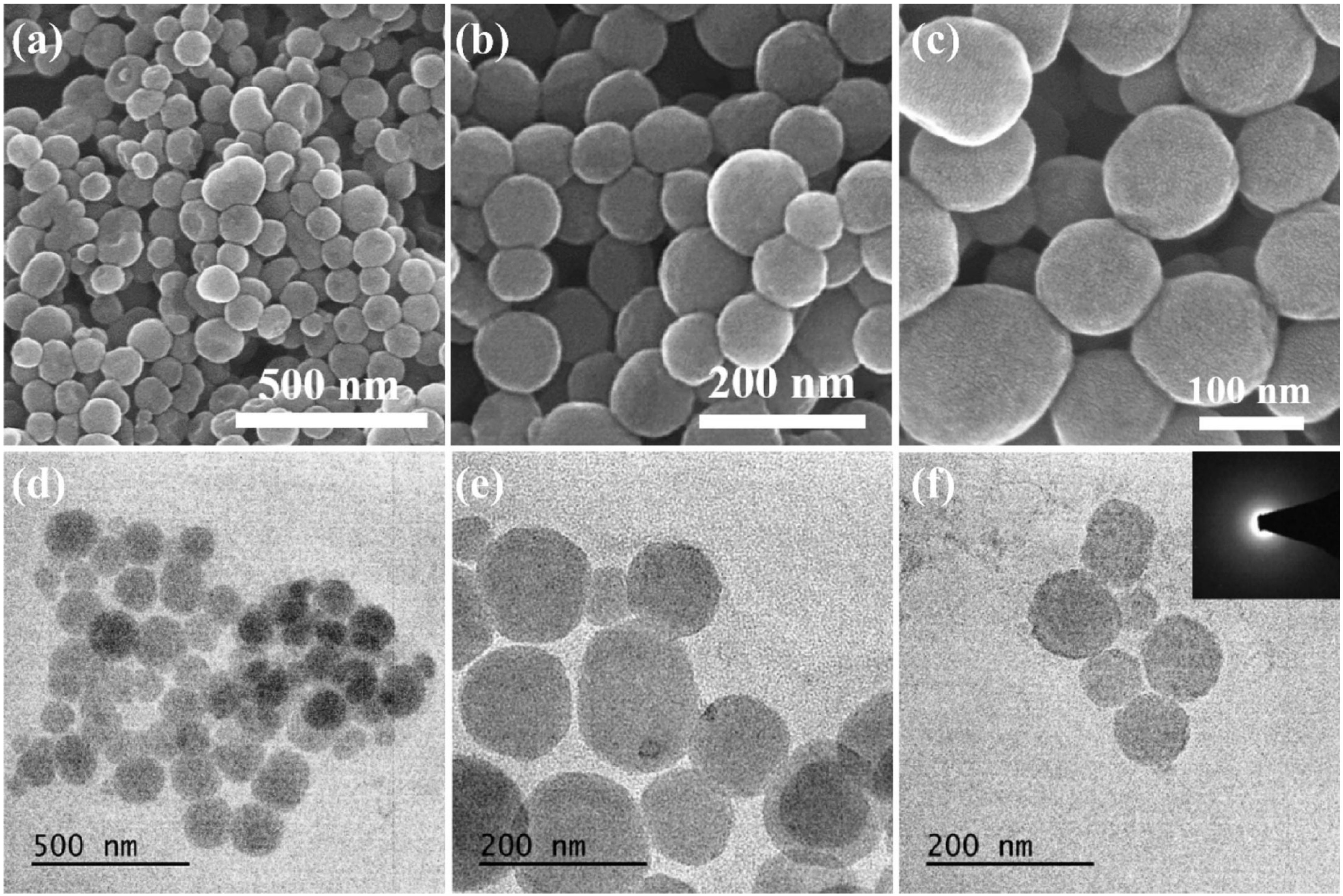

Characterization of RPNP : size dependent and Iodine doping

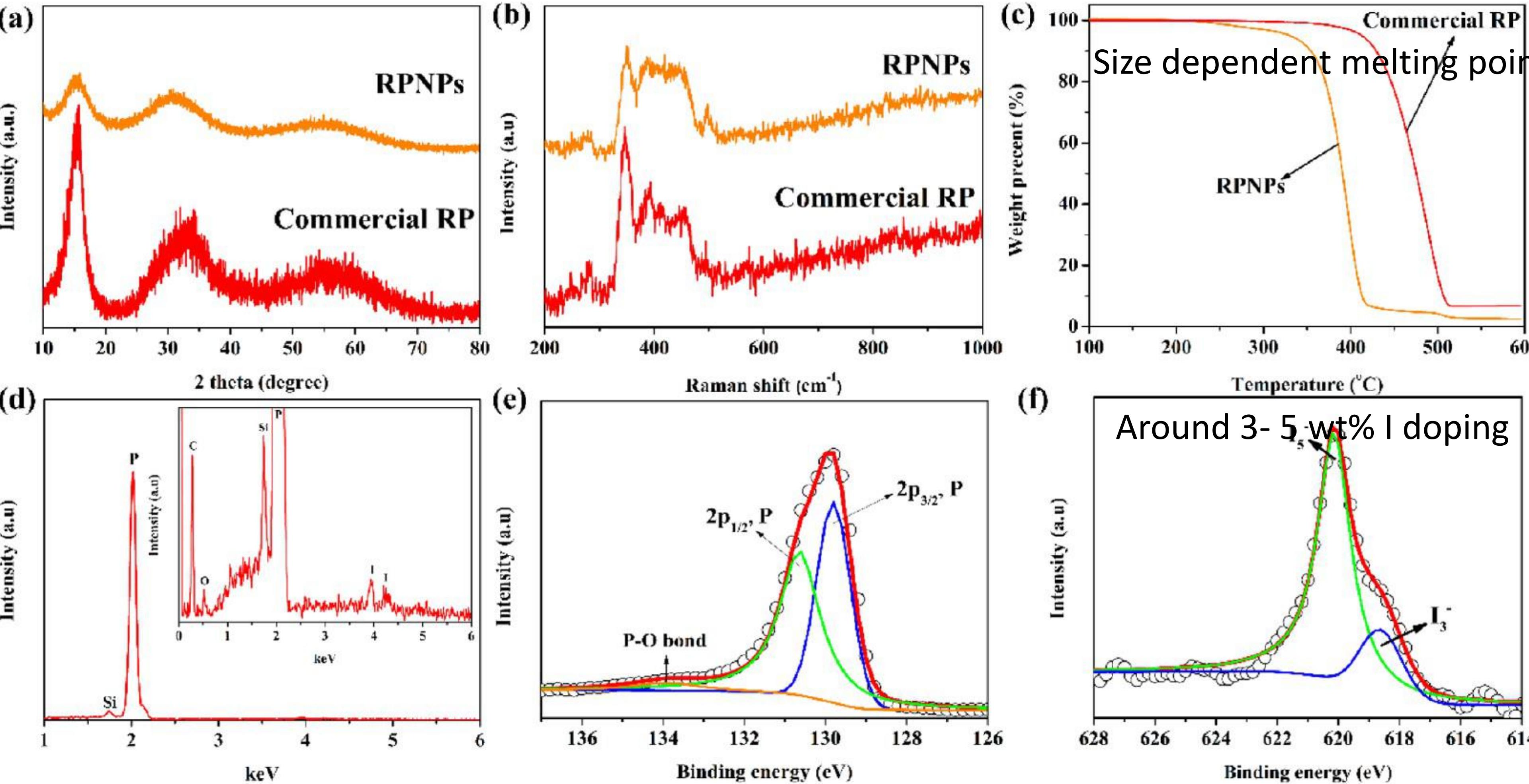

Significantly improved conductitivy

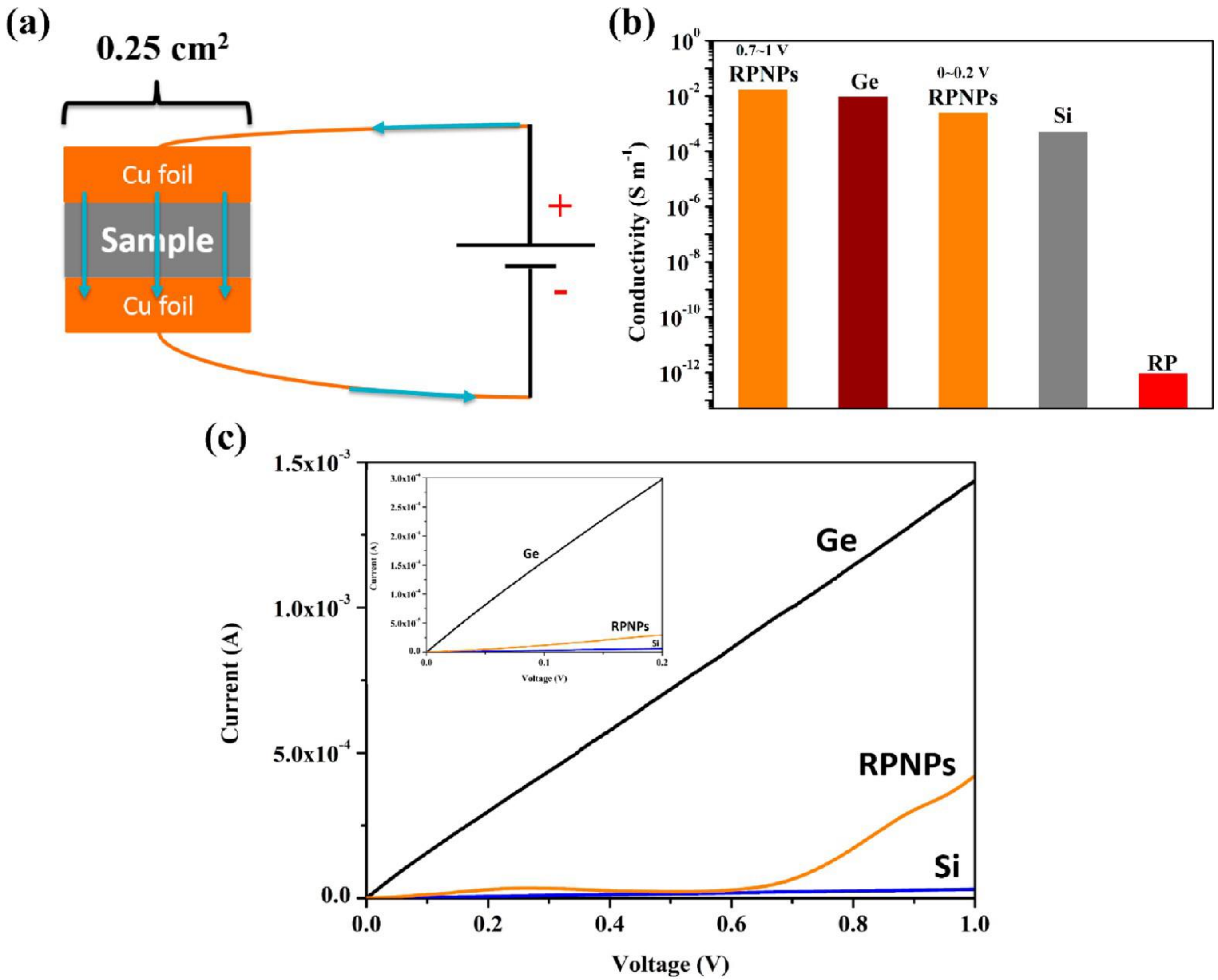

Half-Cell battery test

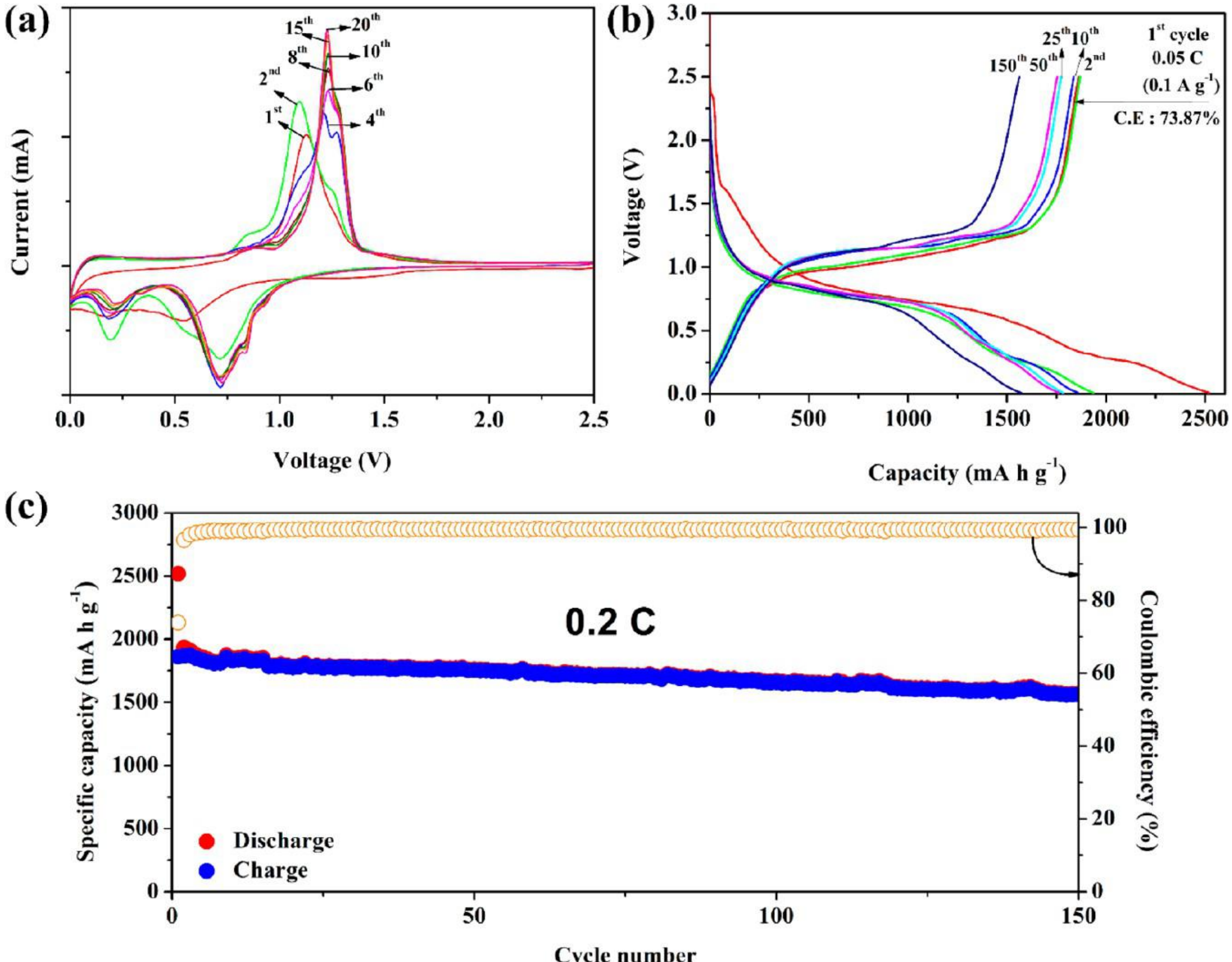

Half-cell battery test

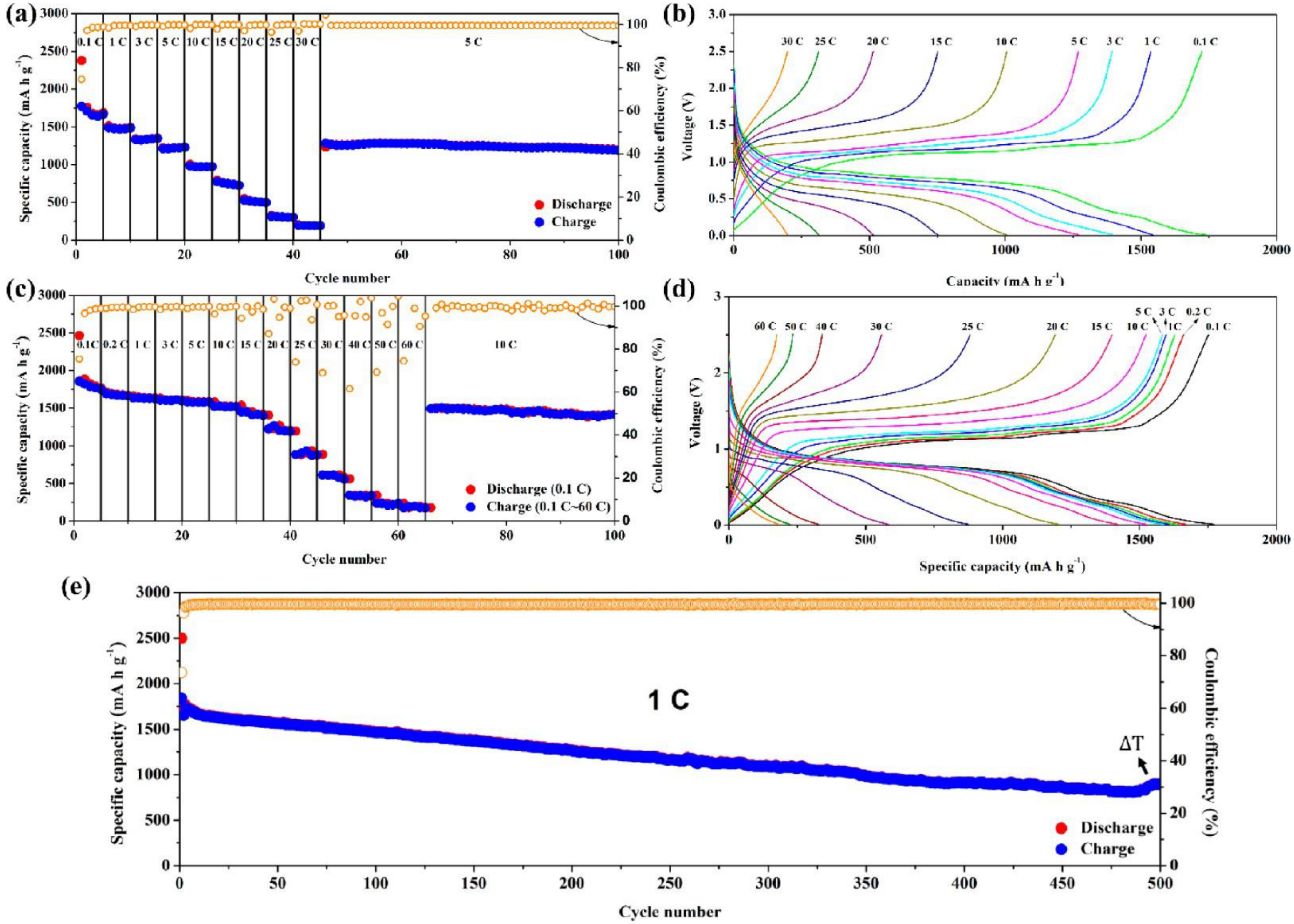

Full cell tests

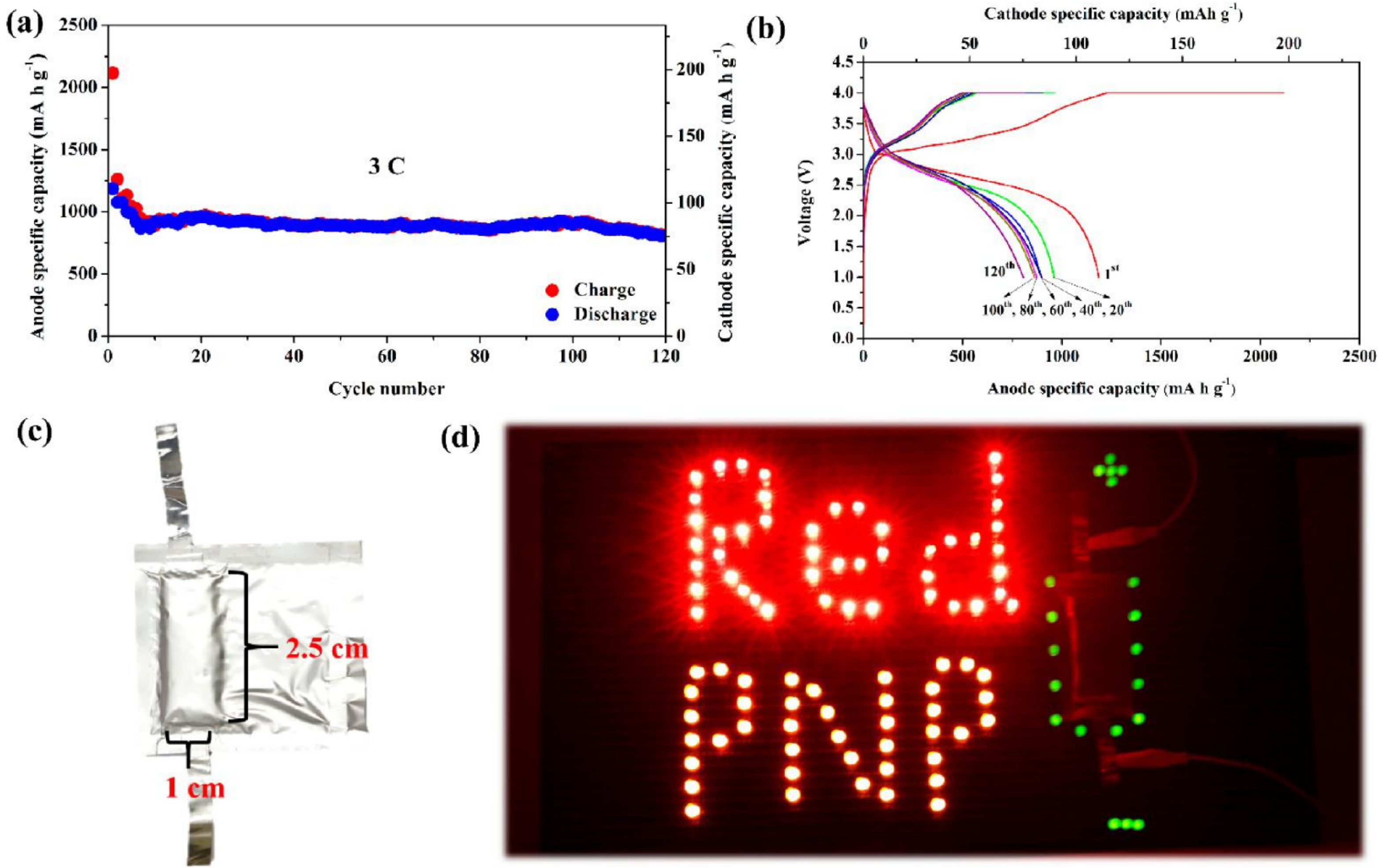

C&EN News: Phosphorus boosts lithium-ion battery charge capacity

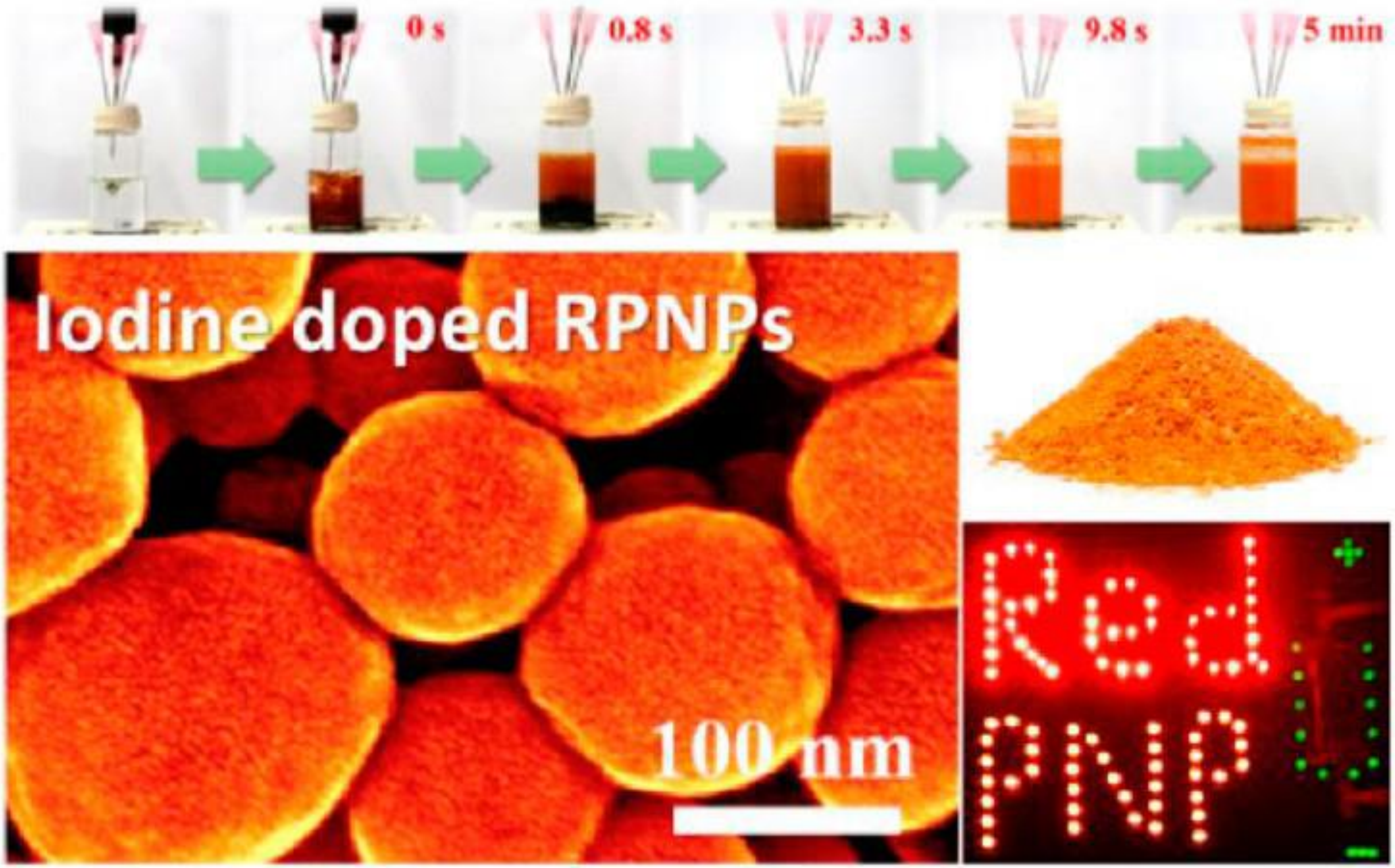

C&EN, **2017**, *95*, pp 8–9

Pouch type full cells as proof-of-concept demonstration for practical applications

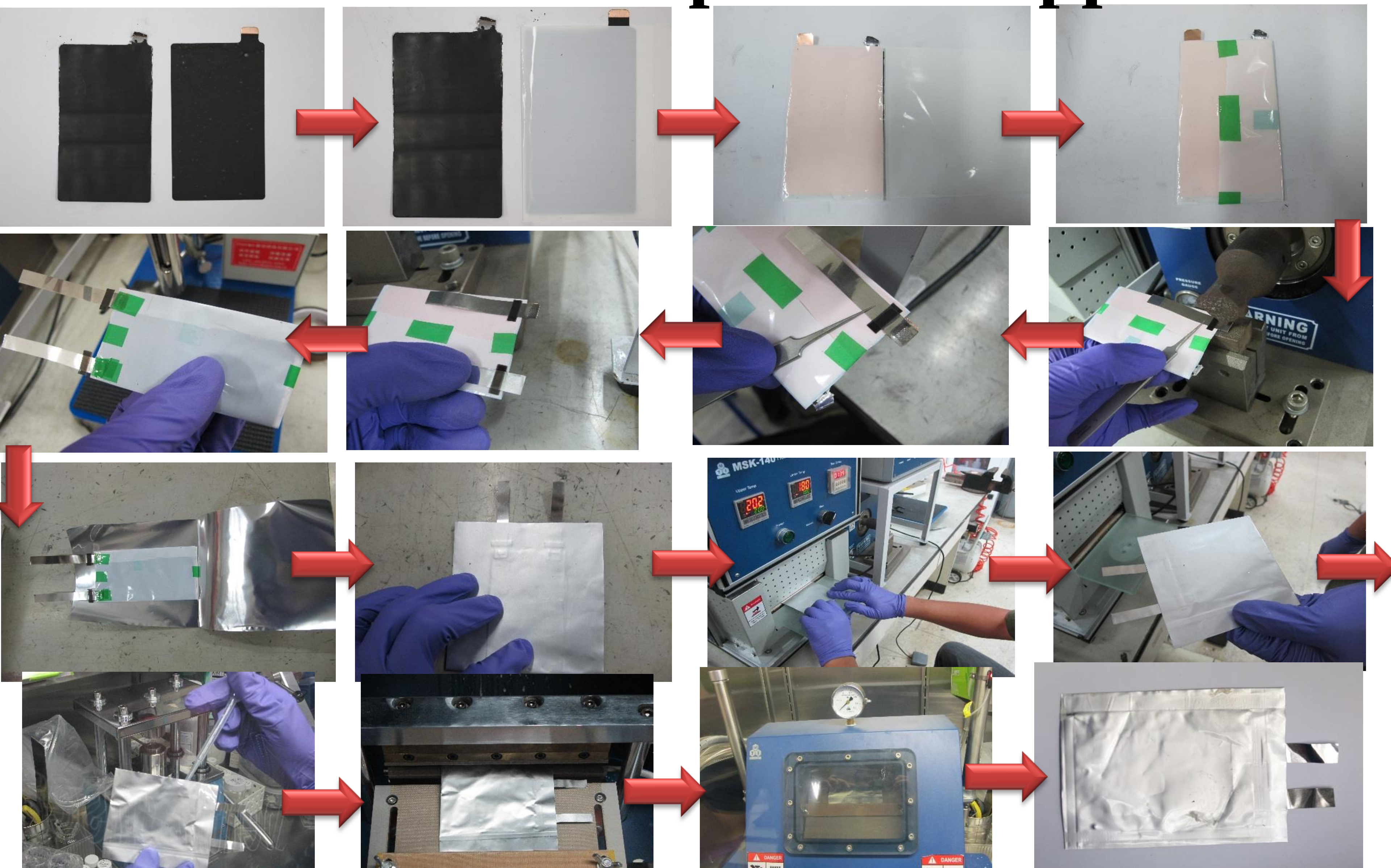

Mobile phone

Mini 4D car

LED Lighting

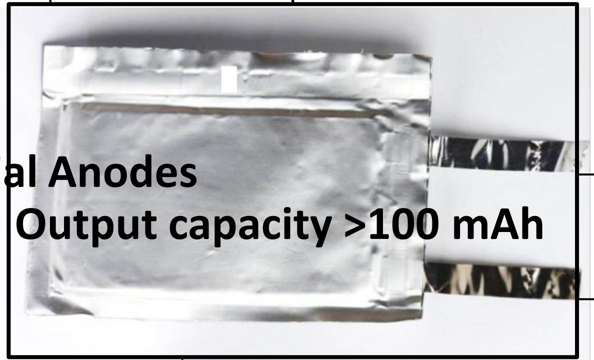

High specfic capacity Nanomaterial Anodes

Ge、Ge/RGO、Ge/MoS_2、

GeO_2、CuP_2、silicon/graphite

Output capacity >100 mAh

fan

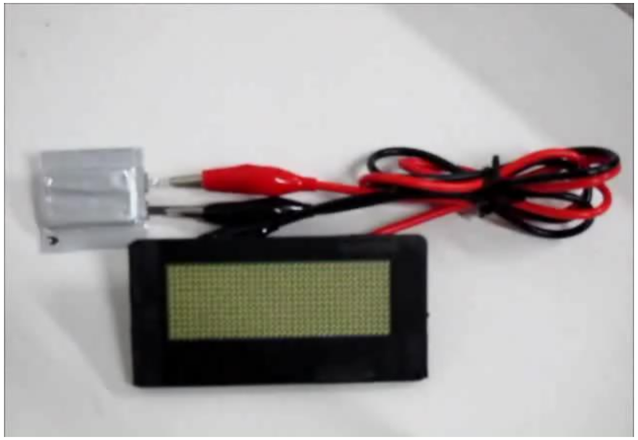

marquee

Nanoscale kerf loss Si :A top-down approach to make high-capacity nanomaetrials

Kerf loss silicon collected from the sawing process of solar-grade silicon

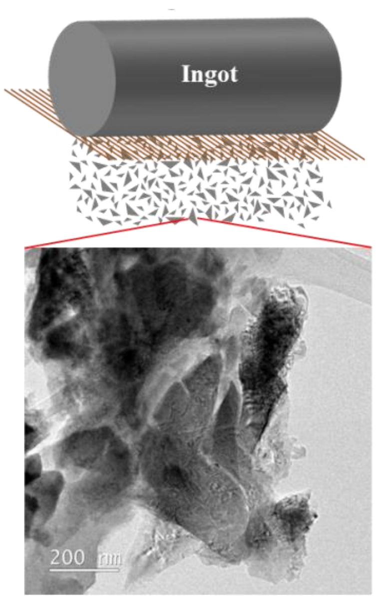

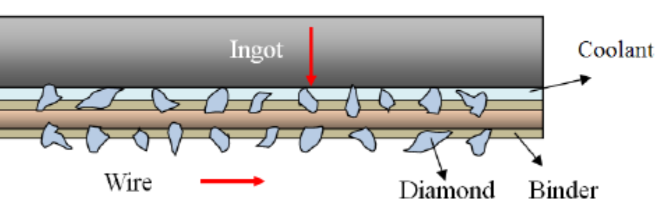

- □Nanoscale kerf loss silicon
- □Low cost (1 USD / kg)
- □A solar cell wafer company can produce ~1000 MT/Y
- ■Sufficient supply : annual consumption of polysilicon: 157000 tons with 20% growth rate

The capacity influence of Si addition into graphite anode full

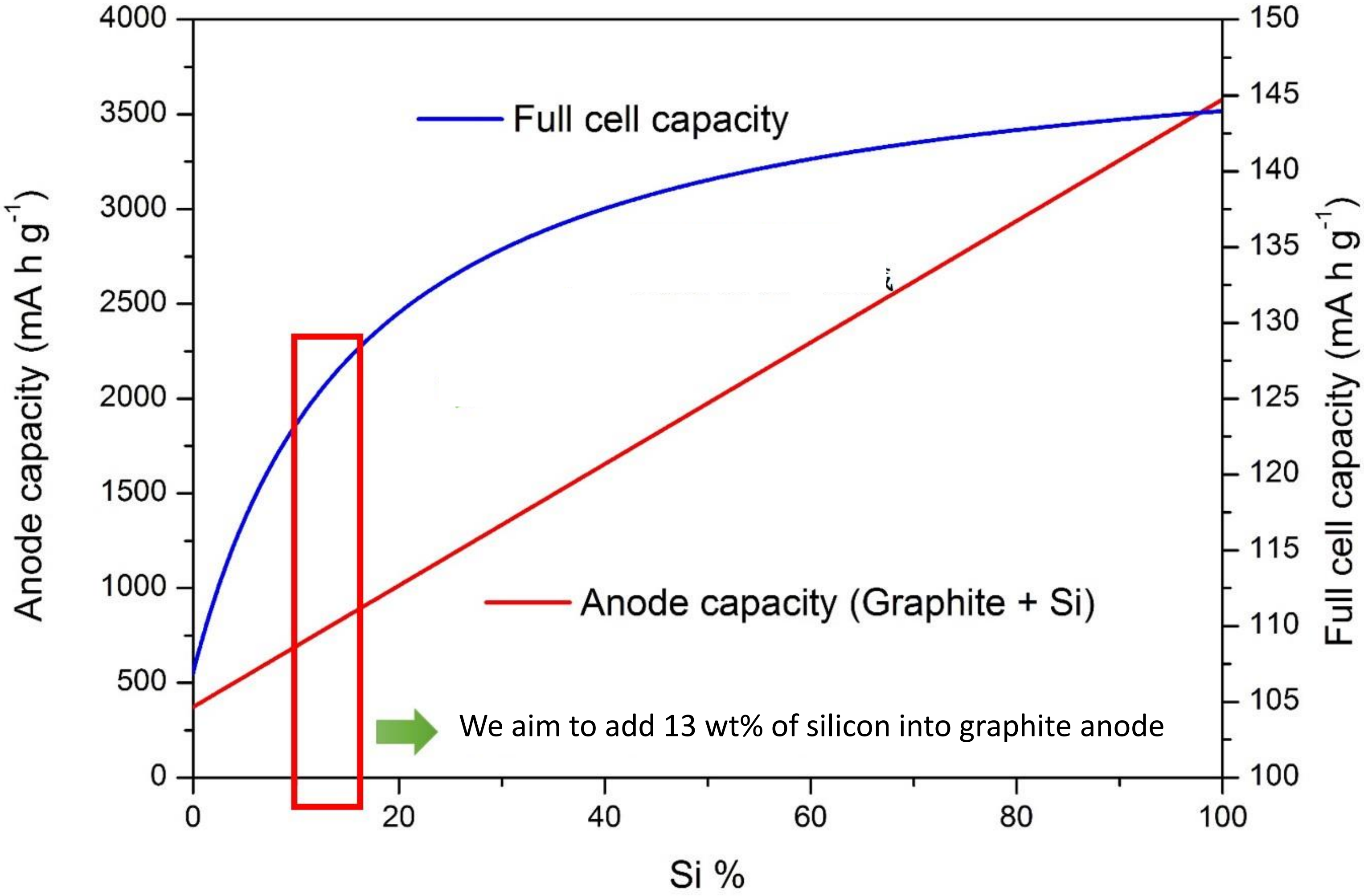

Proposed battery components with volumetric capacity higher than 600 mAh/cm^3

Cathode : Li(NiCoMn)O_2 Double-sided coating 135 μm X 8

Anode : Si/graphite or MCMB double-sided coating 110 μm X 8

Areal capacity 3.2 mA h/cm^2

single layer 25 μm X17

plastic film 110 μm X 2

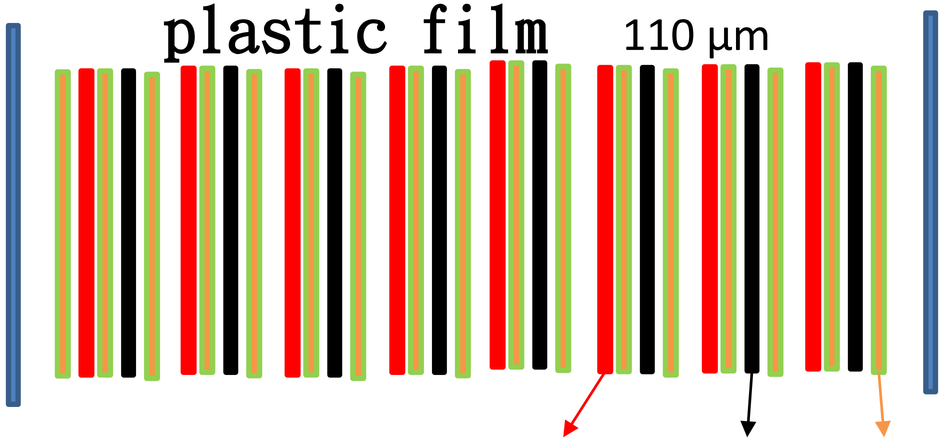

Cell volume 100 x 50 x 2.605 mm 2350 mA h @3.45 V

Characterization of kerf loss silicon

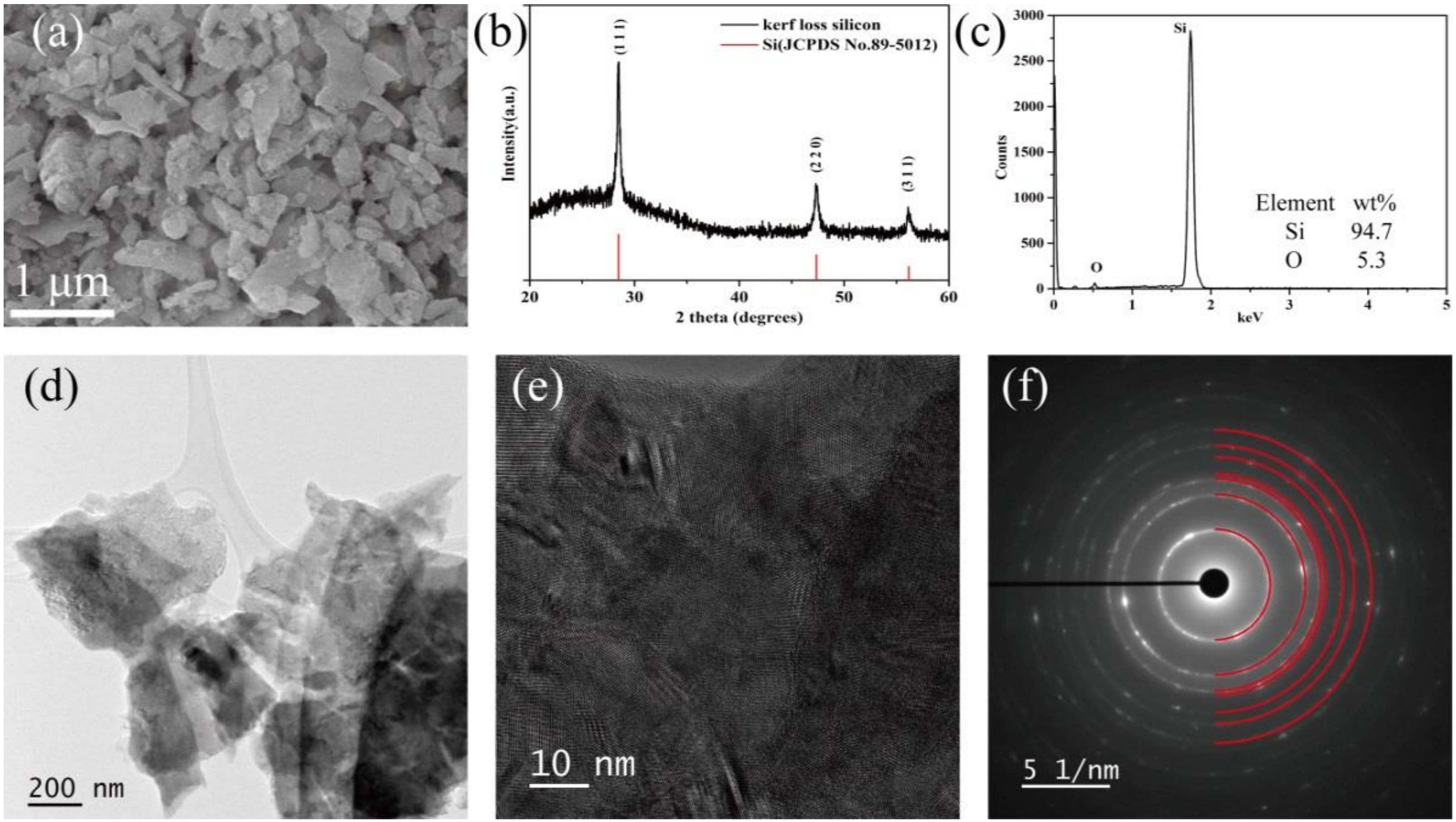

- Average size around 300-600 nm
- Slightly oxidized
- Polycrystalline
- No other metal impurity

Element	Concentration. (ppb)
Si	1000000
P	440
Ca	370
B	190

Coated film of Si/Graphite

(a)

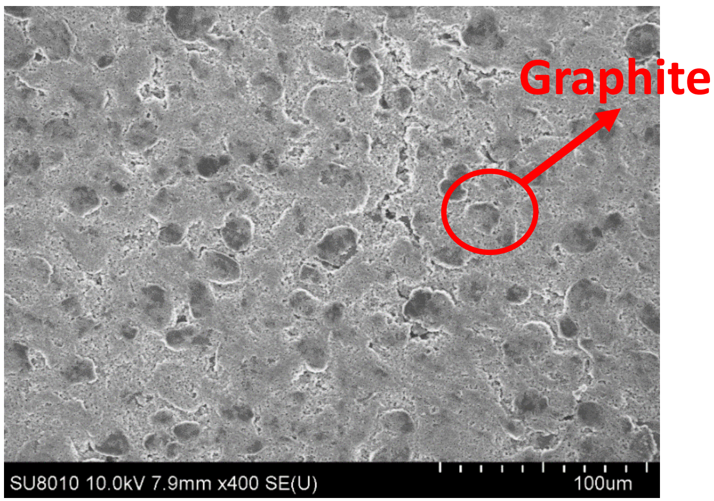

(b)

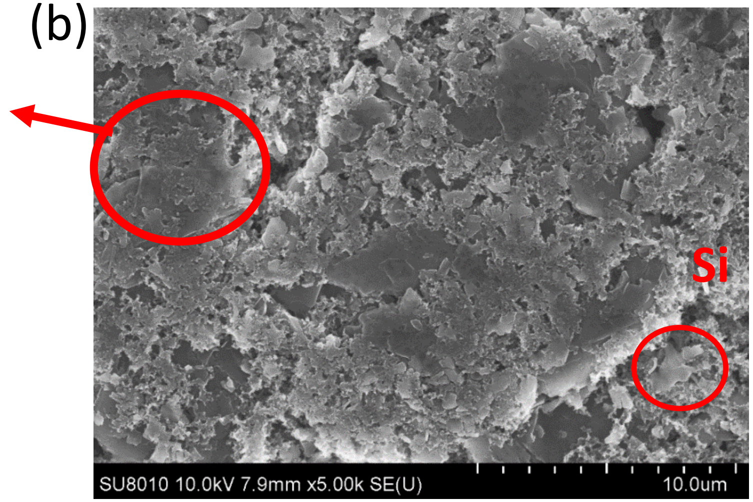

(c)

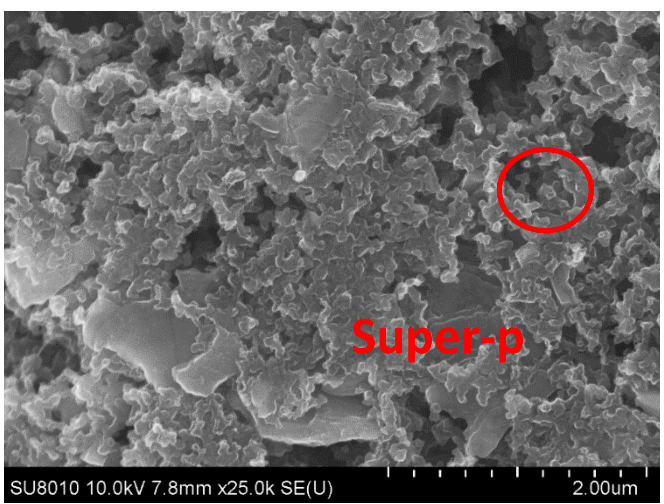

- Graphite：15~30 µm, Si：average size 600 nm
  Super-p：42~66 nm

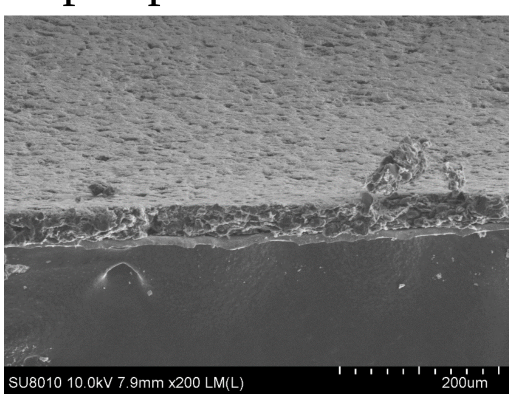

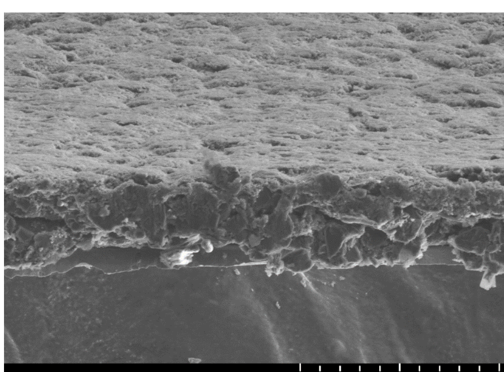

Half-cell performance of Si/graphite anode

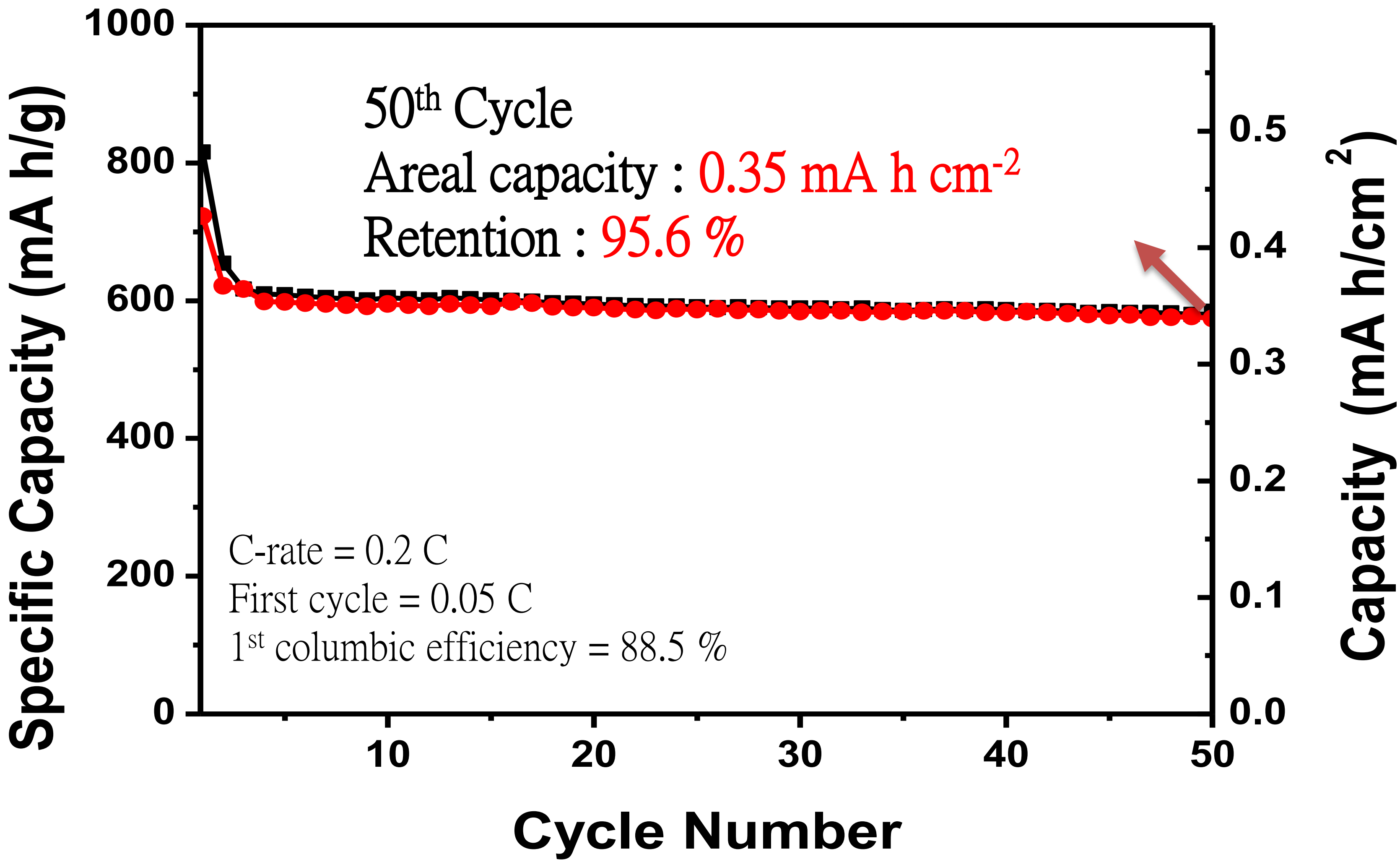

Electrode Appearance-Front view

Before cycle

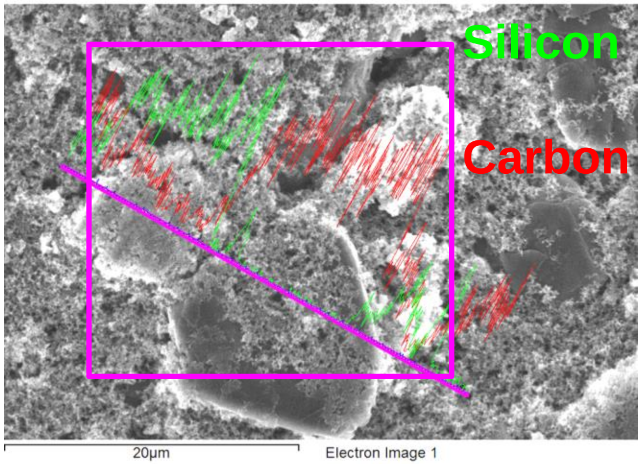

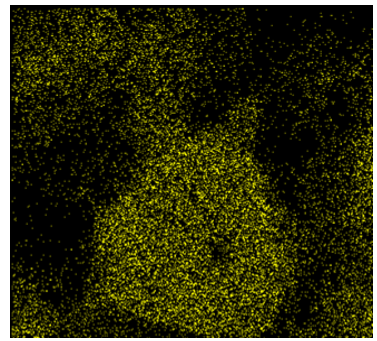

Carbon

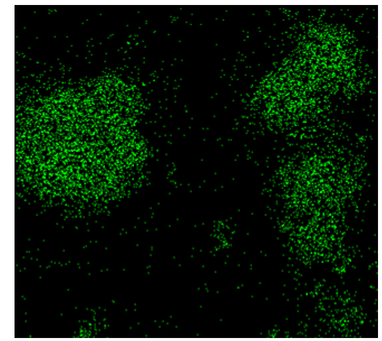

Silicon

After 100 cycles

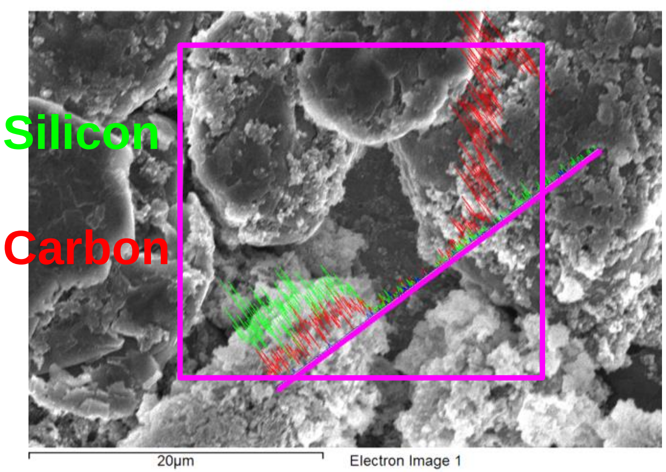

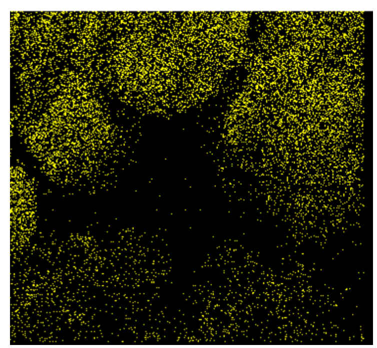

Carbon

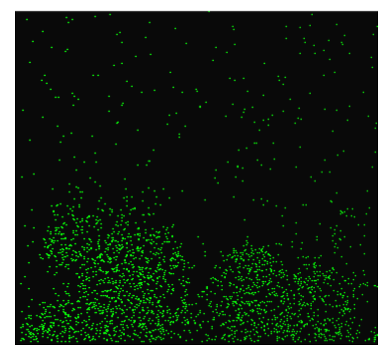

Silicon

Electrode Appearance-Side view

Si-Graphite

Before reaction

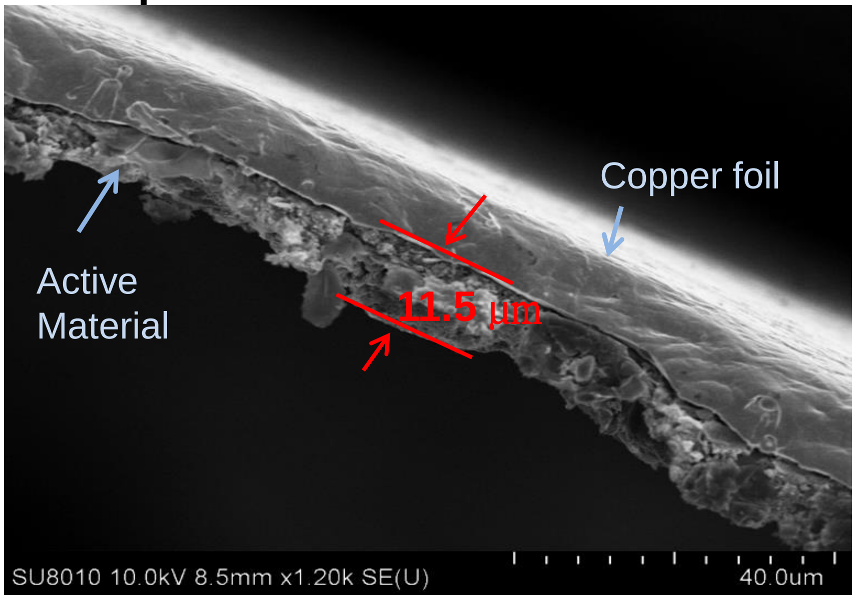

After 50 cycles

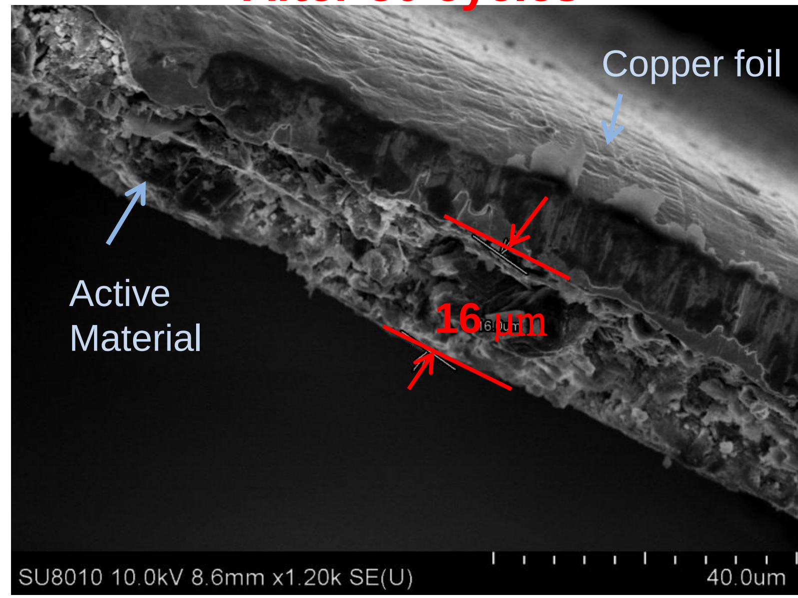

~40%

Ni-Si-Graphite

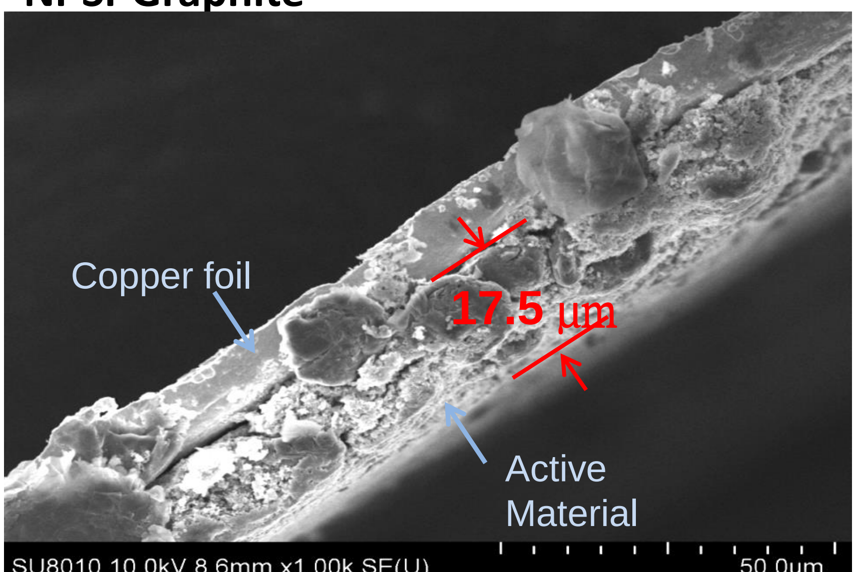

Before reaction

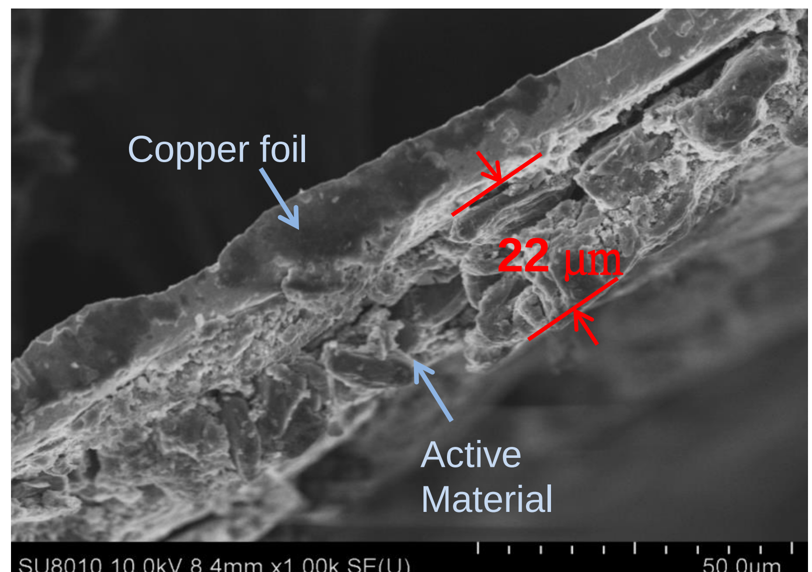

After 100 cycles

~25%

Positive electrode

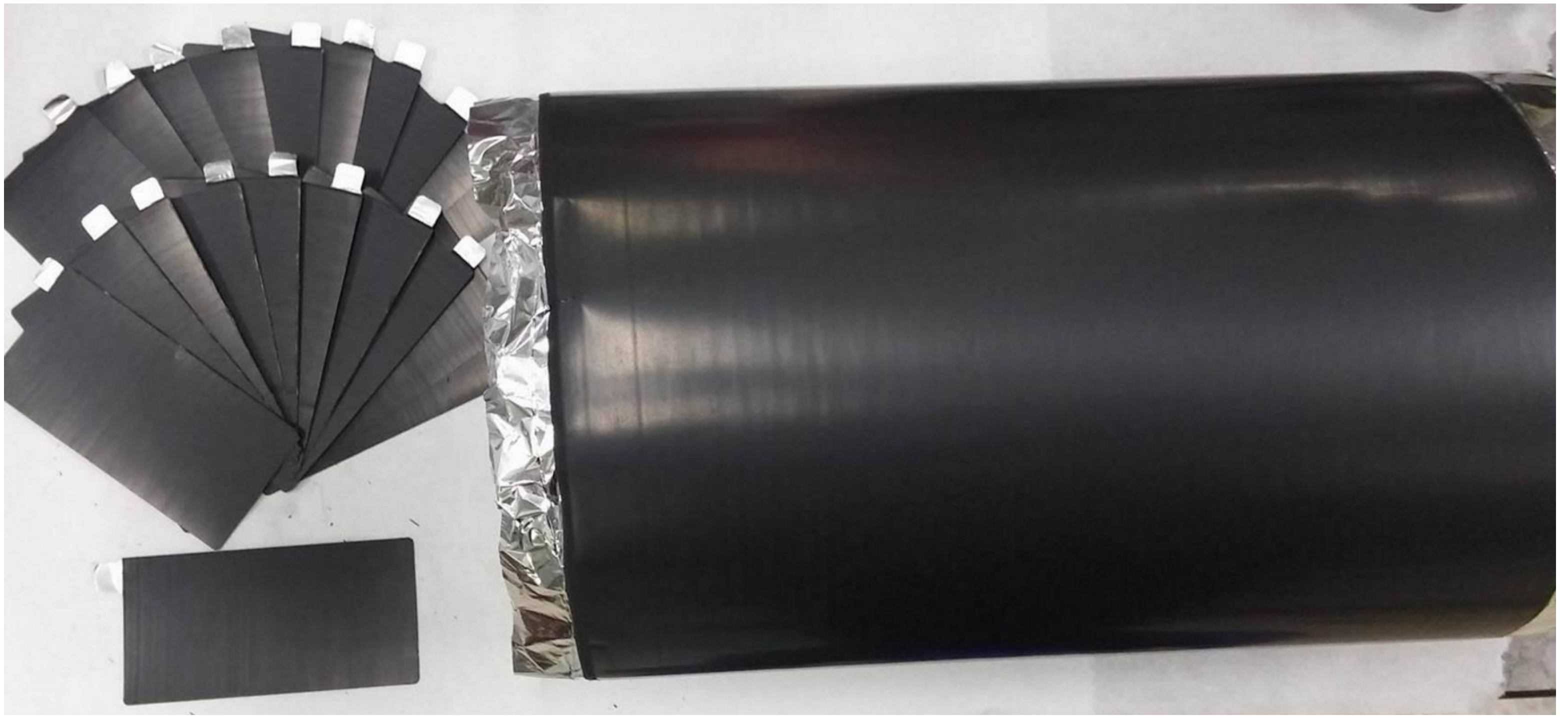

Li(NiCoMn)O_2 (NCM) :

Theoretical capacity : ~160 mA h/g), 4.2V

Operation range: 4.4V~4.5V(4.4V ~192 mA h/g)

Areal capacity :3.6 mA h cm^{-2} 。

Full cell: Si/Graphite-NCM

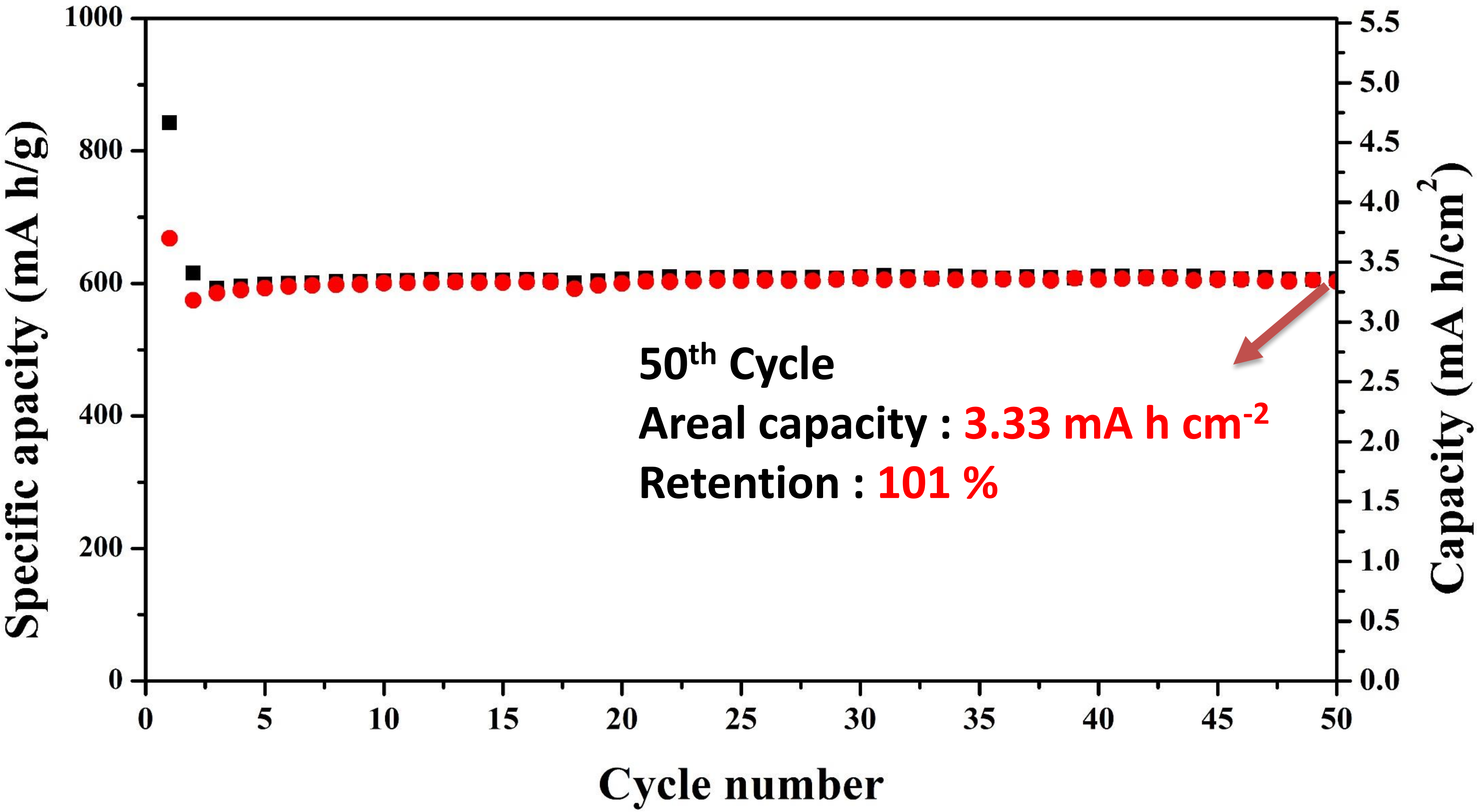

Full cell : Si/MCMB-NCM

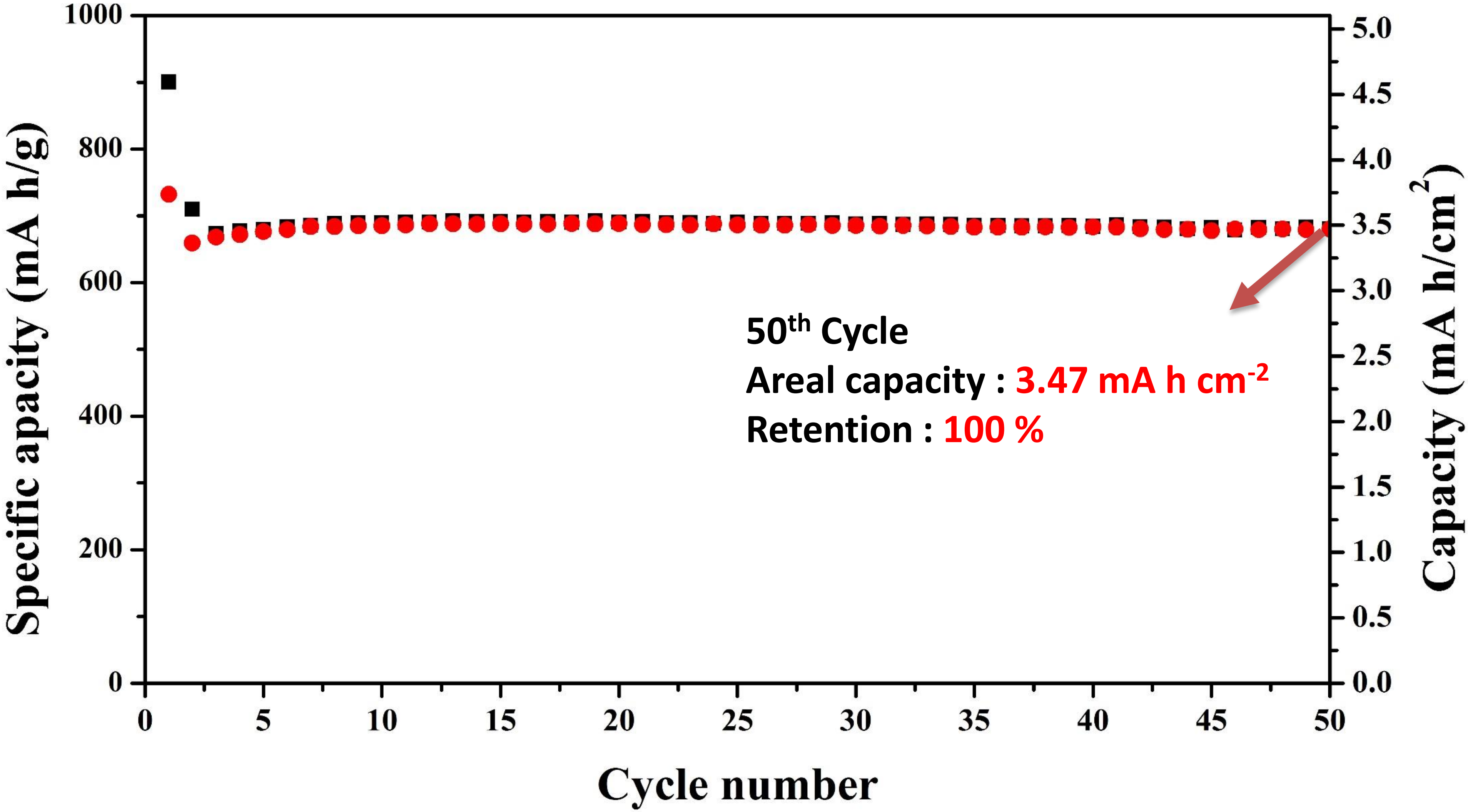

The effect of electrolyte on battery performance

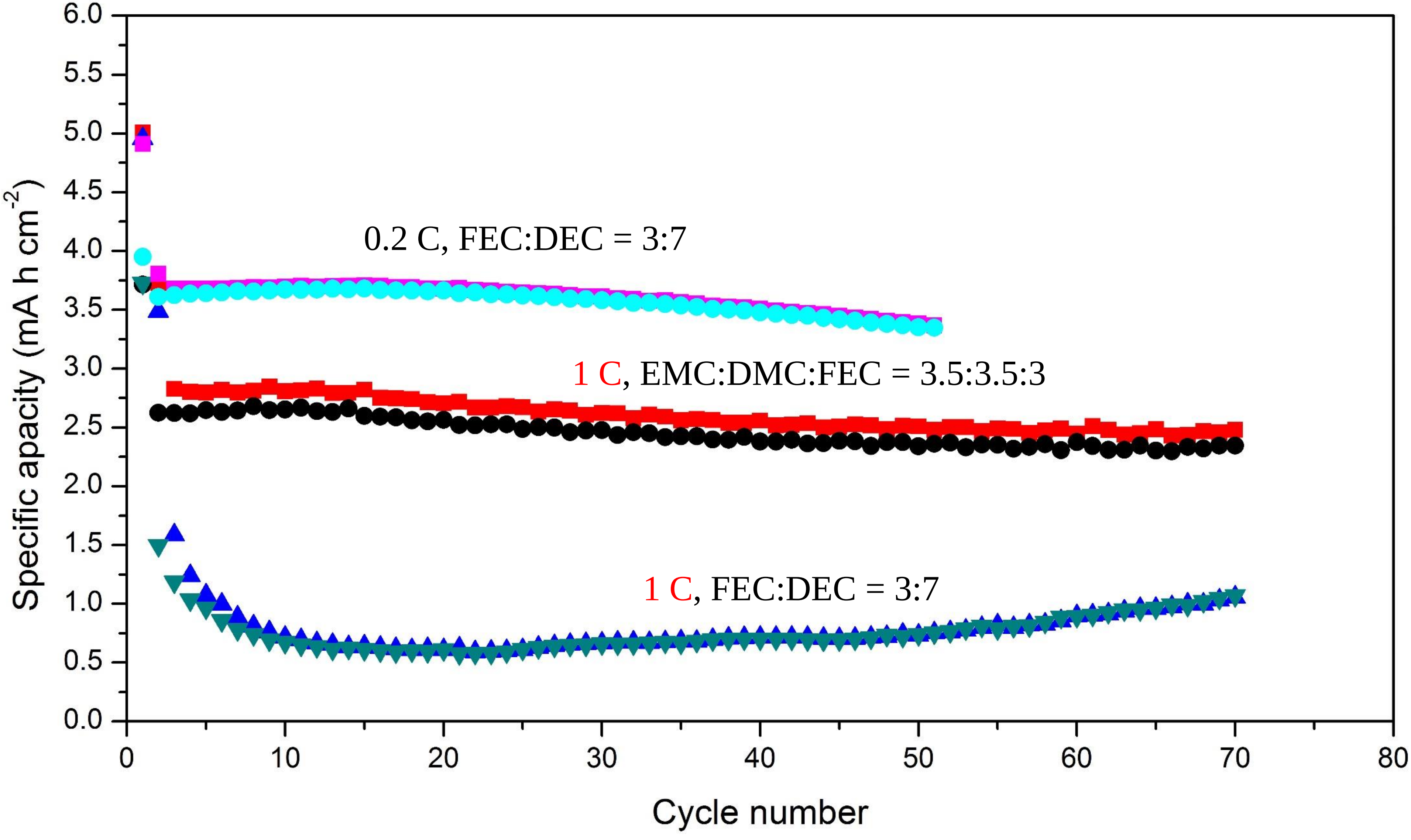

Pouch-type full cell: Si/Graphite -NCM

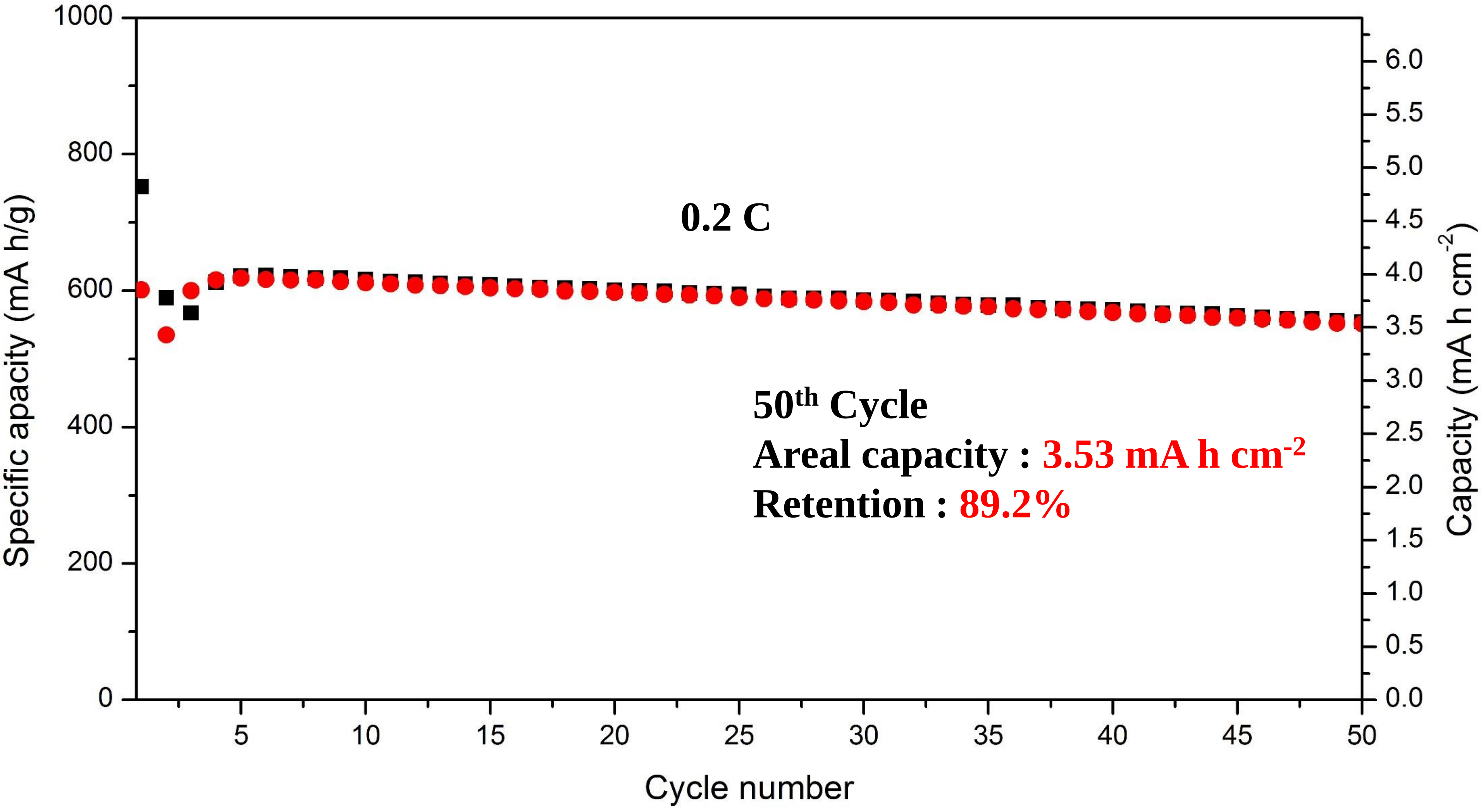

Double sided coating of active materials

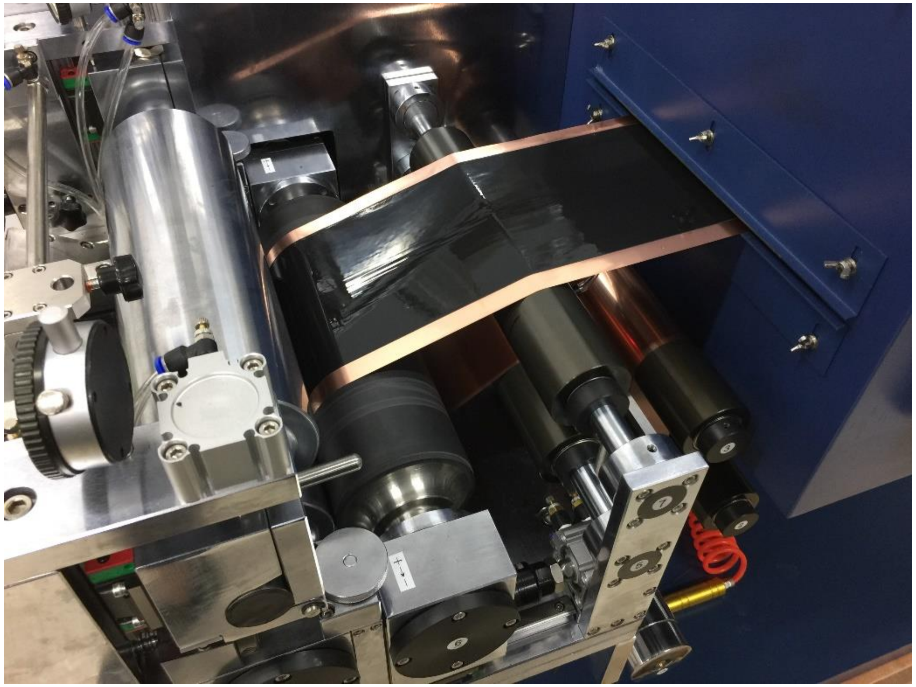

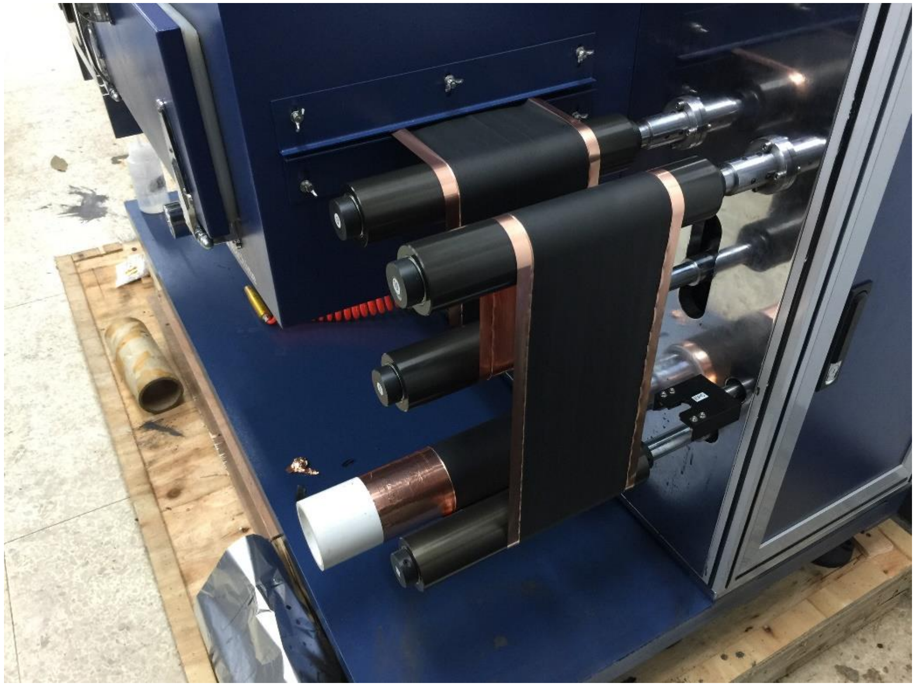

Power bank preparation

Charge (4.3V)

Second cycle charge capacity: 2731 mA h

Average charge voltage：3.90 V

Areal capacity：3.03 mA h cm^{-2}

thickness：3.435 mm

Volumetric energy density：620.1 Wh l^{-1}

Discharge 2.5V

Second cycle charge capacity 2703 mA h

Average charge voltage： 3.50 V

Areal capacity： 3.00 mA h cm^{-2}

thickness： 3.069 mm

Volumetric energy density： 616.5 Wh l^{-1}

Conclusion

Coin half cell

Parameters of
Slurry, coating, rolling

First cycle coulombic efficiency
: 88.5%

Areal capacity retention: 95.6 %

Coin Full cell

Areal capacity: 3.33 mA h cm^{-2}

Areal capacity retention: 101 %

Pouch-type cell: Single layer

Areal capacity: 3.53 mA h cm^{-2}

Areal capacity retention: 90% 50th cycle

Pouch-type Cell: multiple layer

1. Continuous coating technique
2. Cell capacity >2300 mAh
3. Volumetric capacity >600 mAh/cm^3

Introduction

Greenhouse effect

Limited fossil oil reserves

Hydrogen production

=

Develop alternative clean energy

- high heat value of 141.79 MJ/kg
- Benign emission after combustion

http://www.ln.edu.hk/projects/ecfp/ecfp/Environmental%20attitudes/Greenhouse%20Effect.htm
http://baike.sogou.com/v582173.htm

Hydrogen Production Method
Chemical process

- **Metal-hydride (e.g. $NaBH_4$ and MgH_2)**

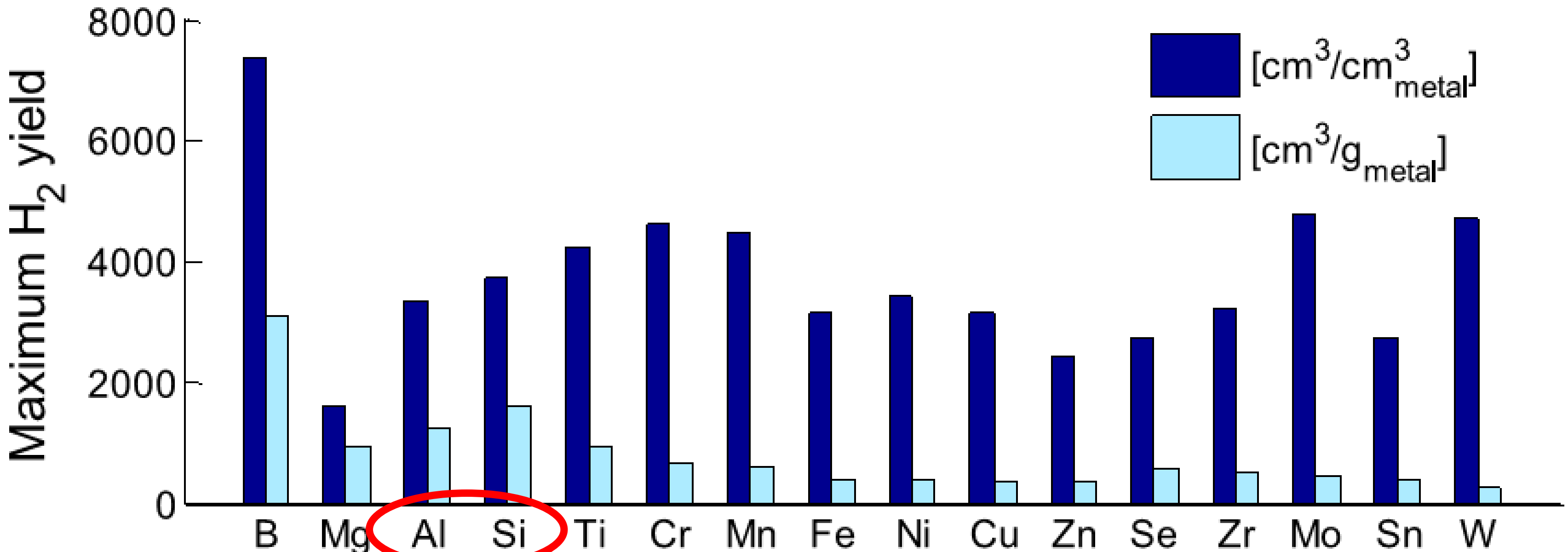

Cheap and safely transported

Yavor, Y., *Int. J. Hydrogen Energy* **2015,** *40* (2), 1026-1036.

Hydrogen Economy

Characteristics of H_2

- ☐ *Heating value (142 MJ/kg)*
- ☐ *Benign end production (i.e. H_2O)*
- ☐ *Extremely low density (0.081 kg/m^3)*

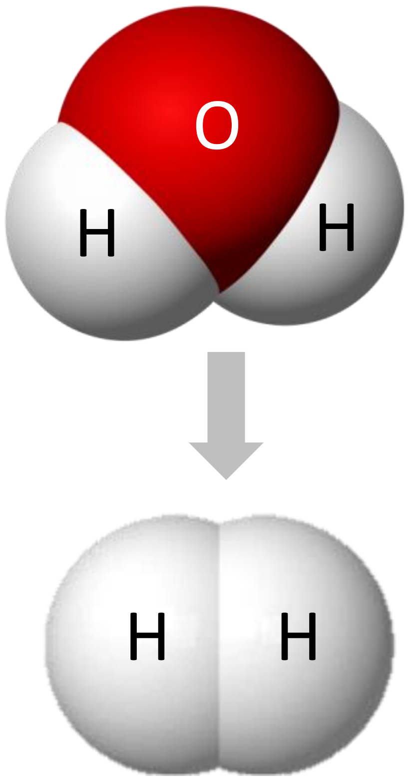

H_2 production method

- ☐ Fossil fuel reforming : CO, CO_2 emit
- ☐ Electrolysis : Energy intensive
- ☐ **Chemical process : Safe Transportation**
- ☐ Photocatalysis : small-scale
- ☐ Fermemtative : small-scale

Metal-Water reaction

Silicon versus Aluminum

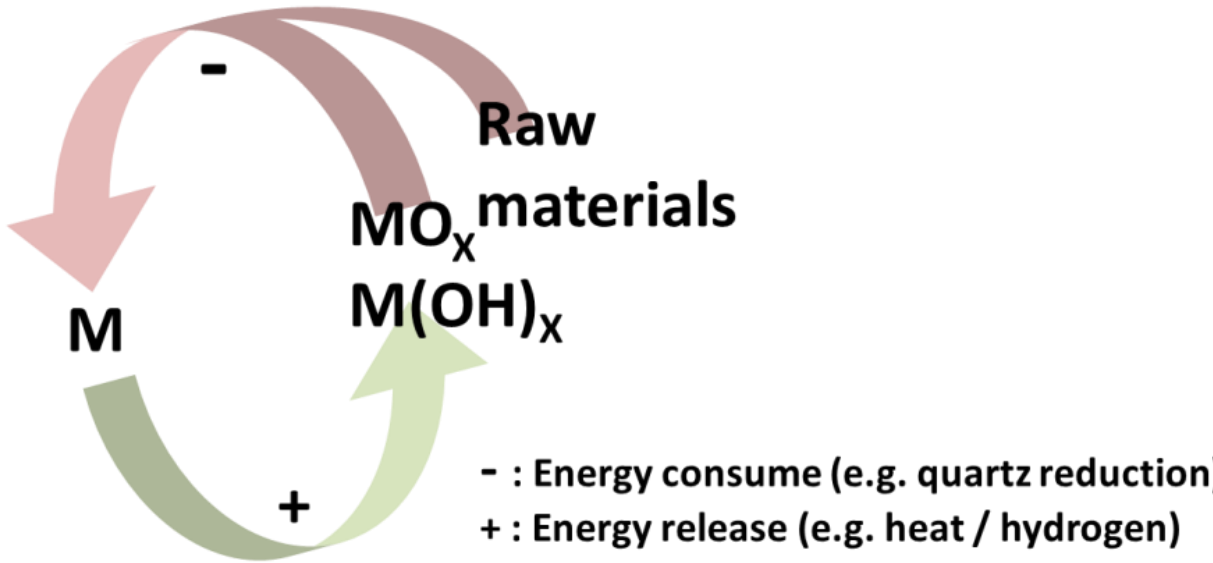

Type of metals	Energy release[1] (MJ kg^{-1})	Price (USD Kg^{-1})	Abundance in earth crust (wt%)
Si	33	2	27.7
Al	31	2	8.2

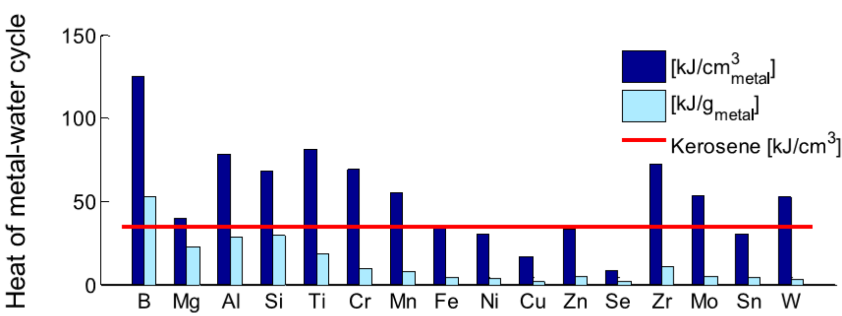

[1]Total energy of metal-water reaction heat and hydrogen released from it.

Yavor, Y., *Int. J. Hydrogen Energy* **2015,** *40* (2), 1026-1036.

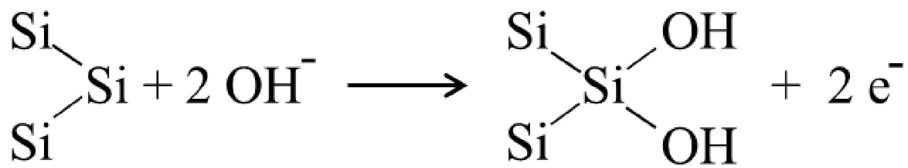

(1)

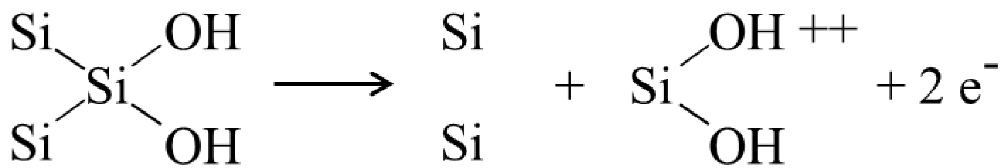

(2)

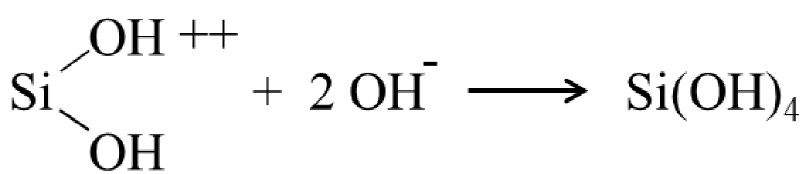

(3)

$$Si(OH)_4 \longrightarrow SiO_2(OH)_2^{--} + 2\,H^+ \qquad (4)$$

$$4\,H_2O + 4\,e^- \longrightarrow 4OH^- + 2H_2 \qquad (5)$$

Overall reaction :

$$Si + 2\,OH^- + 2H_2O \longrightarrow SiO_2(OH)_2^{--} + 2\,H_2 \qquad (6)$$

Scheme Diagram of using kerf loss as energy carrier

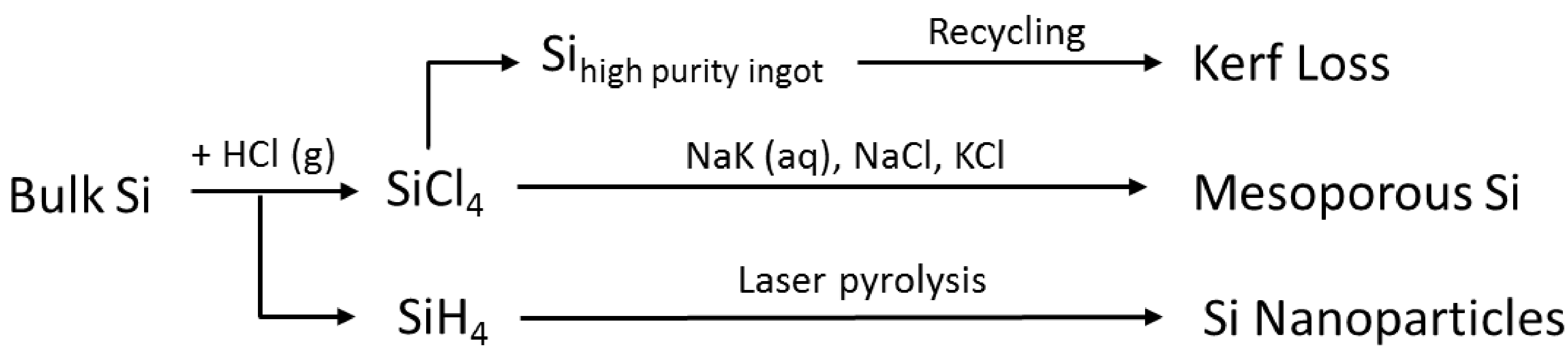

Mesoporous Si

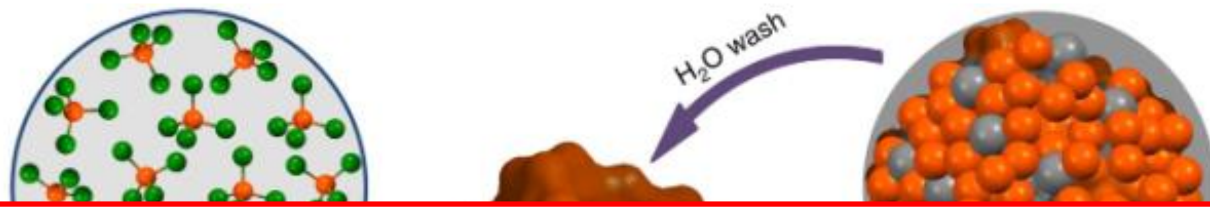

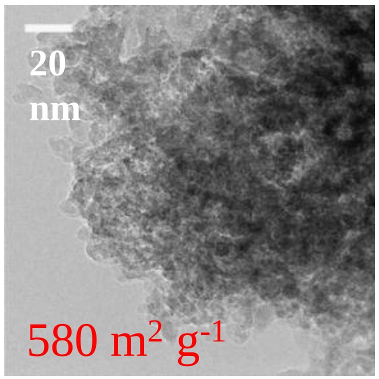

Advantages

- High specific surface area : 580 m^2 g^{-1}
- Hydrogen production rate **(9.5×10^{-2} g_{H2} s^{-1} g_{Si}^{-1})**
- Yield **(90%)**

Disadvantages

- Highly active NaK was used
- Toxic $SiCl_4$ was used

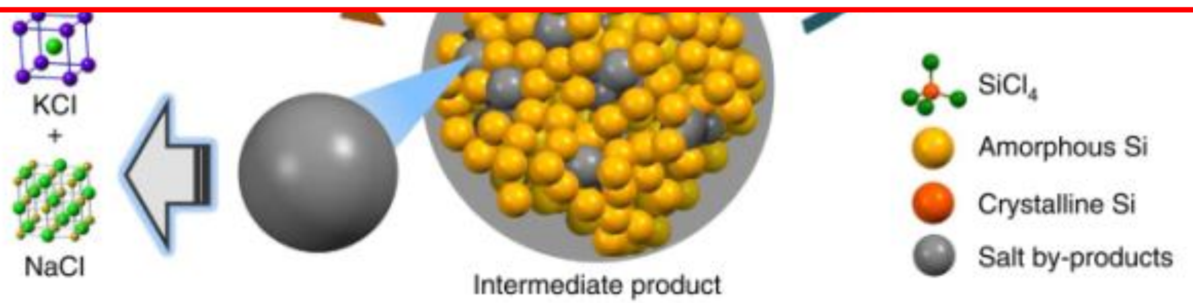

Dai, Fang, et al. "Bottom-up synthesis of high surface area mesoporous crystalline silicon and evaluation of its hydrogen evolution performance." *Nature communications* 5 (2014).

Si Nanoparticles

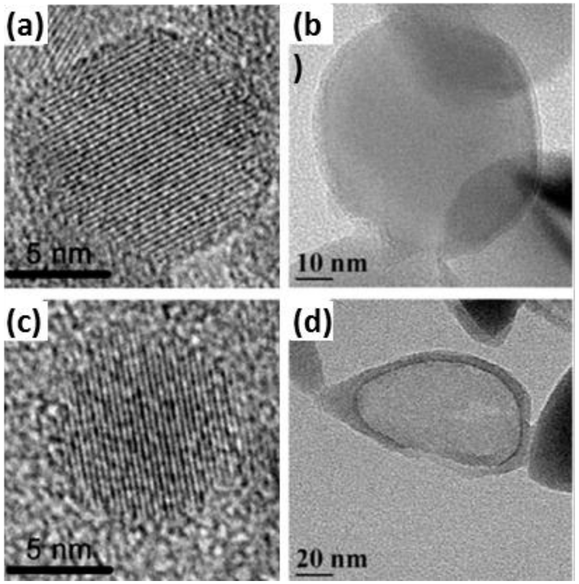

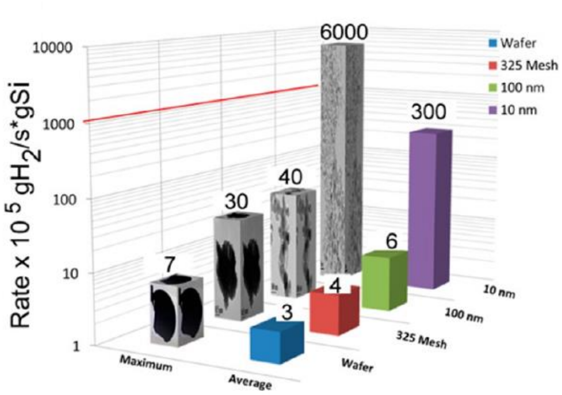

Process description:

Laser-driven chemical reaction using SiH_4 to generate hydrogen-bonded Si nanoparticles.

Advantages

- ☐ Hydrogen production rate **($6.0\times10^{-2}\ g_{H2}\ s^{-1}\ g_{Si}^{-1}$)**
- ☐ Yield **(129%)**

Disadvantages

- ☐ Flammable SiH_4 was used
- ☐ CO_2 laser beam (Heating rate 10^5 K/ sec)

Erogbogbo, Folarin, et al. "On-demand hydrogen generation using nanosilicon: splitting water without light, heat, or electricity." *Nano letters* 13.2 (2013): 451-456.

Motivation

Kerf loss silicon collected from the sawing process of solar-grade silicon

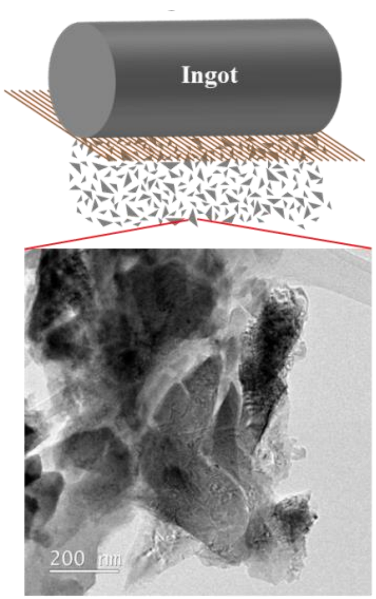

- Micro-sized kerf loss silicon
- Additives-mediated
- Low cost (1 USD / kg)
- Environmental-friendly process

Time-resolved small-scale hydrogen production set-up

Constant temperature

Remove water vapor

Volumetric calculation for small scale (70ml) hydrogen production

Characterization of kerf loss silicon

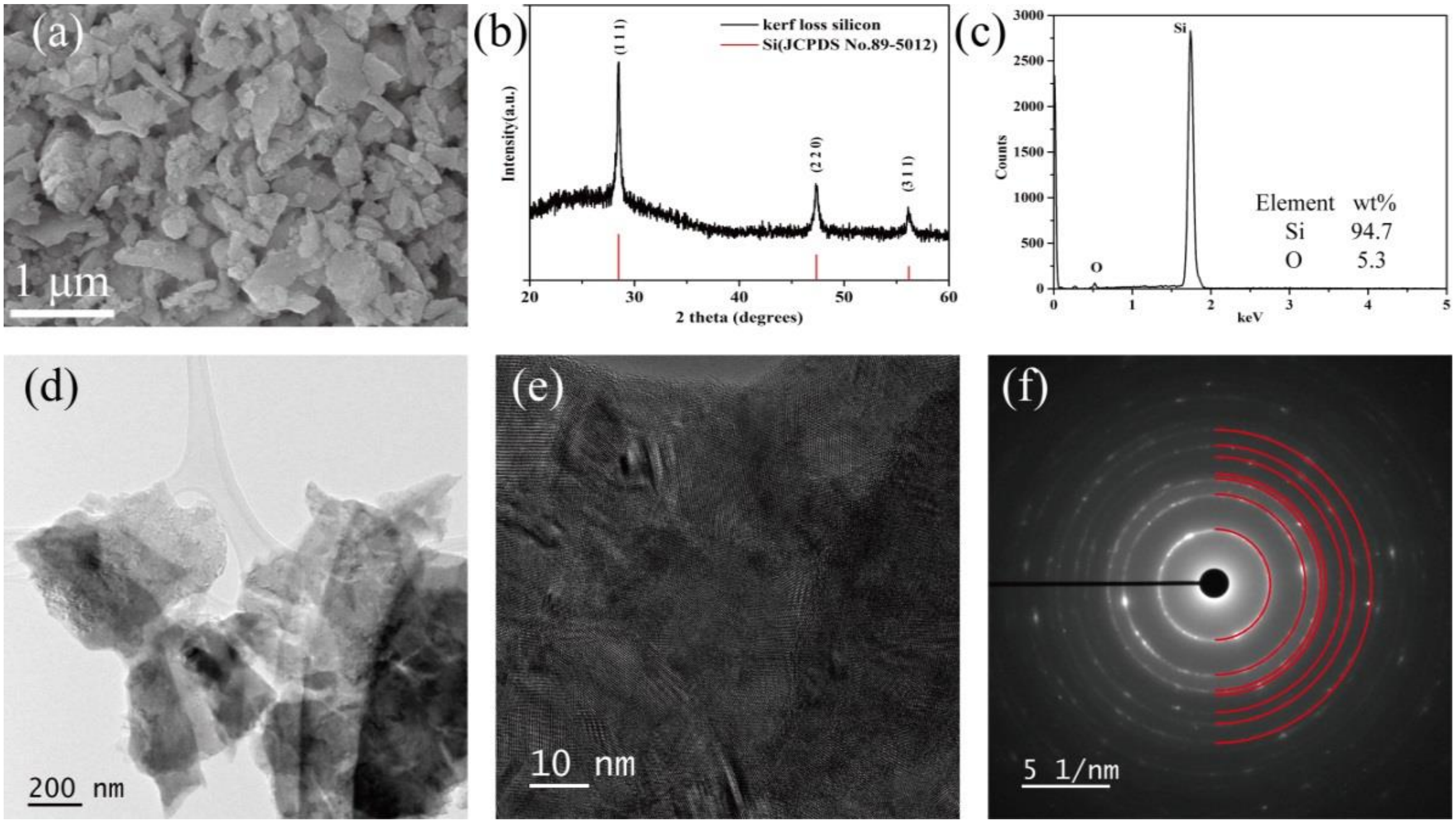

- Average size around 0.5 µm
- Slightly oxidized
- Polycrystalline
- No other metal impurity

Element	Concentration. (ppb)
Si	1000000
P	440
Ca	370
B	190

Real-time observation

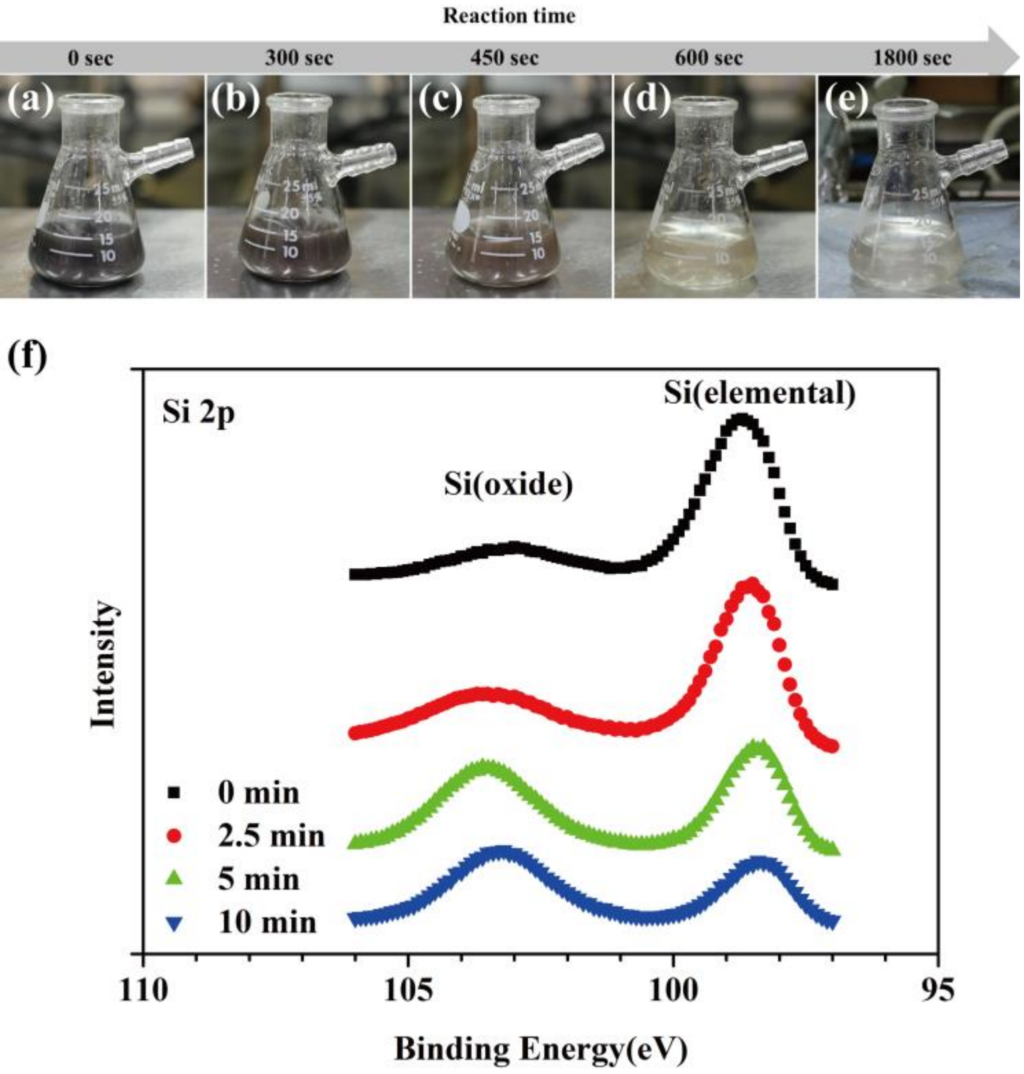

- As reaction time went by, the color of etching solution became lighter gradually.

- The oxide peak at 103.3 eV became relatively strong as reaction time proceeded, indicating the concentration of silicate increased.

Hydrogen Production Video

$$P_iV_i = n_iRT \quad \& \quad P_fV_f = n_fRT$$

$$\Rightarrow (P_i + \Delta P)(V_i + \Delta V) = (n_i + \Delta n)RT$$

$$\Rightarrow P_i\left(1 + \frac{\Delta P}{P_i}\right)(V_i + \Delta V) = (n_i + \Delta n)RT$$

0

$$\Rightarrow P_i(V_i + \Delta V) = (n_i + \Delta n)RT$$

$$\Rightarrow P_iV_i + P_i\Delta V = n_iRT + \Delta nRT$$

$$\Rightarrow P_i\Delta V = \Delta nRT$$

$$\Rightarrow n_{H_2} = \Delta n = \frac{P_i\Delta V}{RT} = \frac{P_iA\Delta h}{RT}$$

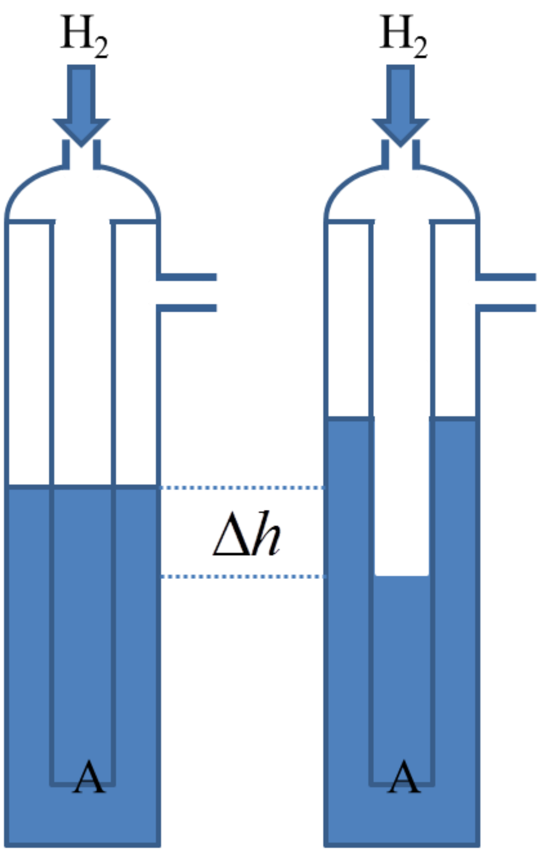

$$\Delta V = A\Delta h$$

Ideal gas and real gas

- Table 2 Density table of real gas and ideal gas regarding hydrogen

P (atm)	T (K)	density(ideal gas, kg m^{-3})	density(NIST, kg m^{-3})	deviation percentage(%)
1	273	0.089990	0.089934	0.063
1	283	0.086811	0.086758	0.061
1	293	0.083848	0.083798	0.059
1	303	0.081080	0.081033	0.059
1	313	0.078490	0.078445	0.057
1	323	0.076060	0.076017	0.057
1	333	0.073776	0.073735	0.056
1	343	0.071625	0.071586	0.055
1	353	0.069596	0.069559	0.053
1	363	0.067679	0.067644	0.051
1	373	0.065864	0.065831	0.051

Effects of Na_2SiO_3 and H_2SiO_3 on the base-catalyzed etching of kerf loss silicon at 303 K

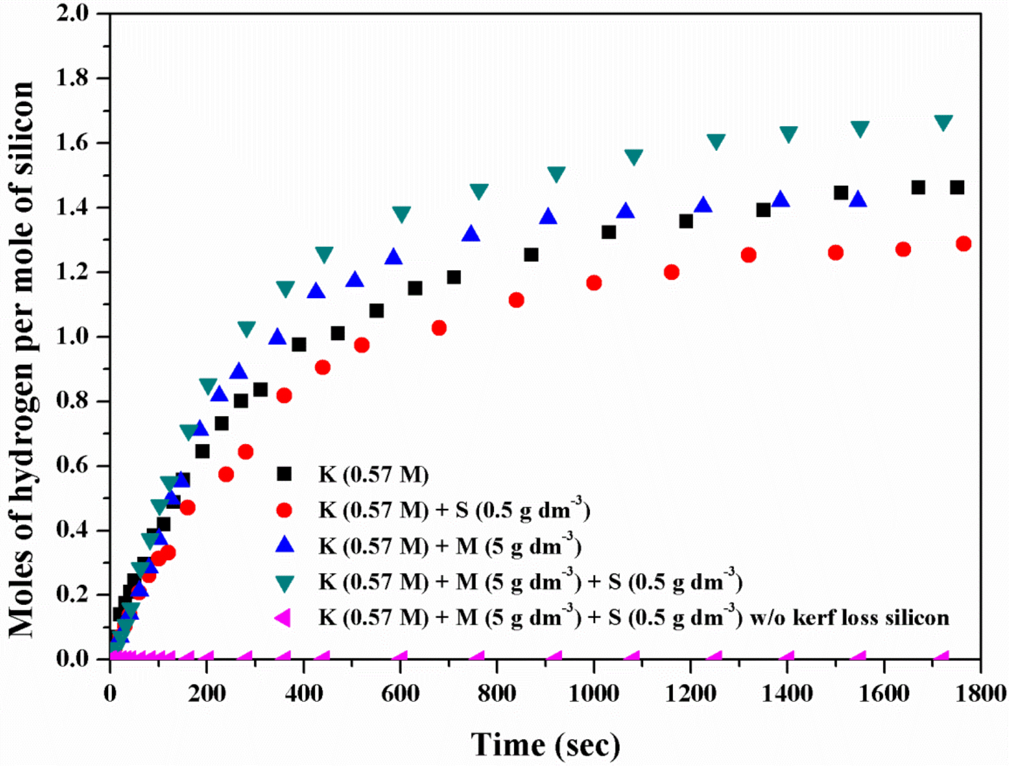

Additives	Hydrogen production rate , $g(H_2)\ s^{-1}\ g^{-1}(Si)$	Yield (%)
K (0.57 M)	6.0×10^{-5}	73
K (0.57 M) + S (0.5 g dm^{-3})	6.3×10^{-5}	64
K (0.57 M) + M (5 g dm^{-3})	6.8×10^{-5}	71
K (0.57 M) + M (5 g dm^{-3}) + S (0.5 g dm^{-3})	7.4×10^{-5}	83
K (0.57 M) + M (5 g dm^{-3}) + S (0.5 g dm^{-3}) w/o kerf loss silicon	0	0

123 %

Effects of reaction temperature on the base-catalyzed etching of kerf loss silicon

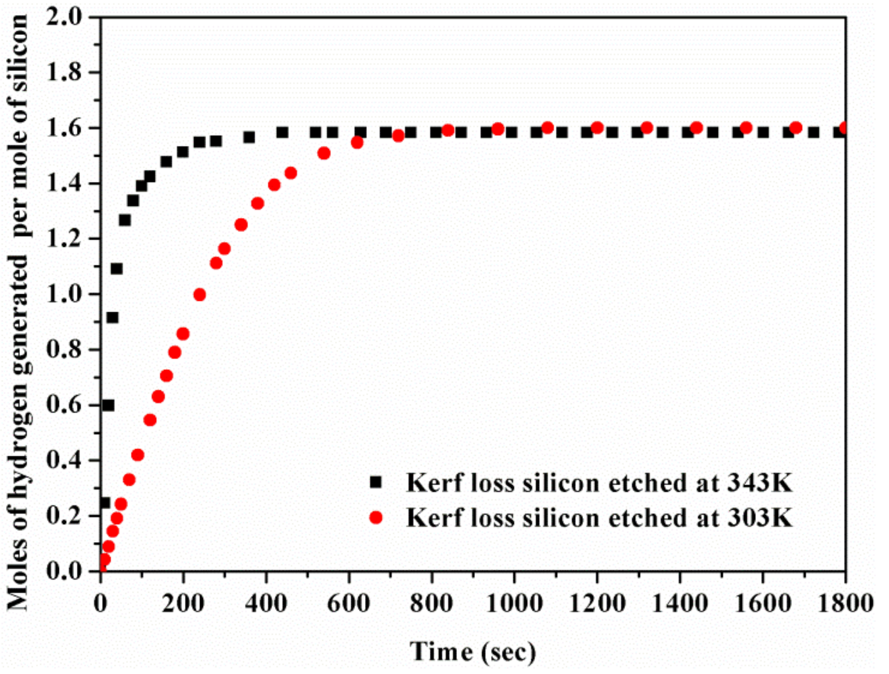

	Hydrogen production rate , g(H_2) s^{-1} g^{-1}(Si)	Yield (%)
K (0.57 M) + M (5 g dm^{-3}) + S (0.5 g dm^{-3}) at 303 K	1.1×10^{-4}	79
K (0.57 M) + M (5 g dm^{-3}) + S (0.5 g dm^{-3}) at 343 K	2.6×10^{-4}	78

230 %

Result and Discussion

Small scale – Optimal quantity of additives

– : low level   + : High level

No. of experiments	K	M	S
1	-	-	-
2	-	+	-
3	+	-	-
4	+	+	-
5	-	-	+
6	-	+	+
7	+	-	+
8	+	+	+

Abbreviation

K: Potassium hydroxide (KOH)

M: Sodium metasilicate (Na_2SiO_3)

S: Silicic acid (H_2SiO_3)

Different compositions of additives at 343K

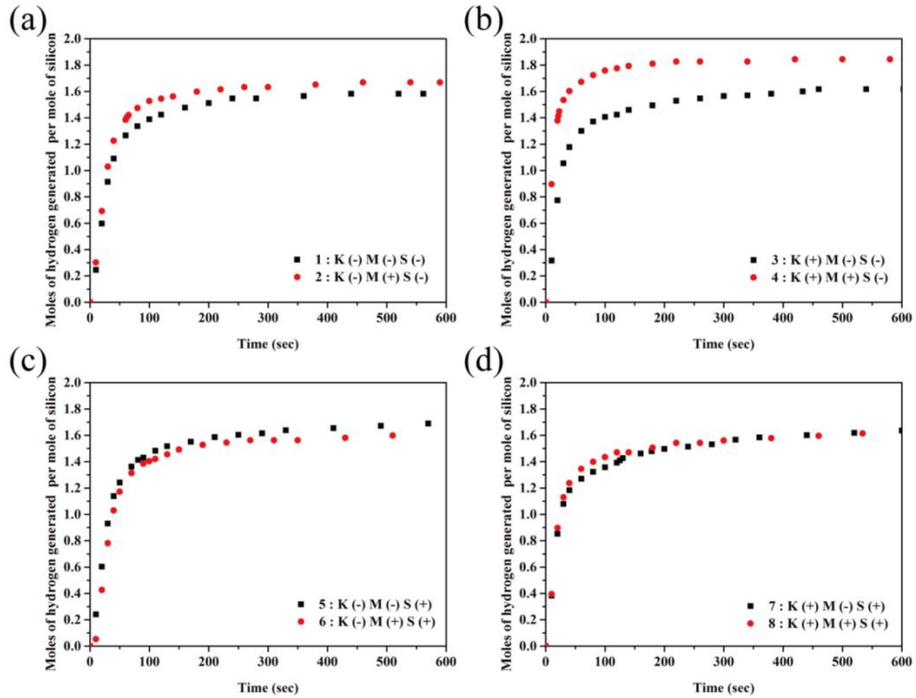

No. of experiment	Composition of additives	70% conversion rate , $g(H_2)\ s^{-1}\ g^{-1}(Si)$	Yield (%)
1	K (0.57 M) + M (5 g dm^{-3}) + S (0.5 g dm^{-3})	9.88×10^{-4}	79
2	K (0.57 M) + M (40 g dm^{-3}) + S (0.5 g dm^{-3})	1.61×10^{-3}	83
3	K (2.14 M) + M (5 g dm^{-3}) + S (0.5 g dm^{-3})	1.00×10^{-3}	81
4	K (2.14 M) + M (40 g dm^{-3}) + S (0.5 g dm^{-3})	4.72×10^{-3}	92
5	K (0.57 M) + M (5 g dm^{-3}) + S (4 g dm^{-3})	1.24×10^{-3}	84
6	K (0.57 M) + M (40 g dm^{-3}) + S (4 g dm^{-3})	9.99×10^{-4}	80
7	K (2.14 M) + M (5 g dm^{-3}) + S (4 g dm^{-3})	8.03×10^{-4}	82
8	K (2.14 M) + M (40 g dm^{-3}) + S (4 g dm^{-3})	1.24×10^{-3}	81

163%

125%

472%

80%

Different hydrogen production methods.

Type	Catalyst	Temp. (K)	Rate (g_{H2} s^{-1} g_{Si}^{-1})	Ref
Etching of Si	KOH	343	4.72×10^{-3}	This work
Etching of Si	NaOH	N/A	9.33×10^{-9} (gH_2 s^{-1})	26
Etching of Si	NaOH	373	2.03×10^{-4}	27
Etching of Si	NH_3	333	6.48×10^{-5}	28
Etching of Si	NaOH	353	5.56×10^{-4}	29
Etching of Si	KOH	R. T.	1.48×10^{-4}	30
Electrochemical	SiNWs/FeP	N/A	9.85×10^{-9} (gH_2 s^{-1})	31
Photoelectrochemical	TiO_2/RGO/Cu_2O	N/A	9.92×10^{-10} (gH_2 s^{-1})	32
Photocatalytic	Si	298	1.89×10^{-7}	34
Ethanol Steam Reforming	Meso-χLaNiAl	873	N/A	37
Fermentative	Microbes	303	N/A	39

Demonstration

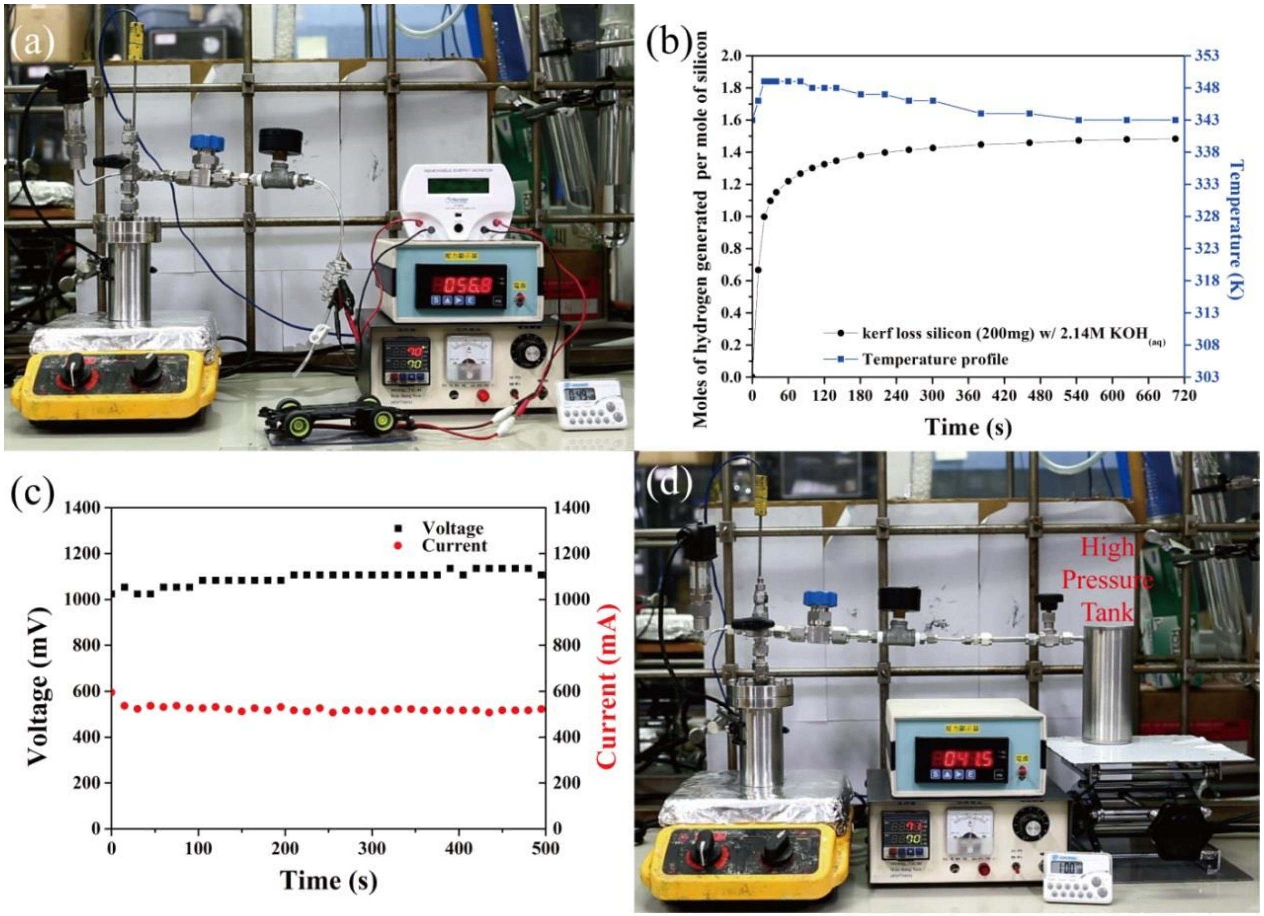

- In coordinate with a fuel cell converting the supplied hydrogen to electricity
- Connected to a gas tank for hydrogen storage

Demonstration

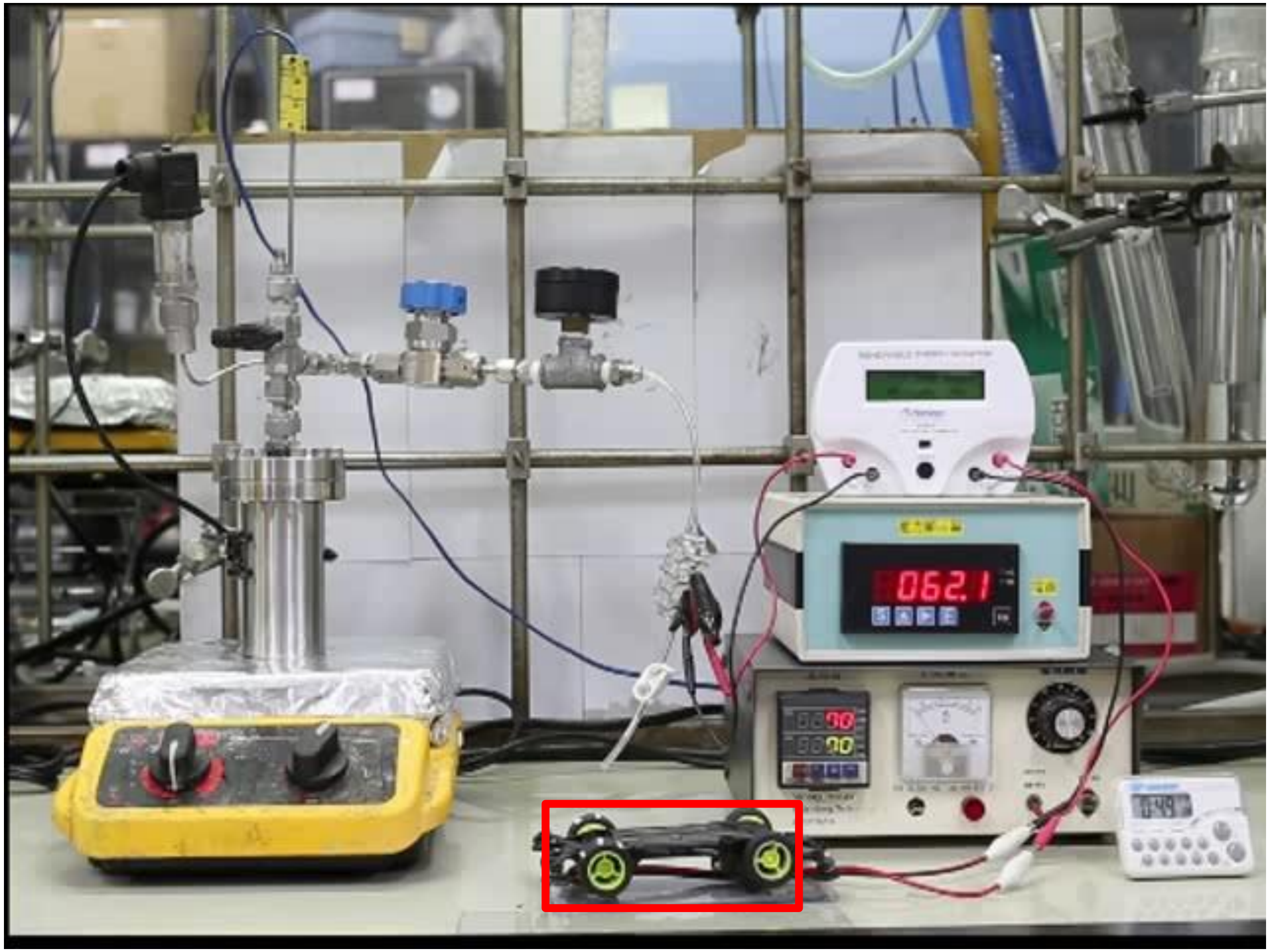

- **Enough to keep a small electric vehicle in motion for minutes.**

Conclusions

Kerf loss silicon collected from the sawing process of solar-grade silicon

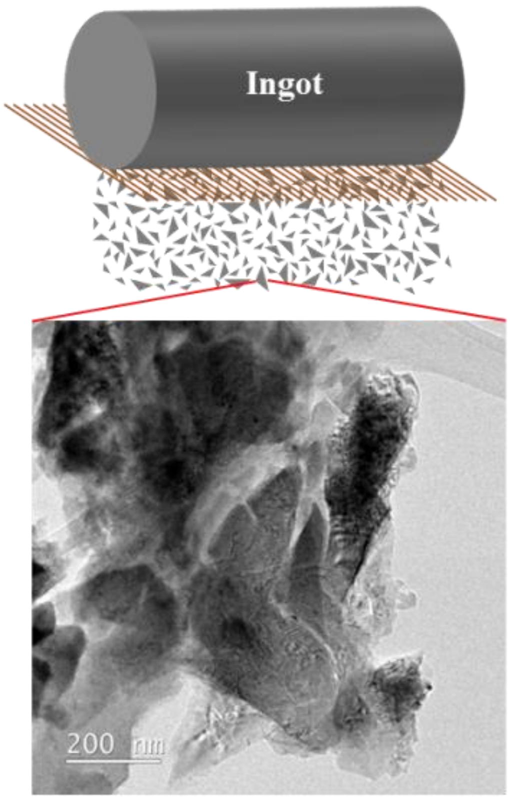

Additives-mediated rapid hydrogen generation

$$Si + 2OH^- + 2H_2O$$

Na_2SiO_3 / H_2SiO_3

$$SiO_2(OH)_2^{--} + 2H_2$$

The H_2 production rate :
$4.73 \times 10^{-3}\ g_{H2}\ s^{-1}\ g_{Si}^{-1}$

The yield of H_2 converted from Si:
92%

Integrated system